UCSF

UC San Francisco Electronic Theses and Dissertations

Title

Gradient amplification during eukaryotic chemotaxis

Permalink

https://escholarship.org/uc/item/94s0d3cr

Author

Weiner, Orion,

Publication Date

2001

Peer reviewed|Thesis/dissertation

eScholarship.org Powered by the California Digital Library
University of California

Gradient Amplification during Eukaryotic Chemotaxis

by

Orion Weiner

DISSERTATION

Submitted in partial satisfaction of the requirements for the degree of

DOCTOR OF PHILOSOPHY

in

Biochemistry

in the

GRADUATE DIVISION

of the

UNIVERSITY OF CALIFORNIA SAN FRANCISCO

[redacted]

Date University Librarian

Degree Conferred: . . . .

Copyright 2001

by

Orion Weiner

I dedicate this thesis to my parents for giving me the freedom and encouragment to pursue my dreams and to Heidi for all of the love and happiness she gives to me.

Acknowledgments

Graduate school has been an immensely rewarding experience for me, largely due to the extraordinary people that I have interacted with here. UCSF is filled with an incredible concentration of extremely sharp internally motivated individuals with whom it has been an absolute joy to share scientific ideas and enthusiasm.

Before I had a specific project carved out, I knew beyond a question of a doubt that I wanted to work with John Sedat, OBM. His fearless approach to attacking scientific questions whose pursuit may span decades and countless new methodologies and his wonderful combination of science and technology have been an inspiration. His genuine weirdness and strange paradoxes have encouraged me to think outside the box and helped me to find the right balance of intensity, humor, and nonconventionality necessary for good science.

My other wonderful labmates and mentors from the 15th floor—Brian, Mike, Bridget, Mats, Julio, and Dave for providing tremendously insightful conversations about science and demonstrating that not all biologists and mathematicians/physicists are afraid of each other, and we have a great deal to learn from one another.

Henry Bourne's incredible clarity of thought helped me to discover the most fundamental questions among all of my interests. To share ideas with Henry, who loves ideas and problem solving so much, has been an absolute joy and at least as rewarding as the many results that followed these investigations. I will be forever grateful for the

tremendous confidence he has inspired in me and the important lessons on what is meaningful in science and what is only a distraction.

The many people in Henry's lab that made it a joy to work there—Tom, Basil, Sonia, Philippe, Elaine. Paul for holding the lab together, and along with Fei and Supriya, being incredible people to share the chemotaxis project.

The other members of my thesis committee—Cori Bargman for her wonderful encouragement, for her immense perceptivity that made it a joy to share ideas, and her emphasis on focus to make sure I didn't spread myself too thin. David Drubin for the valuable opportunity to share my ideas outside of UCSF.

Two of my primary collaborators without whom much of this work would not have been possible. Guy for sticking with the chemotaxis project in the difficult early stages when it looked like it might not yield any fruit and for collaborating in the best sense—sharing ideas and resources instead of competing. Dan for the incredible enthusiasm and joy he brings to science as well as the many fantastic suggestions of beautiful outdoor places to enjoy in Yosemite, the Eastern Sierras, and elsewhere.

My undergraduate advisors George Bittner and Paul Krieg who brought me from the classroom to the wonderful world of experimental science and helped me learn the many benefits of having two PIs. Also for teaching me to start with the question, then choose the experimental organism. It's an important lesson that is easy to miss in the land of model organisms.

All of my wonderful climbing friends who kept me off the ground. After getting used to looking at the world at the level of a single cell, it is spectacular to enjoy the world at the level of Yosemite. In particular, Steve for getting me into climbing out here as well as many great dinners and sun runs to Stanford. Josh, Rachel, and Ettie for introducing me to the heaven that is outdoor climbing. Ettie, Kevin, Simon, and Mark for sharing some memorable climbing epics. Kevin for being a wonderful friend in the lab and on the wall from grad school interviews to late night climbing epics. Melissa for her friendship and enthusiasm.

Joseph for being one of the true friends who I have stayed close to through the years. For convincing me to take the fiendishly depicted Bradshaw taught chemistry course instead of from the soccer coach and his incredible persistance in all of his pursuits.

My parents for giving me exposure to as many ideas and opportunities and experiences possible, for letting me choose my own path, and for all of their encouragement. Also for exposing me to the beauty of nature at an early age which played an enormous part in my pursuit of science later on and approach to it now.

To my Austin family Jim, Deb, Kate, Claire, Meg, and Scott for keeping me young and giving a beautiful example of how wonderful a family can be.

To my inlaws Steve, Suzy, Matt, Laura, Ray, Michael for being a loving home away from home. It has been an absolute joy to be around folks who savor life so much.

To the incredible friends I have made through Heidi—Alyson, Greg, Evelyn, Andrea, Tim, Andy, and Kirsten and for the great dinners and hikes I have had with them. And finally, Heidi for being the most important discovery I made during graduate school. Someone of her perceptivity, fascination, and love of live I wasn't sure I would find ever, much less during the intensity of graduate school. The world is more amazing because I can share it with her. She makes me so happy!

Gradient Amplification during Eukaryotic Chemotaxis

Orion Weiner

Abstract

To carry out their biological responsibilities, many eukaryotic cells depend on their ability to polarize and migrate toward a source of chemoattractant ligand. How do cells appropriately interpret and respond to chemoattractant gradients? To address this question, we study chemotaxis in human neutrophils, cells of the innate immune system that find bacteria by following gradients of formylated peptides released from the bacteria. Our primary goals in these studies were to determine the level at which neutrophils amplify small external gradients into strong internal gradients of response.

In the first project, we develop a transfectable neutrophil system to facilitate quantitative 3-dimensional microscopic analyses of protein dynamics in living cells (Chapter 3). We use this system to demonstrate that chemoattractant receptors are uniformly distributed in living neutrophils during chemotaxis, indicating a lack of gradient amplification at this level of signaling.

In the second project, we developed a permeabilized cell system to address the spatial organization of actin polymerization during chemotaxis (Chapter 4). We also analyzed the dynamics of the Arp2/3 complex, a nucleator of actin polymerization, in living neutrophils. We demonstrate that actin polymerization and the Arp2/3 complex are strongly polarized during

chemotaxis, indicating strong gradient amplification for these final effectors of chemotaxis.

In the third project, we use an effector of PI(3,4,5)P3 and the transfectable neutrophil system to analyze the dynamics of PI(3,4,5)P3 production during chemtoaxis (Chapter 5). We demonstrate that PI(3,4,5)P3 is localized selectively to the up-gradient portion of cells exposed to chemoattractant, the internal gradient of PI(3,4,5)P3 exceeds that of the external chemoattractant, and Rho GTPases are required for PI(3,4,5)P3 generation. These data indicate portions of the signal transduction cascade at which gradient amplification is likely to take place and suggest possible mechanisms for amplification.

In the final project, we use the extracellular parasite enteropathogenic *E. coli* as a model system for the molecular dissection of signals from the cell surface to the cytoskeleton (Chapter 6). We identified the domains of the Wiskott Aldrich Syndrome Protein required for recruitment to the bacterial surface *in vivo* as well as domains required to recruit the Arp2/3 complex, a nucleator of actin polymerization.

Cori Bargmann

Statement Regarding Previously Published Material with Multiple Authors

Chapter Two through Six have previously been published as

Weiner, O.D., G. Servant, C. Parent, P. Devreotes, and H. Bourne (2000) Cell polarity in response to chemoattractants. In *Cell Polarity: Frontiers in Molecular Biology.* D.G. Drubin, editor. Oxford University Press, pp 201-239.

Servant, G., O.D. Weiner, E.R. Neptune, J.W. Sedat, and H.R. Bourne (1999) Dynamics of a chemoattractant receptor in living neutrophils during chemotaxis, *Mol. Biol. Cell.*, **10:** 1163-1178.

Servant, G.*, O.D. Weiner*, P. Herzmark, T. Bhalla, J.W. Sedat, and H.R. Bourne (2000). Polarization of chemoattractant receptor signaling during neutrophil chemotaxis. *Science,* **287:** 1037-1040. (*co-first authors).

Weiner, O.D., G. Servant, M.D. Welch, T.J. Mitchison, J.W. Sedat, and H.R. Bourne (1999) Spatial control of actin polymerization during neutrophil chemotaxis, *Nature Cell Biol.,* **1:** 75-81.

Kalman, D*, O.D. Weiner*, D. Goosney, J. Sedat, B. Finlay, A. Abo, and J.M. Bishop (1999) Enteropathogenic *E. coli.* acts through WASP and Arp2/3 complex to form actin pedestals, *Nature Cell Biol.,* **1:** 389-391. (*co-first authors)

These papers are reprinted here with the permission of Oxford University Press, the American Society for Cell Biology, Macmillan Magazines Ltd., and American

Association for the Advancement of Science, which retain all copyright privileges (see pages xi-xv).

My contribution to Chapter Two was that I wrote all of the chapter with comments from the remaining coauthors and extensive revision by Henry Bourne.

The work described in Chapter Three was a collaboration with Guy Servant, a postdoctoral fellow in the laboratory of Henry Bourne. Guy generated the C5AR-GFP chimera and C5AR-GFP PLB-985 cell line. Enid Neptune provided assistance on how to characterize the functionality of the receptors. All of the experiments with this cell line (Fig1, 2-8) were performed by me with the assistance of Guy Servant.

All of the experiments described in Chapter Four were performed by me. Matt Welch, a postdoctoral fellow in Tim Mitchison's lab, generously provided the Arp3-GFP construct and antibodies to the Arp2/3 complex. Guy Servant generated the promyelocytic leukemia cell line expressing Arp3-GFP.

The work described in Chapter Five was a collaboration with Guy Servant. Guy generated the PHAKT-GFP promyelocytic leukemia cell line and performed the toxin experiments. All of the remaining experiments were performed by me with the assistance of Guy Servant. Paul Herzmark helped set up the microscopy system we used for some of the experiments. Tamas Balla provided the PHAKT-GFP construct.

The work described in Chapter Six was a collaboration with Daniel Kalman, a postdoctoral fellow in the laboratory of Michael Bishop. Dan performed all of the transfections and EPEC infections. Dan and I initiated, planned, and developed this project in close collaboration. Danika Goosney (Finlay lab) helped with some of the experiments, and Arie Abo provided many WASP mutants used in these studies.

Date: Tue, 30 Jan 2001 09:54:33 -0000
From: "Godbolt, Lisa" <L.Godbolt@nature.com>
To: "'oweiner@itsa.ucsf.edu'" <oweiner@itsa.ucsf.edu>
30 January 2001

Mr Orion Weiner
University of California
Department of Biochemistry and Biophysics
San Francisco CA 94143-0450 USA

Invoice No. 00022
Dear Mr Weiner

Macmillan Magazines Limited hereby grants permission for the reproduction of the specified material from Nature Cell Biology for the purpose stated provided that in the event of any written materials being cited, that acknowledgement is made and the author agrees.
Permission is granted for print versions only.

Please use the following form of acknowledgement:

Reprinted by permission from Nature Cell Biology Vol. 1 No.2 pp 75-81
Copyright 1999 Macmillan Magazines Limited

Reprinted by permission from Nature Cell Biology Vol. 1 No. 6 pp389-391
Copyright 1999 Macmillan Magazines Limited

Could you please inform us if you decide not to use the above articles.

Yours sincerely,

Lisa Godbolt
Editorial Assistant
Nature Cell Biology
4 Crinan Street
London N1 9 XW
tel 44-171-843-4924; fax (+) 44 171-843-4794
l.godbolt@nature.com
http://cellbio.nature.com

THE GLOBAL WEEKLY OF RESEARCH
Science

Ref.# weiner 01-0155

Be sure to quote the above reference number in all correspondence

DATE: January 24, 2001

TO:

Orion Weiner
University of California
513 Parnassus Avenue, S-1210
Department of Biochemistry & Biophysics
San Francisco, CA 94143-0450

FROM: Karen Lentz, Permissions Assistant

RE: Your request for permission dated 01/17/01

Regarding your request (see attached copy), we are pleased to grant you non-exclusive, non-transferable permission, **but limited to print and microform formats only**, and provided that you meet the criteria checked below. Such permission is for **one-time use** and therefore does **not** include permission for future editions, revisions, additional printings, updates, ancillaries, customized forms, any electronic forms, braille editions, translations, or promotional pieces. We must be contacted for permission each time such use is planned. This permission does not apply to figures / artwork that are credited to non-AAAS sources. This permission does not include the right to modify AAAS material.

☒ Print the required copyright credit line on the first page that the material appears: "Reprinted (abstracted/excerpted) with permission from [FULL REFERENCE CITATION]. Copyright [YEAR] American Association for the Advancement of Science." Insert the appropriate information in place of the capitalized words.

☒ Permission is limited to the number of copies specified in your request or your first printing.

☐ Obtain the author's permission. *See original article for author's address.*

☐ Remit the following permission fee: $. This letter serves as your invoice. Please make your check payable to "The American Association for the Advancement of Science." A photocopy of this letter must be included with the check. Please remit to SCIENCE, P.O. Box 80144, Baltimore, MD 21280-0144, USA **Please note:** ***Permission is not valid unless payment is received within sixty (60) days of the date on this letter.***

☐ Ensure that no other material is attached to the AAAS article copy.

☐ AAAS must publish the full paper prior to use of any text.

☐ Your publication must not be comprised of more than 30% SCIENCE content.

Note: AAAS does not supply photos or artwork. Also, use of the AAAS material must not imply any endorsement by the American Association for the Advancement of Science. **This permission is not valid for the use of the AAAS and/or SCIENCE logos.**

Thank you for writing. If you have any questions please call me at (202) 326-6765 or write to me via FAX at (202) 682-0816. For international calls, +1 is the country code for the United States.

Headquarters
1200 New York Avenue, NW, Washington, DC 20005 USA • Telephone: 202 326 7073 • Fax: 202 682 0816

AMERICAN ASSOCIATION FOR THE ADVANCEMENT OF SCIENCE

JAN. 24. 2001 11:45AM CMP U C S F +4154765292 NO. 720 P. 2/2
T-302 P.02/02 F-683

01-0155

UNIVERSITY OF CALIFORNIA, SAN FRANCISCO

BERKELEY • DAVIS • IRVINE • LOS ANGELES • RIVERSIDE • SAN DIEGO • SAN FRANCISCO SANTA BARBARA • SANTA CRUZ

SCHOOL OF MEDICINE
DEPARTMENT OF CELLULAR AND MOLECULAR PHARMACOLOGY
513 PARNASSUS AVENUE, S-1210
SAN FRANCISCO, CALIFORNIA 94143-0450

TELEPHONE (415) 476-1951
TELEFAX (415) 476-5292

OK

To: *Science*—Permissions Editor

From: Orion Weiner

I am writing to request permission to reprint the following paper as part of my Ph.D. thesis at the University of California, San Francisco.

Servant, G., O.D. Weiner, P. Herzmark, T. Bhalla, J.W. Sedat, and H.R. Bourne (2000). Polarization of chemoattractant receptor signaling during neutrophil chemotaxis. *Science*, 287: 1037-1040.

Sincerely,

Orion Weiner

Orion Weiner
University of California
Department of Biochemistry and Biophysics
San Francisco, California 94143-0450
Phone: (415) 476-8162
Fax: (415) 476-5292
email: oweiner@itsa.ucsf.edu

Received 01-24-01 08:34am From- To-CMP U C S F Page 02

MOLECULAR BIOLOGY OF THE CELL

PUBLICATIONS OFFICE • 8120 Woodmont Avenue, Suite 750 • Bethesda, Maryland 20814-2755
TEL: 301/347-9300 • FAX: 301/347-9350 • E-MAIL: mbc@ascb.org • www.molbiolcell.org

EDITOR-IN-CHIEF
David Botstein

EDITOR
Keith Yamamoto

ASSOCIATE EDITORS
Mary C. Beckerle
Elizabeth H. Blackburn
Juan Bonifacino
Henry R. Bourne
Joan S. Brugge
Elizabeth Craig
Peter N. Devreotes
David Drubin
Gerald R. Fink
Thomas D. Fox
Joseph Gall
John C. Gerhart
Guido Guidotti
Carl-Henrik Heldin
Tim Hunt
Tony Hunter
Richard Hynes
Chris Kaiser
Judith Kimble
Marc W. Kirschner
Douglas Koshland
Monty Krieger
Vivek Malhotra
Paul T. Matsudaira
J. Richard McIntosh
Elliot Meyerowitz
Marc Mumby
W. James Nelson
Hugh R.B. Pelham
Suzanne R. Pfeffer
Thomas D. Pollard
John Pringle
Martin Raff
Howard Riezman
Ted Salmon
Randy W. Schekman
Richard H. Scheller
Martin Schwartz
Lucy Shapiro
Pamela A. Silver
Mark J. Solomon
Tim Stearns
Harold E. Varmus
Peter Walter
Marvin P. Wickens
Alan P. Wolffe
Mitsuhiro Yanagida

ESSAY EDITORS
Bruce M. Alberts
Thomas D. Pollard

COVER EDITOR
Suzanne R. Pfeffer

VIDEO EDITORS
Jennifer Lippincott-Schwartz
W. James Nelson

January 22, 2001

Orion Weiner
415-476-5292

Dear Dr. Weiner,

We are pleased to grant you permission to reproduce data from the article "Dynamics of a chemoattractant receptor in living neutrophils during chemotaxis", which was published in *Molecular Biology of the Cell*. We require acknowledgment as follows: "Reprinted from *Molecular Biology of the Cell*, (1999, volume 10, 1163-1178), with permission by the American Society for Cell Biology."

Sincerely yours,

Stacie Lemick
Production Editor

Received 01-22-01 01:22pm From-3013479350 To-CMP U C S F Page 01

OXFORD
UNIVERSITY PRESS

Academic Division
Managing Director: Ivon Asquith
Great Clarendon Street
Oxford OX2 6DP
United Kingdom
+44 (0) 1865 556767 *telephone*
+44 (0) 1865 556646 *fax*
www.oup.com

14 May 2001

Our Ref: A/Drubin/AMIZ/mbc

Orion Weiner
Department of Molecular & Cellular Pharmacology
Room S-1222, Box 0450
University of California at San Francisco
513 Parnassus Avenue. San Francisco
CA 94143
USA

Dear Orion Weiner,

Our permission is granted free of charge for the use of the copyright material listed in your letter attached for use in your thesis, subject to the following terms and conditions: - cell Polarity, ed DG Drubin - "Cell Polarity in response to chemoattractants"

1. A credit line should appear in your thesis citing the author/editor, title and year of the Oxford University Press publication that is the source of the material together the copyright line and "by permission of Oxford University Press."

2. The material may not be altered, adapted, added to or deleted from in any way without our written permission.

3. If the credit line or the acknowledgements list indicates that the material was redrawn, modified or reproduced from an earlier source, it will be necessary for you to clear a separate permission for these items with the original publisher.

4. This permission does not cover any electronic use of the material, for which you must apply separately to Liz Mann in the Rights Department.

5. If at some future date your thesis is publisher it will be necessary to re-clear this permission.

Yours sincerely

Mary I. P. [illegible]

PP Anna Zawadzki
Permissions Manager

E-mail: zawadzka@oup.co.uk
Direct Fax: +44 1865 267429

Oxford University Press is a department of the University of Oxford. It furthers the University's objective of excellence in research, scholarship, and education by publishing worldwide

Received 05-14-01 07:48am From-01865 267429 To-CMP U C S F Page 01

Gradient amplification during eukaryotic chemotaxis

Table of Contents

Title Page i

Dedication iii

Acknowledgments iv

Abstract vii

Statement Regarding Previously Published Material with Multiple Authors ix

Table of Contents xvi

List of Figures xix

CHAPTER ONE

Introduction—Gradient amplification during eukaryotic chemotaxis 1

CHAPTER TWO

Background—Cell polarity in response to chemoattractants 9

- Introduction 10
- Chemotactic Receptors and G proteins 12
- Adaptation to chemoattractant 15

Interpreting the chemotactic gradient 18

Polarity effectors: Rho GTPases 25

Other regulators: Calcium and cyclic GMP 32

Coordination of actin polymerization, polarization, and directed movement 33

Perspectives and future directions 39

References 43

CHAPTER THREE

Chemokine receptors are uniformly distributed during neutrophil chemotaxis 49

Summary 50

Introduction 50

Experimental Procedures 51

Results 53

Discussion 60

References 64

CHAPTER FOUR

Actin polymerization and a nucleator of actin polymerization (the Arp2/3 complex) are polarized during neutrophil chemotaxis 66

Summary 67

Introduction 67

Results 68

Discussion 71

Experimental Procedures 72

References 72

CHAPTER FIVE

PI(3.4.5)P3 exhibits an amplified polarity during neutrophil chemotaxis 74

Summary 75

Introduction 75

Results/Discussion 75

Experimental Procedures/ References 77

CHAPTER SIX

Pathogenic E. coli as a system for dissecting signaling to the cytoskeleton —the role of the Wiskott-Aldrich Syndrome Protein. 79

Introduction 80

Results/Discussion 80

Experimental Procedures 82

References 82

CHAPTER SEVEN: Summary 83

List of Figures

CHAPTER TWO

Figure 1: Polarization of a neutrophil in response to a gradient of chemoattractant 11

Figure 2: Requirements for eukaryotic chemotaxis 12

Figure 3: Overview of trimeric G-protein cycle 13

Figure 4: Adaptation at the level of the G-protein-coupled receptor 16

Figure 5: Actin staining of neutrophils converging on point source of chemoattractant 19

Figure 6: PI3K activation localizes to the up-gradient surface in *Dictyostelium.* 21

Figure 7: Comparison of types of signal processing for gradient interpretation 22

Figure 8: Phenotypes of macrophages for gain and loss-of-function of Rho GTPases 27

Figure 9: Modulation of the actin cytoskeleton through activation of Cdc42, Rac, and Rho 29

Figure 10: Review of actin dynamics 34

Figure 11: Model for *Listeria* motility 36

Figure 12: Spatial control of actin polymerization during neutrophil chemotaxis 38

CHAPTER THREE

Figure 1: The promyelocytic leukemia cell line PLB-985 exhibits neutrophil-like responses to gradients of chemoattractant 54

Figure 2: Stable transfection of GFP into PLB-985 cells 55

Figure 3: Functionality and expression of GFP-tagged C5A receptor 56

Figure 4: Internalization of the C5A receptor following stimulation by uniform chemoattractant 57,58

Figure 5: The C5A receptor is uniformly distributed during chemotaxis 59

Figure 6: The C5A receptor parallels the distribution of plasma membrane during chemotaxis in living cells 60

Figure 7: The distribution of C5A receptor parallels that of plasma membrane in fixed optically deconvolved cells 61

Figure 8: Cell surface C5A receptors are uniformly distributed during chemotaxis 62

CHAPTER FOUR

Figure 1: Polarization of a neutrophil in response to a gradient of chemoattractant 67

Figure 2: Spatial distribution of actin polymerization in chemoattractant-stimulated neutrophil 69

Figure 3: Cells with multiple pseudopodia exhibit dominant pseudopod for actin polymerization 69

Figure 4: The Arp2/3 complex accumulates on the up-gradient surface of living neutrophils during chemotaxis 70

Figure 5: The least extractable pool of the Arp2/3 complex colocalizes with sites of actin polymerization 70

Figure 6: Model of actin polymerization in response to chemotactic signal 71

CHAPTER FIVE

Figure 1: Translocation of PHAKT-GFP to the plasma membrane of neutrophil-differentiated HL-60 cells 76

Figure 2: Uniform stimulation by chemoattractant induces a polarized distribution of PI3K activity 76

Figure 3: Asymmetric PI3K activation does not require actin polymerization 77

Figure 4: PI3K activation by G-protein coupled receptors requires Rho GTPases 77

CHAPTER SIX

Figure 1: WASP is recruited to EPEC pedestals via its GTPase binding domain 81

Figure 2: Pedestal formation and localization of the Arp2/3 complex to pedestals require the WASP acidic domain 82

CHAPTER ONE

Introduction

Gradient Amplification during Eukaryotic Chemotaxis

To carry out their biological responsibilities, many eukaryotic cells depend on their ability to polarize and migrate toward a source of chemoattractant ligand. This crucial ability allows single-celled organisms to hunt and mate, axons to find their way in the developing nervous system, and cells in the innate immune system to find and kill invading pathogens. How do eukaryotic cells appropriately interpret and respond to chemotactic gradients? To address this question, we study chemotaxis in human neutrophils, cells of the innate immune system that find bacteria by following gradients of formylated peptides released by the bacteria. During this thesis, we developed a transfectable neutrophil system [1,2] and permeabilized cell system [3] with which we analyzed the dynamics of signal transduction proteins in living neutrophils during chemotaxis. Our primary goals in these studies were to determine the level at which neutrophils amplify small external gradients into strong internal gradients of response and to determine which molecules are good candidates for spatial carriers of information. The basic approaches we use include (1) A permeabilized cell system to address where actin polymerization occurs during chemotaxis, (2) Quantitative 3-dimensional microscopic analyses of protein dynamics in living cells to address how neutrophils interpret the chemotactic gradient and (3) the extracellular parasite enteropathogenic *E. coli* (EPEC) as a model system for the molecular dissection of signal transduction from the cell surface to the cytoskeleton. We pursued the following questions

How do cells convert a relatively shallow external gradient of chemoattractant into a much stronger internal gradient of response?

When exposed to shallow gradients of chemoattractant as subtle as 1-2% across the cell diameter, neutrophils respond with highly oriented cell polarity and motility. To address how neutrophils are able to amplify such subtle external cues, we have developed tools to analyze spatial readouts of activity at a several levels of chemotactic signaling.

◆Neutrophils respond to chemotactic stimuli by increasing the nucleation and polymerization of actin filaments, but the location and regulation of these processes are not well understood. we developed a permeabilized cell system to assay the spatial distribution of actin polymerization during chemotaxis. Similar studies had previously been performed in neutrophils and reported uniform actin incorporation relative to endogenous actin distribution [4]. Using techniques that better preserve the neutrophil actin cytoskeleton and prevent proteolysis, we discovered that chemotactic stimuli cause neutrophils to organize many discrete sites of actin polymerization, the distribution of which is biased by external chemoattractant gradients [1]. Three-dimensional reconstruction of these sites of actin polymerization gave insight into how neutrophils build a complex leading edge in response to chemotactic stimulation. Furthermore, using a transfectable neutrophil system (described below), we found that the Arp2/3 complex, a nucleator of actin polymerization, dynamically redistributes to the region of living neutrophils that receives maximal chemotactic stimulation. These data indicate that strong asymmetry exists at the level of actin polymerization and a putative effector of receptor-mediated actin polymerization. Our subsequent studies probed chemotactic signaling at a more proximal level.

♦ We sought to determine at which level of signaling gradient amplification occurs and which molecules are good candidates for carriers of polarized signals during chemotaxis. Ideally, we would like to know spatial and temporal dynamics of proteins during chemotaxis using GFP-tagged proteins in neutrophils. However, mature neutrophils are terminally differentiated cells that are short-lived in culture and exceedingly difficult to transfect or microinject. In order to deliver foreign proteins into neutrophils, we developed a transfectable neutrophil system in which we use stem cells of the neutrophil lineage (promyelocytic leukemia cell lines) that can be grown indefinitely in culture, transfected with retroviruses or electroporation, and then differentiated into cells in which we analyzed the dynamics of signal transduction proteins in living neutrophils during chemotaxis [2,3]. Using this system, we found that chemotactic receptors [2] and PI(4,5)P2 [unpublished data] are uniformly distributed during chemotaxis..

To develop a probe for signaling events between the chemoattractant receptors and the actin polymerization machinery, we expressed a GFP-tagged pleckstrin homology (PH) domain of the PI3K effector AKT protein kinase (also known as protein kinase B) in neutrophils [3]. Although genetic [5-7] and pharmacological [8] data had demonstrated the importance of PI3K activity for cell polarization and chemotaxis, the subcellular localization of PI3K products during neutrophil chemotaxis were not previously known. Using our living spatial probe for PIP3 localization, we found that PI(3,4,5)P3 is localized selectively to the up-gradient portion of cells exposed to chemoattractant. Furthermore, the internal gradient of PIP3 is stronger than that of the external gradient, and asymmetries of PIP3 are observed even in the absence of actin polymerization [3]. These data indicate that cell polarization and gradient amplification can occur upstream of morphological rearrangements, as for the single-celled amoeba *Dictyostelium* [9]. Surprisingly, polarized PIP3 distributions are observed even for uniform stimulation [3]. These data indicate that neutrophils have an inherent capacity for symmetry breaking and gradient amplification, and that this amplification occurs at a level between the chemotactic receptors and PIP3 metabolism. These data also indicate that the products of PI3K are good candidates for carriers of cell polarity information during chemotaxis.

Because small GTPases of the Rho family mediate certain neutrophil responses to chemoattractant and play important roles in relaying signals to the actin cytoskeleton, we investigated whether Rho GTPases are required for recruitment of the probe for PI3K activity to the neutrophil plasma membrane. Using a toxin that inactivates Rac, Rho, and Cdc42, we found that the Rho GTPases are necessary for PHAKT-GFP recruitment to the cell membrane [3]. These were the first data placing Rho GTPases upstream of AKT activation *in vivo* (and by inference upstream of PI3K activation), and more recent data in T cells implicates Rac (and possibly Cdc42) upstream of AKT activation [10]. Combined with an increasing body of data placing Rho GTPases variably upstream and downstream of PI3K activation, sometimes in the same cell [10], these data suggest that the pathway from chemoattractant receptor and Rho GTPases may not be a simple linear pathway but rather a cyclical one-- placing Rho GTPases both upstream and downstream of PI3K activation-- a possible positive feedback loop with important implications for the actual mechanism of gradient amplification and cell polarity.

How are extracellular cues relayed to the actin cytoskeleton?

Finally, to gain additional insight into how extracellular cues interface with the actin cytoskeleton, our lab (in collaboration with Daniel Kalman in Mike Bishop's lab) studied actin-based pedestal formation of enteropathogenic E. coli (EPEC). Just as the intracellular bacteria *Listeria monocytogenes* has been incredibly powerful in dissecting the most downstream components of actin polymerization and actin-based motility, the extracellular bacteria EPEC has the potential to dissect proteins involved in more upstream stages of signaling for stimulus-induced actin polymerization. We used these bacteria in conjunction with a molecular dissection of WASP (Wiskott-Aldrich Syndrome Protein), a protein involved in signal relay to the actin cytoskeleton, to show that WASP is necessary for pedestal formation by EPEC. This was the first demonstration of a host factor necessary for actin pedestal formation by EPEC. Furthermore, we identified the domains of WASP required for recruitment to the bacterial surface *in vivo* as well as domains required to recruit a downstream nucleator of actin polymerization [11]. The power of this system lies in the fact that EPEC induces actin polymerization at highly localized sites, immediately below the bacterial surface, unlike the much more complex actin rearrangements involved in chemotaxis. Therefore, this system is amenable to address not only which molecules are involved in signal relay to the actin cytoskeleton, but also which domains of the molecules are involved in recruitment versus effector function.

Chemotaxis is an inherently highly spatial signaling event. Its understanding requires more sophisticated tools than those used for other singaling systems. This thesis emphasizes the importance of disparate but complementary techniques such as permeabilized cell systems for pulse-chase experiments and single celled biochemistry, transfectable cell systems for analysis of spatial and temporal dynamics of proteins in living cells, and bacterial pathogens for interfacing with the chemotaxis transduction cascade at intermediate levels, allowing dissection of effectors to the actin cytoskeleton.

References

1. Weiner, O.D., G. Servant, M.D. Welch, T.J. Mitchison, J.W. Sedat, and H.R. Bourne (1999) Spatial control of actin polymerization during neutrophil chemotaxis, *Nature Cell Biol.,* **1:** 75-81.

2. Servant, G., **O.D. Weiner**, E.R. Neptune, J.W. Sedat, and H.R. Bourne (1999) Dynamics of a chemoattractant receptor in living neutrophils during chemotaxis, *Mol. Biol. Cell.*, **10:** 1163-1178.

3. Servant, G.*, **O.D. Weiner***, P. Herzmark, T. Bhalla, J.W. Sedat, and H.R. Bourne (2000). Polarization of chemoattractant receptor signaling during neutrophil chemotaxis. *Science,* **287:** 1037-1040. (*co-first authors)

4. Redmond T and Zigmond SH. (1993) Distribution of F-actin elongation sites in lysed polymorphonuclear leukocytes parallels thedistribution of endogenous F-actin. *Cell Motil Cytoskeleton.***26:**7-18.

5. Sasaki T, Irie-Sasaki J, Jones RG, Oliveira-dos-Santos AJ, Stanford WL, Bolon B, Wakeham A, Itie A, Bouchard D, Kozieradzki I, Joza N, Mak TW, Ohashi PS, Suzuki A, and Penninger JM. (2000) Function of PI3Kgamma in thymocyte development, T cell activation, and neutrophil migration. *Science* **287:** 1040-1046.

6. Li Z, Jiang H, Xie W, Zhang Z, Smrcka AV, and Wu D. (2000) Roles of PLC-beta2 and -beta3 and PI3Kgamma in chemoattractant-mediated signal transduction. *Science* **287:** 1046-1049

7. Hirsch E, Katanaev VL, Garlanda C, Azzolino O, Pirola L, Silengo L, Sozzani S, Mantovani A, Altruda F, and Wymann MP (2000) Central role for G protein-coupled phosphoinositide 3-kinase gamma in inflammation. *Science* **287:** 1049-1053.

8. Niggli, V. and Keller, H. (1997) The phosphatidylinositol 3-kinase inhibitor wortmannin markedly reduces chemotactic peptide-induced locomotion and increases in cytoskeletal actin in human neutrophils. *Eur. J. Pharmacol.* **335:** 43-52.

9. Parent CA, Blacklock BJ, Froehlich WM, Murphy DB, and Devreotes PN. (1998) G protein signaling events are activated at the leading edge of chemotactic cells. *Cell.* **95:**81-91.

10. Genot EM, Arrieumerlou C, Ku G, Burgering BM, Weiss A, and Kramer IM. (2000) The T-cell receptor regulates akt (Protein kinase B) via a pathway involving rac1 andphosphatidylinositide 3-kinase. *Mol Cell Biol.* **20:**5469-78.

11. Kalman, D*, **O.D. Weiner***, D. Goosney, J. Sedat, B. Finlay, A. Abo, and J.M. Bishop (1999) Enteropathogenic *E. coli.* acts through WASP and Arp2/3 complex to form actin pedestals, *Nature Cell Biol.,* **1:** 389-391. (*co-first authors).

CHAPTER TWO

Cell Polarity in Response to Chemoattractants

Reprinted from Weiner, O.D., G. Servant, C. Parent, P. Devreotes, and H. Bourne (2000) Cell polarity in response to chemoattractants. In *Cell Polarity: Frontiers in Molecular Biology*. D.G. Drubin, editor. Oxford University Press, pp 201-239 with permission by Oxford University Press.

7 Cell polarity in response to chemoattractants

ORION D. WEINER, GUY SERVANT, CAROLE A. PARENT,
PETER N. DEVREOTES, and HENRY R. BOURNE

1. Introduction

To carry out their biological responsibilities, many eukaryotic cells depend on their ability to polarize and migrate toward a source of chemoattractant ligand. This crucial ability allows single-cell organisms to hunt and mate, axons to find their way in the developing nervous system, and cells in the innate immune system to find and kill invading pathogens. How do eukaryotic cells interpret a chemotactic gradient? Which signalling molecules carry information from the external world to internal cellular responses? What are the final effectors for cell polarity and migration? How are polarity responses co-ordinated in space and time? To address these and other questions, we will focus on two especially useful systems for the study of eukaryotic chemotaxis: neutrophils and *Dictyostelium discoideum*.

Neutrophils are cells of the innate immune system. All animals from sponges to humans have some version of these amoeboid cells programmed to find and kill invading pathogens. Neutrophils find bacteria by following gradients of formylated peptides released by the bacteria. When isolated in an unpolarized state and presented with a gradient of chemoattractant, neutrophils polarize and migrate towards the highest concentration of chemoattractant (Fig. 1). Constantly interpreting the gradient, they unerringly follow a moving micropipette containing chemoattractant.

Dictyostelium discoideum is a free-living soil amoeba that feeds on bacteria. Under starvation conditions, *Dictyostelium* aggregates to form a multicellular mound that undergoes a complex developmental programme, culminating in the production of hardy spores. Chemotaxis is necessary for *Dictyostelium* to find bacteria during the vegetative phase and to form multicellular aggregates in response to starvation. Both neutrophils and *Dictyostelium* detect and respond to shallow chemical gradients, as small as 2% across the cells' diameter; none the less, the large dynamic range of their responses allows them to respond to concentrations of chemoattractant varying over several orders of magnitude (1).

Chemotaxis, or the directed movement of cells in response to chemotactic gradients, was first discovered more than a century ago in bacteria. In contrast to the

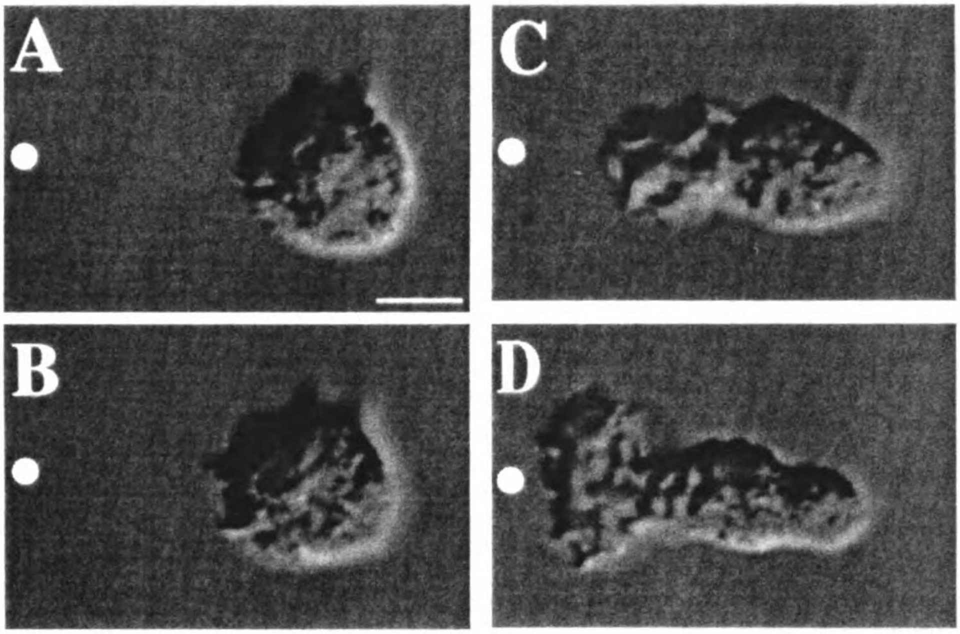

Fig. 1 Polarization of neutrophil in response to gradient of chemoattractant. Nomarski images of unpolarized neutrophil responding to a micropipette containing the chemoattractant FMLP (white circle) at (A) 5 s, (B) 30 s, (C) 81 s, and (D) 129 s. Bar = 5 μm. Figure reprinted from ref. 96 with permission from ***Nature Cell Biology***.

mechanism(s) used by eukaryotes, the *temporal* mechanism used by prokaryotes to interpret a chemotactic gradient and translate it into directed movement is well understood: a bacterium senses the local concentration of chemoattractant as a function of time; an increase in chemoattractant concentration over time makes the bacterium more likely to persist in forward movement and less likely to tumble and travel in a random new direction. The resulting longer duration of runs directed toward the chemoattractant produces a biased random walk that eventually delivers the bacterium close to the highest concentration of chemoattractant. For bacterial chemotaxis, we understand the basic input of the system (the chemoattractant concentration at successive points in time), the basic output (turning the flagellar motor in the direction that generates smooth movement or random tumbling), and much of the molecular machinery in between (2).

What are the basic requirements for eukaryotic chemotaxis? First, a neutrophil or an amoeba needs an external gradient of a *chemotactic ligand* and *a receptor* that transmits a signal into the cell upon binding the ligand. The receptor (or the signal it generates) needs an *adaptation* (or background subtraction) mechanism to allow responses to shallow gradients over a large range of ligand concentrations. Each cell must *interpret* the gradient—that is, identify the portion of its surface that receives the most intense external signal. The cells need *second messengers* to transmit information

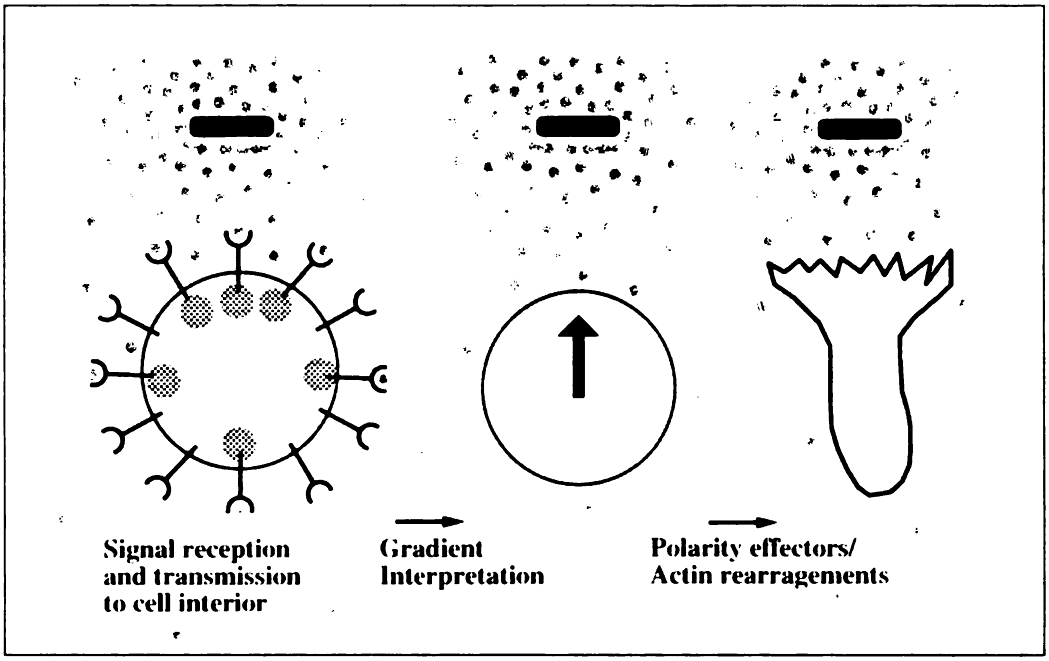

Fig. 2 Requirements for eukaryotic chemotaxis. In order to respond appropriately to chemotactic gradients, eukaryotic cells must contain receptors that transmit a signal to the cell interior upon binding chemoattractant. Each cell must manipulate this information to determine which region of its surface is exposed to maximal chemoattractant. Finally, the cell must transmit this information to the final effectors responsible for spatial regulation of actin rearrangements and cell motility.

about the chemoattractant gradient from receptors to the final effectors that determine cell polarity and mediate cell movement. Here we shall focus on the effects of spatial gradients of chemoattractant on the actin cytoskeleton and the regulation of actin polymerization, which is necessary for morphological polarization and migration of neutrophils, *Dictyostelium*, and almost all motile eukaryotic cells (Fig. 2).

2. Chemotactic receptors and G proteins

To interpret external gradients, eukaryotic cells require receptors to relay to the cell interior information about ligand concentration outside the cell. Both neutrophils and *Dicytostelium* cells use ligand-sensing transmembrane proteins known as G-protein-coupled receptors (GPCRs). Upon binding specific extracellular ligands, GPCRs undergo conformational changes that lead to activation of trimeric G-proteins, which are located on the cytoplasmic side of the plasma membrane. In its inactive form, the G-protein trimer includes a GDP-bound α subunit, associated with a stable $\beta\gamma$ heterodimer. Interaction of the G protein with ligand-bound receptor induces the α subunit to exchange its bound GDP for GTP, with the result that α–GTP dissociates from $\beta\gamma$. In their dissociated states, both α–GTP and $\beta\gamma$ can interact with down-

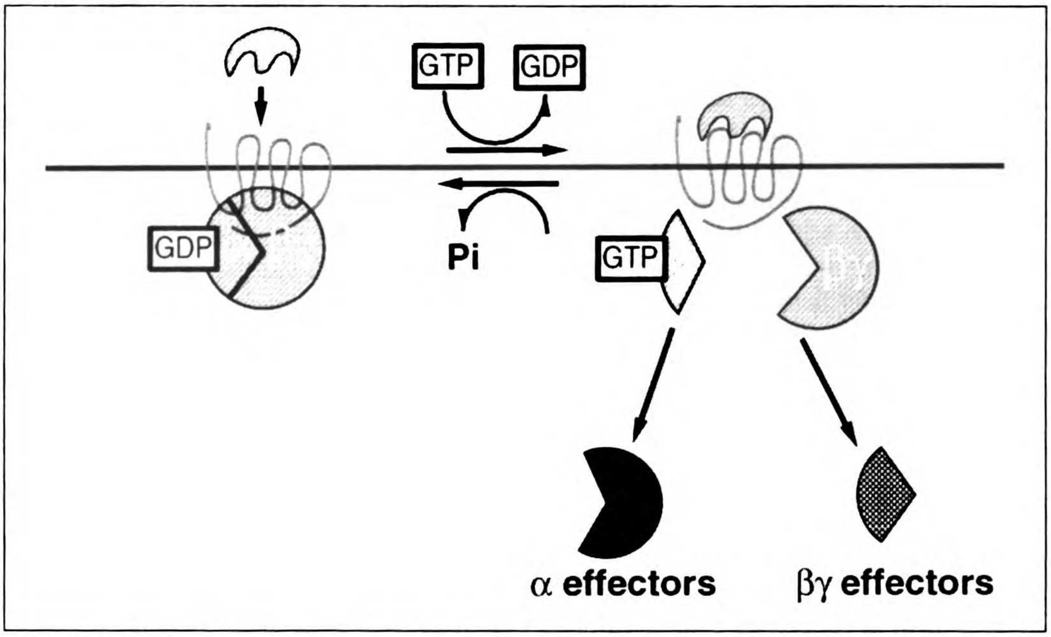

Fig. 3 Overview of trimeric G-protein cycle. Binding of ligand to the extracellular domain of G-protein-coupled receptors induces GTP-charging of α and dissociation of α from βγ. In their dissociated states, both α and βγ can interact with downstream effectors. Hydrolysis of GTP by α regenerates the inactive G protein and terminates the signal. For details, see text.

stream effectors, which recognize surfaces of the two proteins that are inaccessible in the heterotrimer. Hydrolysis of bound GTP by α and reassociation of α–GDP with βγ regenerate an inactive G protein and terminate the signal (Fig. 3). Structurally and functionally heterogeneous, mammalian trimeric G-proteins are made up of polypeptides from three large families, encoded by at least 16 α, 5 β, and 11 γ genes. Individual G proteins are usually denoted by their distinctive α subunits, each of which regulates a different subset of downstream effectors. In addition to chemotactic ligands, GPCRs in mammalian cells detect and relay signals mediated by a host of hormones and neurotransmitters, as well as sensory stimuli, including light, sound, odorants, and tastants.

While any GPCR can relay information about the concentration of an extracellular ligand, only G_i-coupled receptors trigger chemotaxis of mammalian cells. Neutrophils respond to a very large number of chemotactic signals. In addition to the formylated peptides produced by bacteria, these include interleukin-8 (IL-8), a component of the complement cascade (C5a), and several other chemokines that are produced by endothelial cells, immunocytes, and other inflammatory cells at sites of tissue injury. All the GPCRs stimulated by these and other chemoattractants in mammals couple to the G_i class of trimeric G-proteins, as indicated by the sensitivity of chemotactic responses to inhibition by a bacterial toxin, pertussis toxin (PTX), which specifically attaches ADP-ribose to a cysteine in the C terminus of α_i, thereby uncoupling G_i from GPCR stimulation. Several other G_i-coupled receptors whose ligands are not classically considered chemoattractants also mediate chemotaxis in cultured cells, but GPCRs coupled to other G proteins do not (3, 4).

What is special about G_i-coupled receptors? One obvious distinction is that only G_i-coupled receptors activate α_i. Is α_i–GTP then a necessary mediator of chemotaxis? This α subunit is probably not a necessary mediator, as indicated by experiments in which HEK293 cells were tricked into using a G_i-coupled receptor to activate a G-protein trimer that does not contain α_i (5). The cells were made to express an α_q/α_z chimera, in which the C-terminal four residues of α_q were replaced by the corresponding residues of α_z, a member of the α_i family that can be activated by G_i-coupled receptors but whose C terminus lacks the cysteine that confers sensitivity to inhibition by PTX. In PTX-treated cells, CXCR1, a G_i-coupled receptor for IL-8, could mediate a chemotactic response (migration across a filter toward a chamber containing chemoattractant, in a device called a Boyden chamber) if the cells expressed the α_q/α_z chimera, but not in untransfected cells or in cells expressing recombinant α_q. As expected, in PTX-treated α_q/α_z-expressing cells, IL-8 stimulated an α_q effector, phospholipase C, but had no effect on an α_i effector, adenylyl cyclase. Thus, although a G_i-coupled GPCR is required for chemotaxis, specific α_i-dependent signals are not. Until this experiment is repeated in a professional chemotactic cell, like the neutrophil, this result does not rule out the possibility that α_i–GTP transmits messages that contribute to efficient chemotaxis of cells that move faster than HEK293 cells; the result suggests, none the less, that α_i–GTP is probably not *required* for neutrophil chemotaxis.

If α_i is dispensable for chemotaxis, what components downstream of the GPCR are necessary? In mammalian cells, one necessary component is the $\beta\gamma$ subunit released by G-protein activation. Chemotaxis in HEK293 or lymphocyte cells is blocked by expression of either of two proteins that bind and sequester free $\beta\gamma$ (3, 4). One of these proteins, the α subunit (α_t) of G_t, can be activated by rhodopsin, but not by G_i-coupled receptors; consequently, recombinant α_t expressed in HEK293 cells or lymphocytes remains in its GDP-bound form and sequesters free $\beta\gamma$, thereby inhibiting chemotaxis. In HEK293 cells, expression of a C-terminal fragment of the β-adrenergic receptor kinase (βARK) similarly sequesters $\beta\gamma$ and prevents chemotaxis (the C-terminal fragment binds $\beta\gamma$ but lacks the kinase catalytic domain). Although α_t and βARK sequester free $\beta\gamma$, they do not prevent CXCR1 from mediating an α_i–GTP-dependent response to IL-8-inhibition of adenylyl cyclase.

What roles do α and $\beta\gamma$ subunits play in the chemotactic responses of *Dictyostelium*? Homologous recombination, or site-directed insertion of foreign DNA at specific locations in the *Dictyostelium* genome, makes it possible to inactivate specific genes in this haploid organism—to create, for example, cells with null alleles for any one of the eight α genes or for the single β or γ gene. This approach has been used to study chemotaxis toward two ligands that are detected by different GPCRs: folate, a bacterial product that tells amoebae where to find their prey, and cAMP, the ligand that mediates aggregation of starved amoebae to form a slug that will later produce spores. Chemotaxis toward folate is impaired in *Dicytostelium* null for one α subunit,

α_4, while a different null mutation (in the α_2 gene) impairs chemotaxis toward cAMP; in neither case does the null α gene affect chemotaxis toward the other ligand (6, 7). Thus the two receptors mediate chemotaxis by activating G-protein trimers containing different α subunits, but the results do not tell us whether the α subunit specificity reflects a requirement for interaction with specific receptors or with specific downstream effectors. The latter interpretation, implying that the two chemotactic responses depend on different downstream effectors, seems possible but unlikely. The former interpretation suggests that specific α subunits in *Dicytostelium* act primarily as tools for coupling release of free $\beta\gamma$ to ligand stimulation of a specific subset of GPCRs, which discriminate among α subunits of the trimers they activate—that is, a role similar to that of α_i in mammalian cells.

What about $\beta\gamma$? Cells null for the gene encoding the single β subunit of *Dictyostelium* do not migrate toward any chemoattractant (8). This result indicates that $\beta\gamma$ is essential for chemotaxis but by itself does not tell us whether $\beta\gamma$ signals directly to downstream effectors for chemotaxis or whether the primary function of $\beta\gamma$ is to mediate receptor activation of α subunits. The amenability of *Dicytostelium* to homologous recombination made it possible to address this question, by rescuing β null cells with mutated versions of the β gene (9). One β mutant supported chemotaxis very poorly, but allowed proper coupling of G protein to receptor (assayed by a GTP-induced loss in ligand affinity) and proper activation of G protein by ligand-bound receptor (assayed by ligand-induced actin polymerization). This result strongly suggests that in *Dicytostelium* $\beta\gamma$ directly regulates downstream effectors for chemotaxis. Indeed, it seems likely that both *Dicytostelium* and neutrophils use $\beta\gamma$ as the principal mediator of chemotaxis, and specific α subunits to couple the process to specific GPCRs.

3. Adaptation

In both neutrophils and *Dictyostelium*, exposure to chemoattractant elicits a number of transient responses, including actin polymerization, cell-shape changes, activation of adenylyl cyclase, and phosphorylation of myosin heavy and light chains (1). After the immediate transient response to a given concentration of chemoattractant, the cells become refractory to stimulation with that concentration, but can respond to a chemotactic stimulus of greater intensity. This process is called 'desensitization' or 'adaptation'. The ability to adapt to a given concentration of chemoattractant probably contributes to the ability of neutrophils and *Dictyostelium* to undergo chemotaxis over ranges of ligand concentration that span several orders of magnitude. Although adaptation could occur at many different levels in the signalling cascade, we will focus on adaptation at the levels of GPCR and G protein, which is best understood.

A common mechanism for adaptation of G-protein-mediated signals is to phosphorylate the GPCR, thereby marking it for physical uncoupling from G protein. This marking process is crucial for proper visual transduction in the rod photoreceptors of the vertebrate retina. Photoexcited rhodopsin itself initiates adaptation

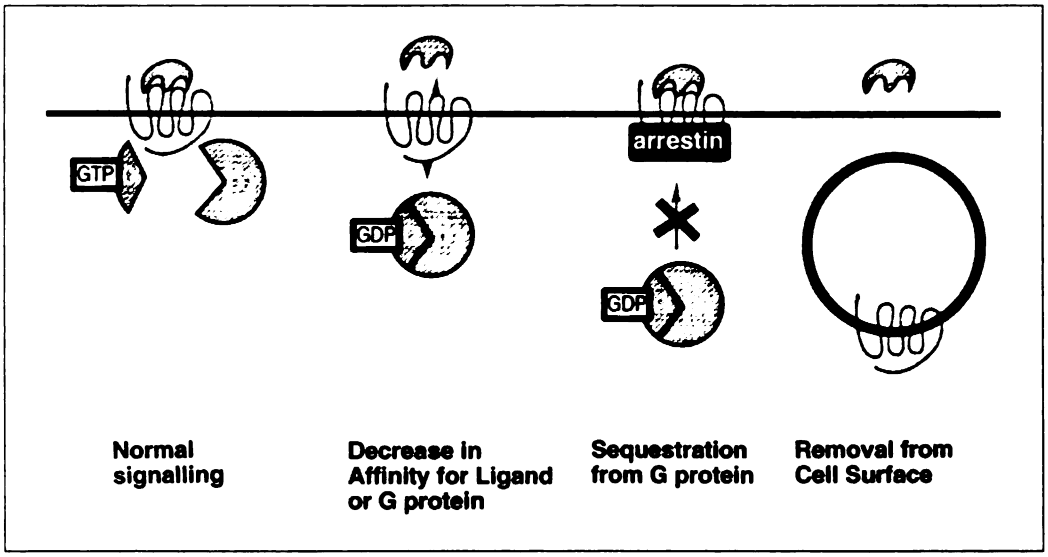
GTP
GDP
arrestin
GDP
Normal signalling
Decrease in Affinity for Ligand or G protein
Sequestration from G protein
Removal from Cell Surface

Fig. 4 Adaptation at the level of the G-protein-coupled receptor. G-protein-coupled receptor signalling can be downregulated through a decrease in affinity for ligand or G protein (some types of receptor phosphorylation produce these effects), sequestration of receptor from G protein (arrestin is thought to operate in this fashion), or removal of the receptor from the cell surface (for example, clathrin-mediated receptor internalization). For comparison, normal GPCR signalling is shown at far left.

by activating rhodopsin kinase, a member of a large class of G-protein receptor kinases (GRKs). The kinase, in turn, phosphorylates rhodopsin on multiple serine and threonine residues. This phosphorylation marks the receptor for binding by another protein, arrestin, which sterically prevents rhodopsin from coupling to and activating G_t. For other GPCRs, such as the β-adrenergic receptor, βγ helps to recruit the GRK (e.g. βARK) to the receptor (10). In these cases, members of the arrestin family act not only to turn off the GPCR but also as adapters between the GPCR and clathrin, leading to internalization of the GPCR (but not of the G protein) (11). Thus the GRK/arrestin mechanism, activated by the GPCR in combination with βγ, uncouples the GPCR from the G protein not only by sterically blocking their association but also by physically separating the GPCR from the G protein (Fig. 4).

Does eukaryotic chemotaxis require a GRK/arrestin mechanism for adaptation? Although GPCRs induce phosphorylation of chemotactic receptors in both neutrophils and *Dicytostelium*, available evidence indicates that neither receptor phosphorylation nor receptor internalization is necessary for adaptation during chemotaxis. For instance, chemotaxis and adaptation of multiple cellular responses, including actin polymerization and activation of adenylyl and guanylyl cyclases, are unaffected in *Dictyostelium* cells whose wild-type cAMP receptor is replaced by a cAMP receptor lacking sites for phosphorylation (12). Similarly, mutation of all the carboxy-terminal serine and threonine residues in the CCR2B chemokine receptor markedly impairs ligand-dependent internalization of this GPCR but has no effect on its ability to mediate chemotaxis in pre-B lymphocytes (13), and phosphorylation of the *N*-formyl peptide receptor is required for receptor internalization but not chemotaxis of myeloid cells (14).

It is likely that cells can use alternative mechanisms to uncouple GPCRs from G proteins. One such mechanism would reverse the order of regulation so that the uncoupler and not the receptor is marked or regulated (in contrast to GRK-mediated desensitization where the receptor to be uncoupled is marked by phosphorylation). Imagine, for instance, that GPCR activation leads to localized activation of an uncoupler, making it able to bind the GPCR and prevent activation of the G protein. Alternatively, GPCR activation could induce signals that alter the GPCR's microenvironment (physical location or interaction with the actin cytoskeleton) and thereby alter signal transduction from GPCR to signalling components downstream. Indeed, GPCRs and G proteins are reported to interact differently with the actin cytoskeleton of stimulated neutrophils, and certain signalling cascades are potentiated by depolymerization of the actin cytoskeleton.

Other adaptation mechanisms could act directly on the G protein. Strong candidates for roles in such a mechanism belong to the growing family of RGS (regulators of G-protein signalling) proteins, which increase the rate of GTP hydrolysis by α_i and α_q, thereby decreasing the duration of G-protein activation and the intensity of the transmitted signal. The activity of an RGS is essential for the GPCR-mediated mating response of the budding yeast, *Saccharomyces cerevisiae*. During mating this organism responds to a pheromone gradient by orienting its polarity toward the source of pheromone, the mating partner (described in Chapter 2). Mutational inactivation of the yeast RGS protein renders the mating response pathway hypersensitive, resulting in saturation of the response at very low concentrations of pheromone and consequently preventing the organism from mating with partners that express a normal amount of pheromone. However, such a yeast cell *can* mate with partners expressing very low concentrations of pheromone and can correctly orient its polarity in response to a sufficiently low pheromone gradient (15, 16).

While these results suggest that the RGS protein sets the *perceived* intensity of the pheromone signal within a range that the yeast cell can interpret, they do not tell us whether the RGS machinery participates in actual adaptation, defined as *a stimulus-triggered change* in responsiveness. It is quite likely that extracellular signals do in fact regulate the activities of RGS proteins, including that of *S. cerevisiae*. For instance, most mammalian RGS proteins contain large N-terminal domains, separate from the GTPase-stimulating RGS domain itself; these domains appear to control the subcellular location of RGS activity and may, in some cases, make the RGS protein more effective in damping signals mediated by specific receptors. The N-terminal domain of the yeast RGS protein probably contains a site of regulation, as suggested by a point mutation in that domain which produces a dominant increase in the protein's RGS activity and a decrease in pheromone signalling (17). In summary, RGS proteins furnish an ideal mechanism for damping the signal intensity perceived by a cell, a mechanism that should allow a cell to expand its dynamic range of responsiveness, perhaps in a stimulus-dependent fashion. Very little is known about the importance of RGS signalling for chemotaxis. The observation (18) that certain overexpressed

RGS proteins impair chemotaxis of leukocytes identifies RGS proteins that can inhibit signals, but does not address the actual role of any RGS protein in regulating chemotaxis. Given the large number of different RGS proteins, specifying their individual roles by studying loss-of-function mutations appears a daunting task. As an alternative, a more general role of RGS proteins could be defined in experiments requiring that chemotaxis be mediated by a mutant Gα_i that cannot interact with known RGS proteins (19) (for instance, by making the mutant resistant to PTX and using PTX to inactivate endogenous α_i).

Proteins that sequester α or (more likely) $\beta\gamma$ would also decrease transmission of the chemotactic signal to downstream effectors. Such proteins certainly exist, as shown by identification (20–23) of $\beta\gamma$-sequestering proteins in *S. cerevisiae* (where their role in regulating signals is poorly understood). Other evidence raises the possibility that chemoattractants can act at a level downstream of the G protein to induce adaptation. For instance, preincubation of *Dicytostelium* with cAMP decreases the ability of the hydrolysis-resistant GTP analogue GTPγS (which directly activates G protein in a receptor-independent fashion) to activate adenylyl cyclase. This effect could reflect either adaptation downstream of the G protein or a decrease in the pool of G protein available for stimulation. Similarly, stimulation of neutrophils with IL-8 or C5a decreases FMLP-mediated IP_3 production without affecting the ability of the FMLP receptor to activate G protein, as determined by a GTPγS-binding assay (24).

4. Interpreting the chemotactic gradient

To mount an appropriately graded response, most cells need only decide *how much signal* they are receiving. In addition, chemotaxis requires a cell to decide *where the signal is coming from,* by comparing signal intensity over the cell's entire surface, in which some areas are exposed to greater concentrations of chemoattractant than others. Consider, for instance, two cells at different distances from a point source of chemoattractant (Fig. 5). Both cells move toward the source and exhibit greater actin polymerization and accumulation of filamentous actin on their up-gradient edges (as discussed in a later section). The down-gradient edge of cell 1 shows morphology characteristic of a trailing edge, despite the fact that it is exposed to a higher concentration of chemoattractant than the up-gradient edge of cell 2, in which the characteristic asymmetry of the actin cytoskeleton directly parallels that seen in cell 1. In other words, behaviour of any portion of a cell depends not only on the absolute intensity of the signal it receives, but also on that intensity *relative* to the intensity of signals received by other portions of the cell. Such comparisons require communication between different regions of the cell surface. What is the nature of this communication, and what is the basis of the comparison? At which level(s) of the signalling cascade is this comparison performed?

4.1 Asymmetrical intracellular signals

To understand how cells interpret the chemotactic gradient, it would be helpful to pinpoint the level at which asymmetry first appears in the signalling cascade between

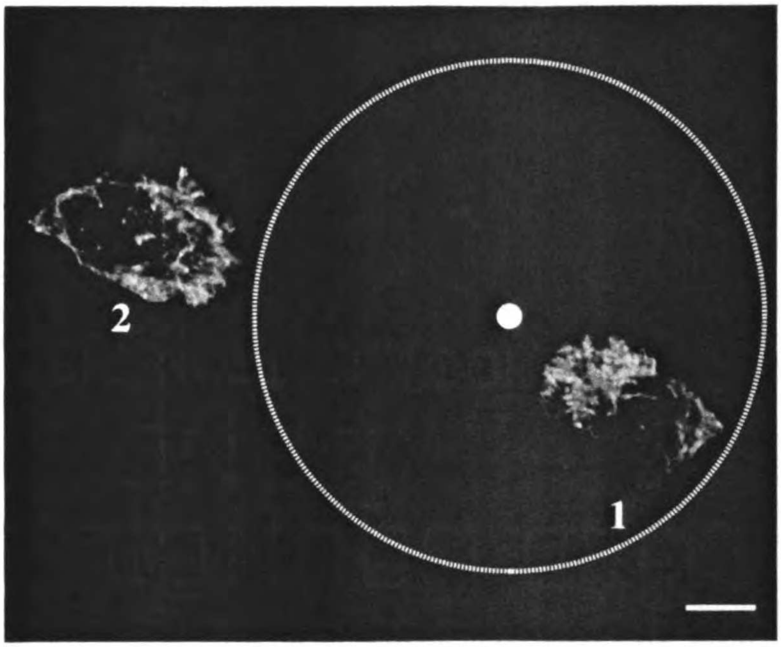

Fig. 5 Actin staining of two neutrophils converging on a point source of chemoattractant. The morphology of a region of a cell depends on signal intensity elsewhere in the cell rather than on the absolute level of chemoattractant. Thus the down-gradient region of cell 1 exhibits less actin ruffling than the up-gradient region of cell 2, despite the fact that the down-gradient region of cell 1 is exposed to a higher concentration of chemoattractant (for relative distances, note the position of the circle centred on the point source of chemoattractant). Bar = 5 μm.

ligand detection and actin polymerization. Are the primary sensors, the GPCRs, asymmetrically localized? Despite conflicting inferences drawn from observations of fixed mammalian cells, chemotactic GPCRs tagged with green fluorescent protein (GFP) are distributed uniformly on the surfaces of living *Dictyostelium* (25) and neutrophils (26) during chemotaxis. In contrast, actin accumulation, actin polymerization, and a variety of actin-associated proteins are asymmetrically distributed during chemotaxis (discussed in the final section). Thus the decision for directional polarization must occur at a level between localization of the GPCR and the actin cytoskeleton.

If receptor localization is uniform during chemotaxis, what about receptor *activity*? Does activity of the receptor and/or the G protein constitute a direct readout of the concentration of extracellular ligand, or does it exhibit signs of local amplification at the leading edge? To address this question, we need a spatial readout of receptor activity, distinct from the actin cytoskeleton and proximal to it in the signalling cascade. One approach is to determine the subcellular distribution of a GFP-tagged protein that is recruited to the plasma membrane upon activation of the GPCR. If the site for docking of the GFP-tagged probe is sufficiently discrete, it can be used as an indirect spatial indicator of GPCR activity.

Several properties of a *Dicytostelium* signalling protein, the cytosolic regulator of adenylyl cyclase (CRAC) made it a useful probe for GPCR activation and for the location of free βγ generated in response to a chemotactic stimulus. *Dicytostelium* cells genetically lacking CRAC are capable of chemotaxis toward cAMP, but cannot activate adenylyl cyclase, increase cAMP secretion, or aggregate normally (27). G-protein activation in wild-type *Dicytostelium*, in response either to extracellular cAMP or to GTPγS, induces CRAC to translocate from the cytosol to the plasma membrane (28). The pleckstrin homology (PH) domain of CRAC is sufficient for stimulus-mediated recruitment to the plasma membrane. It is likely that free βγ or a signal generated in response to βγ recruits CRAC to the plasma membrane, because GTPγS induces CRAC translocation to the plasma membrane in *Dicytostelium* cells genetically lacking every component of the pathway *except* Gβ.

On this basis, GFP-tagged CRAC was used as a probe—direct or indirect—for the location of free βγ generated by a chemotactic stimulus (29). In cells stimulated with a uniform concentration of cAMP, CRAC–GFP transiently translocates to the plasma membrane in a symmetrical fashion and returns to the cytosol within 1–3 minutes. Increases in chemoattractant concentration elicit repeated cycles of symmetrical recruitment and release of CRAC–GFP from the plasma membrane. In contrast, gradients of chemoattractant recruit CRAC–GFP to the up-gradient surface of the cells; the asymmetry of this recruitment substantially exceeds the asymmetry of receptor occupancy, inferred from the chemoattractant's extracellular concentration (Fig. 6). The apparent lack of GPCR-generated signalling at the back of the cell depends not on an absolute inability to respond, but instead on the relative intensities of signals in different parts of the cell, as inferred from a simple observation (29): replacement of the chemotactic gradient by a high and *uniform* concentration of chemoattractant causes CRAC–GFP to be recruited symmetrically to the entire cell surface.

Thus GPCRs are uniformly distributed through the plasma membrane during chemotaxis, but their activity is NOT. Asymmetry of the CRAC–GFP signal in excess of the asymmetry of external ligand concentration strongly suggests that the cells' perception of the gradient is amplified at the level of the GPCR or the G protein. Moreover, signalling on the down-gradient surface must somehow be inhibited, because this surface is exposed to chemoattractant but does not show a response to the GPCR. A second probe constructed from a PI3 kinase effector, the PH domain of AKT tagged with GFP, shows similarly asymmetrical patterns of apparent GPCR activity in both *Dicytostelium* (30) and neutrophils (105).

4.2 Initiation and maintenance of the asymmetrical signal: models

How might signals communicated between different regions of the plasma membrane induce apparent inhibition of the chemotactic signal at the down-gradient

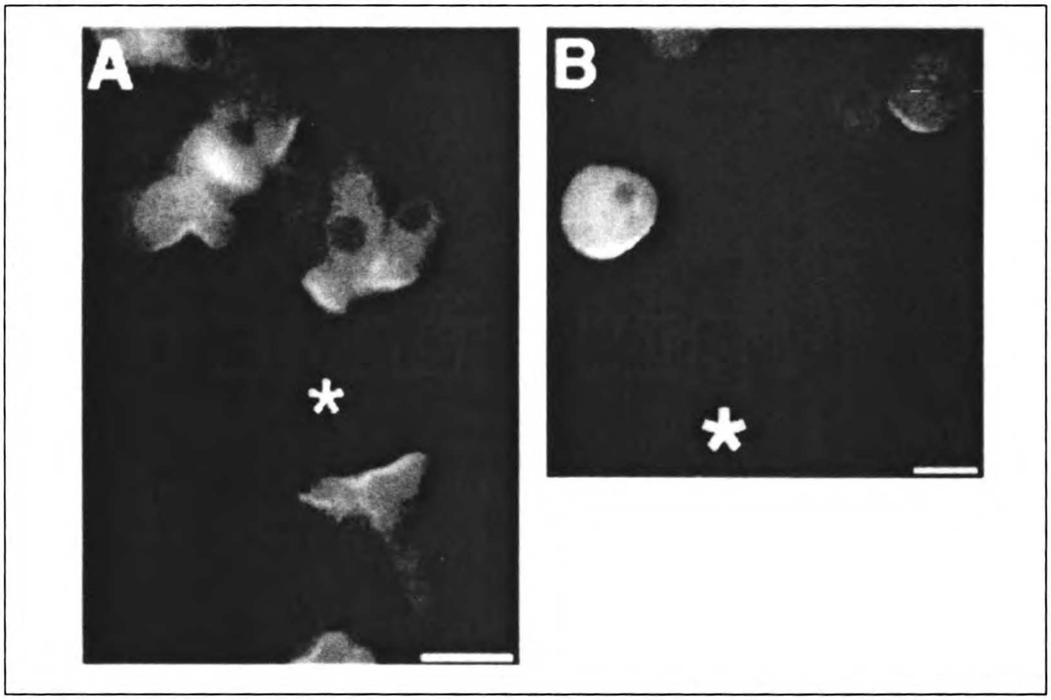

Fig. 6 (A) CRAC–GFP is exclusively found at the leading edge of chemotaxing *Dictyostelium* amoebae. CRAC-null cells expressing CRAC–GFP were exposed to a gradient of chemoattractant generated by a micropipette containing 1 μM cAMP (asterisk). The image represents cells 90 seconds after exposure to the micropipette. Bar = 7 μm. (B) *Dictyostelium* amoebae can sense chemoattractant gradients in the absence of actin polymerization. CRAC-null cells expressing CRAC–GFP were treated with latrunculin-A (final concentration 0.5 μM) for 15 min and then exposed to a micropipette containing 1 μM cAMP (asterisk) for 65 seconds. Bar = 12 μm.

surface? One potential mechanism would rely on exquisitely well-tuned *global inhibition* (31). Suppose that the sum of GPCR activities produces a rapidly diffusing global inhibitor, which reduces, by an absolute amount, the signal transmitted by each GPCR. If this inhibition were sufficiently well-tuned, only the GPCRs on the up-gradient surface would exhibit net activation (Fig. 7). This conceptually straightforward model requires relatively simple machinery—a diffusible regulator that controls responsiveness to the signal. A disadvantage is that regulation by inhibition alone may not amplify small differences effectively enough.

A potentially more effective mechanism combines *global inhibition* with *local enhancement* of the signal. This more complex model is thought to explain how developing organisms solve a similar problem in using gradients of morphogens to create polarity and sculpt the shapes of organs and tissues. In order to produce *exactly one* signalling organizer at the site of the maximal concentration of a morphogen in a gradient (or even in the presence of an initially uniform concentration of morphogen), each responding cell in the tissue produces both a *long-range inhibitor* of activity and a *short-range enhancer* of activity. The combination of positive and negative regulation results in positive feedback that amplifies small initial asymmetries in morphogen concentration (32–34).

Applying this model to chemotaxis, we focus our hypothesizing lens on a single cell, rather than on a developing tissue (Fig. 7). GPCRs at the plasma membrane of a single cell generate both a global inhibitor of signalling AND a local activator of signalling (which might, for example, *inhibit inhibition* locally). It is important to note that local enhancement is not simply the local activation of G proteins by GPCRs but is a layer of regulation superimposed on normal signalling whereby each activated

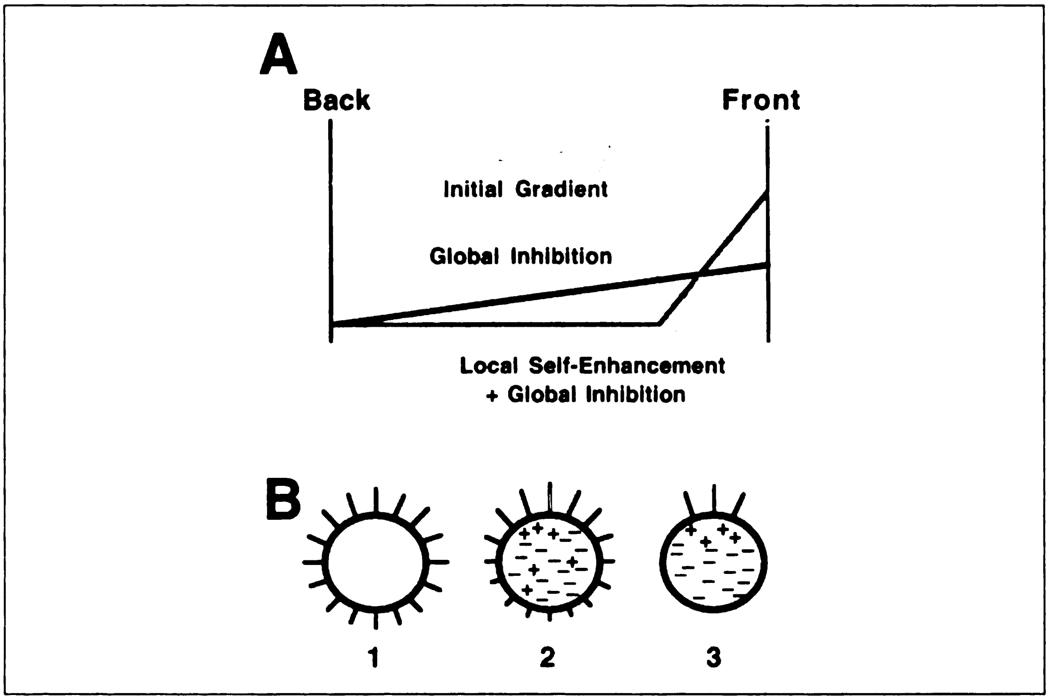

Fig. 7 (A) Comparison of types of signal processing for gradient interpretation. The horizontal axis represents the position along a cell exposed to a chemotactic gradient to the right. The vertical axis represents the intensity of an intracellular signal generated by the chemoattractant. The light grey line represents the signal in response to the initial gradient in the absence of processing. The black line represents the signal following global inhibition. Note that the percentage difference in signal from front to back of the cell increases, but the absolute difference does not. The dark grey line represents the signal following global inhibition and local self-enhancement. Note that both the percentage and absolute difference from front to back of the cell increase. (B) Spatial example of global inhibition and local self-enhancement amplification of a gradient. Each activated receptor generates a global inhibitor of signalling (–) and a local self-enhancer of signalling (+), with the net result that each receptor favours signalling in its own region and inhibits signalling elsewhere. It is important to note that local enhancement is not simply the local activation of G proteins by GPCRs but is a layer of regulation superimposed on normal signalling, whereby each activated GPCR increases its own activity in a short-range fashion. Lines outside of the circles represent the level of intracellular signal generated in response to the chemoattractant. (1) Cell initially exposed to a chemotactic gradient experiences slight asymmetry in intracellular signalling. (2) Global inhibition and local self-activation generated by each receptor dramatically amplify the difference in intracellular signalling across the cell when iterated over time (3).

GPCR increases its own activity in a short-range fashion. To make the model more concrete, imagine possible biochemical mechanisms in which the activated GPCR stimulates synthesis of a rapidly diffusible global inhibitor that damps signalling throughout the cell—by stimulating an appropriate RGS protein, by sequestering free G-protein βγ subunits, or by otherwise uncoupling the GPCR from its G-protein target. Localized signal enhancers would act in the opposite direction—for instance, by inducing phosphorylation of an RGS protein to decrease its ability to accelerate GTP hydrolysis by the α_i subunit.

Available evidence restricts the number of potential mechanisms for either global inhibition or local enhancement of the signal. Neither type of regulation is likely to be mediated solely by altering localization, phosphorylation, ligand affinity, or internalization of GPCRs, for reasons outlined above; similarly, neither is likely to be exerted solely at the level of actin polymerization (see below). Note, however, that our emphasis on regulation at the level of receptor and G protein depends on an assumption that may not be correct. This assumption is that free βγ in the plasma membrane of cells exposed to a chemotactic gradient *directly* mediates recruitment of the cytoplasmic proteins used as markers for receptor activity. Several observations suggest that the asymmetrical signals studied so far may instead reflect regulation of signalling events downstream of GPCR and G protein. CRAC–GFP is recruited normally to macropinosomes, even in *Dictyostelium* cells lacking Gβ (C. Parent and P. Devreotes, unpublished). AKT–GFP, a marker recruited by chemoattractants to the up-gradient edges of both *Dictyostelium* (30) and neutrophils (105), is considered a specific probe for $PI(3,4)P_2$ and $PI(3,4,5)P_3$, rather than for βγ.

Wherever regulation takes place, the simple global inhibition model exhibits two disadvantages in comparison to the combined inhibition/enhancement model. First, it can generate a robustly asymmetrical signal only by exquisite fine tuning and thresholding; to allow signalling solely on the cell's up-gradient edge, the inhibitor must damp the signal by *precisely* the right amount to drop the down-gradient (but not up-gradient) edge below the threshold for response. Quantitatively precise inhibition is not as crucial in a model that incorporates positive feedback as well. Secondly, it is difficult to imagine how a model based on global inhibition alone could account for the ability of neutrophils in a *uniform concentration of ligand* to establish unequivocal polarity of their actin cytoskeletons. Indeed, a uniform concentration of chemoattractant can also recruit the GFP-tagged PH domain of AKT asymmetrically to the leading edge of a neutrophil (105). In contrast, as in a developing tissue responding to a morphogen, the combination of positive and negative signals may not merely generate appropriate polarity more efficiently in response to a small gradient, but may also generate random polarity in response to small stochastic fluctuations in a uniform concentration of ligand.

This apparent advantage of the combined inhibition/enhancement model also implies a potential disadvantage—that is, it might generate an internal gradient of signal intensity so strong that the cell finds it difficult to change polarity in response to changing external conditions. Slight variations in the model could make it easier to change polarity (106). For instance, a cell could 'clean the slate' by cyclically destroying the strong amplified peak of internal activity to allow a different interpretation of the external gradient during the next activation cycle; this could account for the cyclical pattern of receptor activation in *Dicytostelium* during chemotaxis, as assayed by cycles of recruitment and dissociation of CRAC–GFP during chemotaxis (29). Alternatively, it may be easier to move an amplified internal peak of activity than to destroy it. In *Dictyostelium* cells unable to polymerize actin, CRAC–GFP redistributes smoothly in response to a moving external point source of chemoattractant, without exhibiting cyclical turn-off and turn-on of the signal (29). Similarly, neutrophils tend to reorient an existing front rather than to generate a new front in response to a moving point source of chemoattractant (35).

Neutrophils and *Dicytostelium* cells are unlikely to interpret gradients using a simple temporal mechanism, like that of prokaryotes, because they pursue a moving point source of chemoattractant smoothly (35, 36), rather than approach it in a biased random walk. In contrast to the simple temporal mechanism of gradient interpretation in which cells compare levels of global signalling before and after movement of the entire cell, for the 'pilot pseudopodia model' cells compare levels of signalling at each point of their surface during extension of projections—the region of the surface experiencing the largest *temporal* increase in signalling (i.e. extending maximally up the chemotactic gradient) exhibits continued extension. The pilot pseudopodia model is difficult to distinguish behaviourally from spatial gradient interpretation in which the region of the cell surface experiencing maximal signalling (in an absolute sense) becomes the leading edge. None the less, one straightforward prediction is that temporal—but not spatial—interpretation of a stable gradient should require movement of the cell, or part of it. In contrast to this prediction, a stationary neutrophil extends its first projection towards a point source of chemoattractant (36). Moreover, CRAC–GFP is recruited preferentially to the up-gradient edge of *Dicytostelium* cells that are paralysed by a toxin, latrunculin, that causes depolymerization of the dynamic actin cytoskeleton, inhibits actin polymerization, and prevents actin-dependent morphological changes; the GFP-tagged PH domain of AKT shows similarly asymmetrical recruitment to the plasma membrane of latrunculin-treated neutrophils (105). Thus interpretation of the gradient takes place upstream of actin polymerization and does not require motility, suggesting that the primary interpretation of a gradient is spatial, although an additional temporal mechanism cannot be ruled out.

Interpretation of a pheromone gradient by *S. cerevisiae* may differ from interpretation of chemoattractant gradients by neutrophils and *Dictyostelium*. Whereas GPCRs in the latter cells are distributed uniformly throughout the cell surface during chemotaxis (25, 26), exposure of yeast cells to pheromone induces a massive internalization of mating factor receptors, followed by synthesis of new receptors which later reappear at the tip of the mating projection. Moreover, depolymerization of the yeast actin cytoskeleton inhibits proper induction of morphological polarity and asymmetrical accumulation of mating factor receptors and other polarity markers in response to stimulation with uniform pheromone (37). In contrast, as we have seen, loss of actin polymerization does not prevent asymmetrical signalling polarity (i.e.

distribution of markers for receptor activation) in either neutrophils or *Dicytostelium*. Thus development of polarity in yeast cells appears to require actin rearrangements, perhaps as a way of reinforcing asymmetrical distribution of receptors, while *Dicytostelium* and neutrophils polarize without rearranging the actin cytoskeleton or redistributing GPCRs. An important caveat: the yeast experiments were performed in a uniform concentration of pheromone, rather than (like neutrophils and *Dicytostelium*) in a gradient, raising the possibility that a pheromone *gradient* could induce yeast cell polarity even in the absence of the actin cytoskeleton.

5. Polarity effectors: Rho-GTPases

Once a cell has interpreted the gradient, how does it point itself in the right direction and move? Rapidly accumulating evidence indicates that members of the family of Rho-GTPases transmit spatial interpretation of the chemoattractant gradient from GPCRs and trimeric G-proteins at the cell surface to the ultimate effectors of polarity and motility. In *Dictyostelium*, neutrophils, and virtually every motile eukaryotic cell, these effectors regulate polymerization of actin and rearrangements of the actin cytoskeleton. Deferring more detailed description of actin polymerization to the next section of this chapter, here we describe the roles of three Rho-GTPases—Cdc42, Rac, and Rho—in chemotaxis. Rapidly accumulating evidence is beginning to identify parts of the machinery responsible for regulating each GTPase and to define the mechanisms underlying their intertwined but distinct functions in rearranging the actin cytoskeleton. We begin by introducing the GTPases and their effects on actin polymerization in cells and cell extracts, move to genetic analysis of their roles in intact cells responding to a gradient of chemoattractant, and finally focus in greater detail on each individual member of the family.

5.1 Rho-GTPases in cell extracts

Early evidence that GTPases regulate actin polymerization in chemotactic cells came from experiments in which a hydrolysis-resistant GTP analogue, GTPγS, was introduced into neutrophils (by electroporation or permeabilization of the plasma membrane): the analogue, which directly activates G proteins, induced polymerization of actin. Development of a cell-free system, in which GTPγS stimulates actin polymerization of cytosolic extracts from neutrophils or *Dictyostelium* cells (38), opened the way to identifying the specific G proteins involved. The effect of GTPγS was not impaired in cytosol from *Dictyostelium* mutants lacking Gβ, indicating that one or more G proteins distinct from the heterotrimers suffice to support actin polymerization. These G proteins belong to the Rho family of small GTPases, as indicated by experiments in which GTPγS-induced actin polymerization is blocked by three classes of inhibitors (38–40): *Clostridium difficile* toxin (which glucosylates Rho-GTPases and prevents their interaction with effectors), Rho-GDI (which prevents nucleotide exchange and insertion of Rho-GTPases into membranes), or dominant-negative constructs (which are thought to sequester proteins that activate the Rho-GTPases).

First identified by analysing mutations in *S. cerevisiae* (41), the Rho family of GTPases is implicated in a vast array of cell functions, including modulation of the actin and tubulin cytoskeletons, adhesion, secretion, transcription, cell proliferation, and neoplastic transformation. Like other GTPases in the Ras superfamily, Rho-GTPases cycle between GTP- and GDP-bound forms with the assistance of a variety of proteins which enhance GTP-loading (guanine nucleotide exchange factors, or GEFs) or GTP-hydrolysis (GTPase activating proteins, or GAPS), and their GTP- and GDP-bound forms interact with different subsets of effectors and regulatory proteins. Specific point mutations produce Rho-family proteins that are constitutively active (GTP-bound) or inactive (GDP-bound).

The corresponding dominant-positive and dominant-negative effects of such Rho mutants helped to identify their effects on the actin cytoskeleton. Injection of different constitutively activated Rho-GTPases into tissue-culture cells produces distinctive rearrangements of the actin cytoskeleton: activated Cdc42 induces thin finger-like projections, called filopodia; activated Rac induces sheet-like ruffles, called lamellipodia; and activated Rho induces formation of actin bundles, called stress fibres (42). Dominant-negative versions of these proteins inhibit the corresponding actin rearrangements produced by extracellular stimuli (42). (As described below and in Chapter 2, yeast and mice genetically lacking specific members of the Rho family are beginning to extend our understanding of the roles played by these proteins in cell polarity and chemotaxis.)

So far, cell-free extracts have proved useful for studying effects of Cdc42 on actin polymerization, but not for understanding biochemical roles of other Rho family members or for analysing the links that connect activation of Rho proteins to ligand-stimulation of GPCRs in the plasma membrane. In cytosolic extracts from neutrophils and *Dictyostelium*, activated Cdc42 induces actin polymerization and dominant-negative Cdc42 blocks GTPγS-induced actin polymerization, but the corresponding Rac mutants have no effect—despite the fact that activated Rac induces actin polymerization in whole or permeabilized cells (see below).

5.2 Rho-GTPases in whole cells

Chemotaxis of macrophages, which are larger than neutrophils and more accessible to microinjection of foreign proteins, provides a useful experimental model for studying the effects of mutant Rho-GTPases. Videomicroscopy allows quantitative observation of individual microinjected cells migrating up a gradient of a chemoattractant (43). Dominant-activated versions of Cdc42, Rac, and Rho all inhibit cell motility and chemotaxis, but exert different effects on cell morphology: activated Cdc42 induces filopodia around the entire cell periphery, activated Rac induces ruffling throughout the cell periphery, and activated Rho induces cell rounding and inhibits cell adhesion (43) (Fig. 8). Similarly, dominant-negative versions of the same GTPases inhibit chemotaxis but exert different effects on cell motility and morphology: dominant-negative Cdc42 randomizes the direction of motility of cells exposed to a chemoattractant, but the cells show polarized morphology and increased

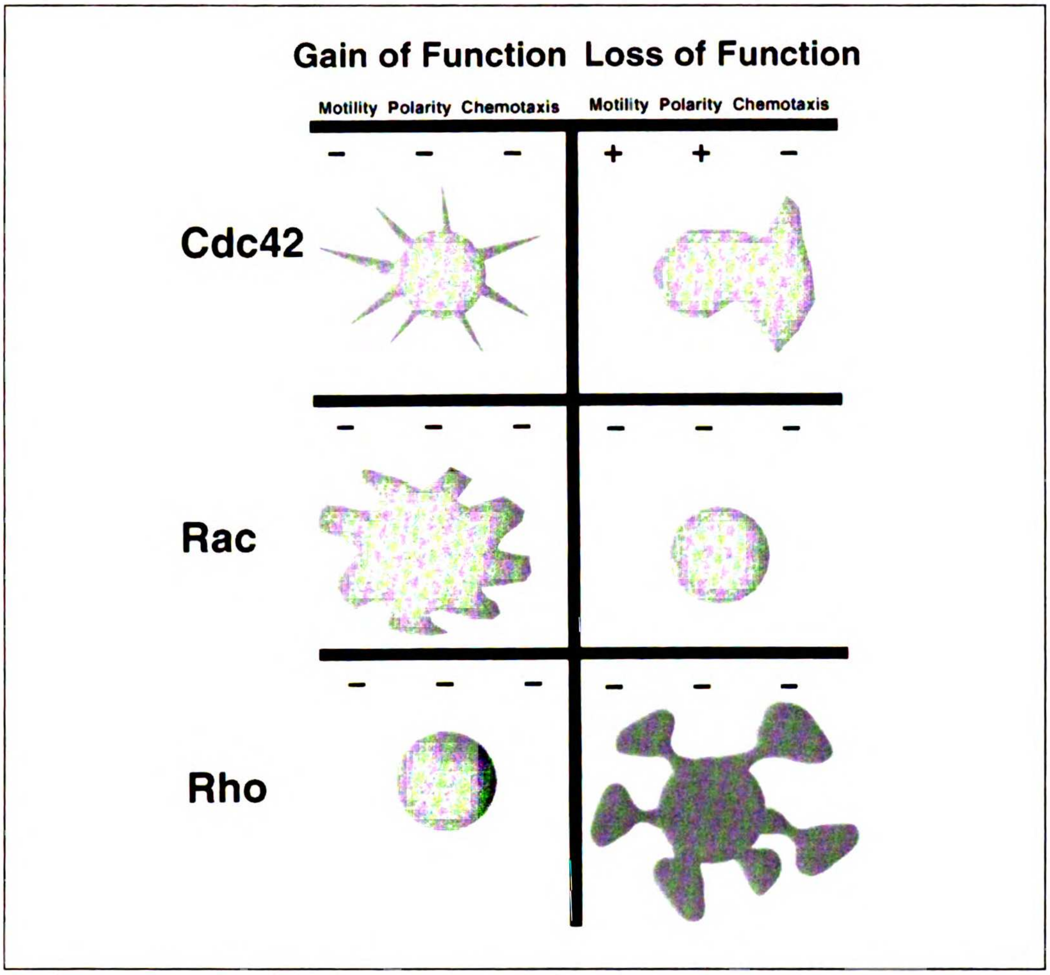

Fig. 8 Phenotypes of macrophages for manipulations that effect gain or loss of function for Rho-GTPases. All phenotypes represent macrophages injected with dominant-activated or dominant-negative versions of Rho-GTPases, except for the Rho loss-of-function studies, which were performed with the botulinum C3 toxin, which inactivates endogenous Rho.

motility (43). Dominant-negative Rac inhibits both migration and morphological cell polarity. Dominant-negative Rho produces a dendritic cell morphology, with many extensions in all directions. A consistent interpretation of these observations is that Cdc42 matches cell polarity to the gradient of chemoattractant (perhaps in part by regulating Rac), while Rac plays a key role in chemoattractant-induced actin polymerization and generation of lamellipodia, and Rho is involved in cell adhesion and retracting aberrant cell projections (perhaps by modulating myosin, the actin motor protein; see below).

How does activation of a GPCR regulate activities of the Rho-GTPases? Here the most comprehensive answer comes from genetic analysis of the role of Cdc42 in the pheromone response of *S. cerevisiae*. Pheromone activation of the yeast GPCR induces release of $\beta\gamma$, which binds to an adaptor protein, Far1. Far1 also interacts with Cdc24, a GEF that activates Cdc42. Genetic manipulations that prevent interaction of $\beta\gamma$, Far1, and Cdc24 prevent activation of Cdc42, recruitment of this GTPase to the cell surface, and oriented polarization in response to gradients of pheromone (44–46) (for more details, see Chapter 2). In larger eukaryotes, a number of specific and non-specific GEFs are candidates for transmitting signals from GPCRs to Rho-family GTPases. A direct biochemical mechanism is understood in only one case, however: a GEF for Rho, called p115 RhoGEF, also serves as an RGS for α_{12} and α_{13} (i.e. it increases the rate at which these α subunits hydrolyse GTP). Moreover, association of α_{13} with p115 RhoGEF activates its GEF activity (47). The specific GEFs responsible for activating Rac and Cdc42 in response to specific stimuli are not yet identified.

Knockout mice lacking a Rac protein, Rac2, reveal the crucial importance of this Rho-GTPase in chemotaxis (48). Neutrophils from these mice show marked defects in chemoattractant-induced actin polymerization and chemotaxis. (Embryonic lethality, the quite different phenotype of mice genetically lacking another Rac, Rac1, probably reflects the more ubiquitous expression of Rac1; Rac2 is restricted to the immune system.)

5.3 Cdc42 and actin polymerization

How do Rho-GTPases regulate rearrangements of the actin cytoskeleton? Here we understand the biochemical machinery best for Cdc42, principally because of this protein's ability to stimulate actin polymerization in cytosolic extracts (Fig. 9). Cdc42 does not induce pure G-actin to polymerize, but can do so in the presence of protein fractions prepared from cytosol of frog eggs; one such fraction contains a heptameric protein complex, called Arp2/3 (49). This complex, first identified as the profilin-binding complex of *Acanthamoeba* (50) and conserved from yeast to humans (51, 52), contains two actin-related proteins, Arp2 and Arp3 (50). Structural models position amino acids required to interact with actin at the barbed ends of Arp2 and Arp3, suggesting that the complex acts as a nucleus for barbed-end actin polymerization (53) (the biochemistry of actin polymerization is described more fully below). Indeed, the human Arp2/3 complex is necessary and sufficient to mediate ActA-dependent actin polymerization at the surface of an intracellular bacterial pathogen, *Listeria monocytogenes* (54, 55), where the complex stimulates nucleation of actin filaments that elongate only from their barbed ends (56, 57). Defective actin-dependent functions in conditional Arp2 and Arp3 mutants (52, 58, 59) indicate a critical role for the Arp2/3 complex in controlling the yeast actin cytoskeleton. Consistent with the notion that Cdc42 and the Arp2/3 complex act in a common pathway, function-blocking antibodies to the complex inhibit Cdc42- or GTPγS-mediated actin polymerization in *Acanthamoeba* extracts (60). Because cytosol extracts can serve as models only for some types of actin polymerization, this observation does not indicate whether the Arp2/3

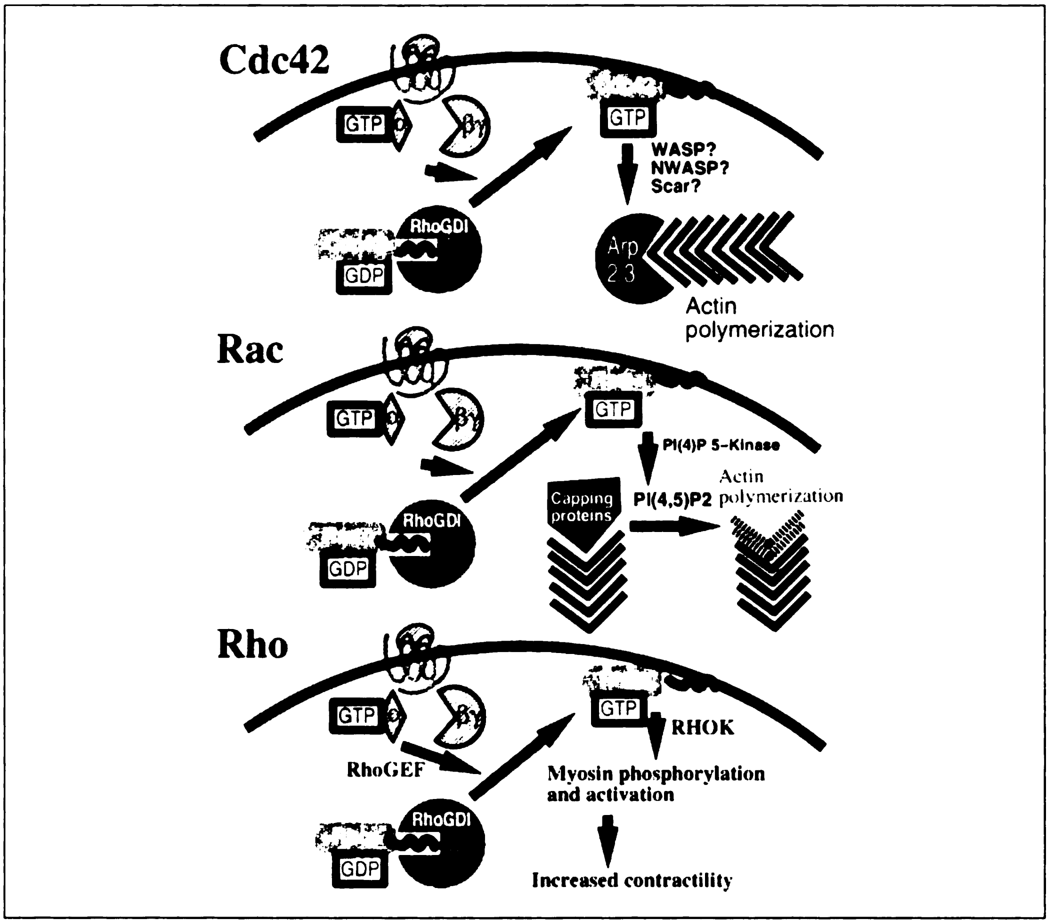
Cdc42
GTP
βγ
GTP
WASP?
NWASP?
Scar?
RhoGDI
GDP
Arp
2 3
Actin
polymerization
Rac
GTP
βγ
GTP
PI(4)P 5-Kinase
Actin
polymerization
Capping
proteins
PI(4,5)P2
RhoGDI
GDP
Rho
GTP
βγ
GTP
RHOK
RhoGEF
Myosin phosphorylation
and activation
RhoGDI
GDP
Increased contractility

Fig. 9 Modulation of the actin cytoskeleton through activation of Cdc42, Rac, and Rho. In their inactive states, Cdc42, Rac, and Rho are in their GDP-bound forms and reside in the cytoplasm with their lipid tails embedded in Rho-GDIs, proteins that prevent both GTP-charging and membrane association of the Rho-GTPases. Upon receptor activation, the Rho-GTPases are charged with GTP and driven into a membrane-bound pool. In general, it is not known whether dissociation from Rho-GDI or activation of exchange factors is the regulated step for Rho-GTPase activation. It is not known what product of receptor activation leads to activation of Cdc42 and Rac, but α_{13}–GTP is known to directly activate the exchange factor for Rho. Activated Cdc42 induces *de novo* actin polymerization by causing activation of the Arp2/3 complex. Activated Rac induces liberation of barbed end of actin filaments by stimulating formation of the phosphoinositide $PI(4,5)P_2$ which removes capping proteins from the barbed end of actin filaments. Rac is also thought to stimulate Arp2/3 complex activation and inhibit myosin-based contractility (see text). Activated Rho induces cell contractility by promoting activation and cortical association of the actin motor protein, myosin.

complex is necessary for actin polymerization induced by other signals, including Rac activation. In other cells, overexpression of protein fragments postulated to interfere with recruitment of the Arp2/3 complex does prevent actin rearrangements in response to activation of Rac and Rho, as well as Cdc42 (61), but the specific target of inhibition in these experiments is difficult to assess.

By itself the Arp2/3 complex nucleates actin polymerization rather weakly in the absence of activating proteins, such as the ActA protein of *L. monocytogenes* (56, 57). Three eukaryotic proteins that mimic the potentiating effect of ActA are candidates for roles as important links between Cdc42 activation and regulation of the actin cytoskeleton: the mammalian Wiskott–Aldrich syndrome protein (WASP, which is expressed predominantly in haematopoietic cells) (55), N-WASP (a close relative expressed more widely) (62), and a WASP-related protein of *Dictyostelium*, Scar-1 (63). Scar-1 mutants in *Dicytostelium* show defects in actin polymerization and chemotaxis (64). WASP mutations cause the human immunodeficiency disorder of patients with the Wiskott–Aldrich syndrome, whose haematopoetic cells exhibit a variety of defects related to actin function, including defects in monocyte chemotaxis, platelet function, T-cell signalling, and actin polymerization (65 and references therein). Injection of WASP into cultured cells induces actin polymerization (66), and N-WASP potentiates Cdc42-induced formation of filopodia in neuronal cells (67).

The combined efforts of several laboratories are just beginning to explore *how* these proteins link Rho-GTPases to actin polymerization of actin. A G-protein-binding domain (GBD) enables WASP and N-WASP to bind specifically to GTP-bound forms of Rac or Cdc42 (66). WASP, N-WASP, and Scar-1 contain a conserved C-terminal domain, which suffices for binding and activation of the Arp2/3 complex (61, 63). In cell-injection experiments, WASP lacking the GBD induces actin polymerization more potently than does full-length WASP (A. Abo, personal communication), raising the possibility that Cdc42 or Rac activate normal WASP by abrogating an autoinhibitory effect of the GBD and exposing the C-terminal Arp2/3 complex activation domain. Consistent with this idea, Cdc42–GTP (in the presence of PI(4,5)P_2) increases the ability of purified N-WASP to stimulate the Arp2/3 complex *in vitro* (62). Furthermore, N-WASP depletion prevents Cdc42-mediated actin polymerization in cell extracts (62). However, the complete cascade is not likely to be as simple as Cdc42–GTP activates N-WASP which in turn activates the Arp2/3 complex. First, the ability of N-WASP to activate the Arp2/3 complex *in vitro* requires activated Cdc42 *and* PI(4,5)P_2 (62), but activated Cdc42-mediated actin polymerization in extracts is insensitive to the sequestration of PI(4,5)P_2 (38). Thus, the role for PI(4,5)P_2 in normal N-WASP activation is uncertain. Secondly, N-WASP exists in a large protein complex in extracts and only partially purifies with the biochemical fraction necessary to mediate Cdc42-dependent activation of the Arp2/3 complex (L. Ma and R. Rohatgi, personal communication). Biochemical fractionation of cell-free systems (38, 49) should eventually make it possible to fully reconstitute Cdc42-dependent activation of the Arp2/3 complex.

5.4 Rac and actin polymerization

A primary effect of Rac activation is to increase the *availability* of barbed ends by promoting uncapping of previously formed filaments (Fig. 9). Here the best evidence comes from studies of permeabilized platelets (68), blood cells that promote formation of thrombi in response to thrombin and other agents and that are essential for normal haemostasis. In the resting state, most barbed ends of actin filaments are capped by barbed-end capping proteins, such as gelsolin (see below for general description of actin polymerization and capping proteins). Activation of the thrombin receptor increases the proportion of *uncapped* barbed ends from around 4% to 20–25%, resulting in massive polymerization of actin and striking changes in morphology. The number of exposed barbed ends correlates strongly with the amount of actin polymerization, making their exposure a convenient assay for signalling events that trigger actin polymerization. Indeed, these signals can act in detergent-permeabilized platelets: the proportion of barbed ends increases in response to activation of the GPCR for thrombin, addition of constitutively active Rac, or GTPγS.

In this system, ligand activation of the thrombin receptor triggers transient accumulation of a polyphosphoinositide, $PI(4,5)P_2$, which closely parallels the kinetics of barbed-end exposure. The following series of observations in permeabilized platelets (68) suggests that $PI(4,5)P_2$ is necessary and sufficient to induce actin polymerization, that it acts downstream of one or more G proteins, including Rac, and that it promotes polymerization by removing gelsolin or some other capping protein from barbed ends:

1. Direct addition of Rac-GTP increases accumulation of $PI(4,5)P_2$.
2. Addition of $PI(4,5)P_2$ induces exposure of barbed ends.
3. Barbed-end exposure triggered by activation of the thrombin receptor is inhibited by a GDP analogue that blocks G-protein activation, and this inhibition can be overcome by addition of $PI(4,5)P_2$.
4. Because $PI(4,5)P_2$ induces gelsolin and other capping proteins to dissociate from the barbed ends of actin filaments in purified systems (69), the $PI(4,5)P_2$-binding domain of gelsolin was used to sequester endogenous $PI(4,5)P_2$; this sequestration inhibits exposure of barbed ends triggered by activation of the thrombin receptor, by activated Rac, and by GTPγS.
5. Finally, Rac is thought to increase production of PIP_2 by binding to and activating PI(4)P 5-kinase, which converts PI(4)P to $PI(4,5)P_2$; PI(4)P 5-kinase lacking its Rac-interaction domain acts as a dominant negative for Rac-induced actin polymerization in platelets (J. Hartwig, personal communication).

It is not known whether the product of the kinase reaction, $PI(4,5)P_2$, always regulates the actin cytoskeleton directly, as it does in platelets. In some systems $PI(4,5)P_2$ appears to act upstream of Rho-GTPases; probably by facilitating nucleotide exchange on Cdc42. The polyphosphoinositide suffices to induce Cdc42-mediated actin polymerization in *Xenopus* extracts (40) and potentiates GTPγS-mediated actin polymerization in neutrophil extracts (38).

More recently a putative protein effector of Rac, known as WAVE, has been identified. Dominant-negative versions of WAVE prevent Rac-mediated actin polymerization, and overexpression of WAVE induces actin polymerization even in the presence of dominant-negative Rac, suggesting that WAVE is a downstream effector of Rac (70). WAVE shares sequence similarity to WASP and N-WASP and, importantly, contains a conserved C terminus, which has been shown in Scar-1 and WASP to be sufficient to activate the Arp2/3 complex (63). These data suggest that Rac may mediate its effects on actin polymerization through both PI(4,5)P$_2$-mediated uncapping of actin filaments *and* WAVE-mediated activation of the nucleation ability of the Arp2/3 complex.

5.5 Regulation of the actin cytoskeleton by Rho

In contrast to Cdc42 and Rac, Rho seems to control actin rearrangements indirectly, by regulating activity of myosin (Fig. 9) rather than polymerization of actin. Indeed, botulinum C3 toxin—which ADP-ribosylates and inactivates Rho—impairs neutrophil chemotaxis without preventing chemoattractant-induced actin polymerization (71). If Rho is not required for polymerizing actin, what role might it play in chemotaxis?

The most likely function of Rho in chemotaxis is to regulate cell contractility, allowing a cell to retract or inhibit surface projections that otherwise prevent the cell from moving. This idea is consistent with the appearance of macrophages, described above, in which Rho is inactivated by C3 toxin (43): these macrophages, their surfaces covered with dendritic projections, are unable to move. If loss of Rho allows unbridled formation of projections, it is not surprising that expression of activated Rho inhibits formation of actin projections triggered by Rac or Cdc42 in several systems (42). Rho is thought to modulate cell contractility by activating Rho-kinase (RHOK), which phosphorylates the light chain of the actin motor protein, myosin. This phosphorylation leads to bundling of actin filaments into contractile fibres (72, 73). Neutrophils treated with a RHOK inhibitor spread spontaneously in the absence of chemotactic stimulation (O. Weiner, unpublished observation). Also consistent with the idea that contractility and process formation are competing processes, Rac opposes the effect of Rho on cell contractility. Rac activates the kinase Pak1, which in turn phosphorylates and inhibits myosin light chain kinase (MLCK), reducing myosin phosphorylation and blocking the contractile effect of myosin (74).

6. Other regulators: Ca^{2+} and cGMP

One ubiquitous second-messenger molecule, intracellular Ca^{2+} ion, is *not* absolutely required for chemotaxis. Neutrophils do exhibit transient elevations of intracellular Ca^{2+} during random motility and in response to stimulation by chemoattractant; motility and chemotaxis can proceed normally, however, when Ca^{2+} elevations are inhibited by calcium chelators and calcium ionophores (75, 76). It is likely that intracellular Ca^{2+} does play an adjuvant role, however, in facilitating ability of the trailing edge of a motile cell to detach from the underlying substrate; detachment *is* inhibited when calcium-depleted neutrophils are plated on certain substrates, such as fibronectin, but directional polarity is not (76). This Ca^{2+}-dependent detachment from fibronectin is thought to reflect severing by calcium-activated proteases of integrin contacts with the extracellular matrix.

Analysis of several *Dicytostelium* mutants has suggested that another second messenger, cGMP, does play a role in chemotaxis (77). These mutants, found by screening for defective chemotaxis toward both cAMP and folic acid, are defective in cGMP regulation; chemoattractant-induced accumulation of cAMP and IP_3, however, are normal in most of the mutants. Thus in comparison to two other second messengers, cGMP appears to play a much more important role in one or more signal cascades leading from GCPR activation to chemotactic effectors.

One such cascade may regulate cyclical association of myosin with the cell cortex. Thus, elevated cGMP leads to activation of myosin heavy chain kinase (MHCK), which, along with myosin II, associates with the cortex in response to chemoattractant stimulation. Next, MHCK phosphorylates myosin II, causing it to dissociate from the cortex (78, 79). In keeping with this idea, both defects in cGMP accumulation and MHCK mutations result in persistent association of myosin with the cortex (78–80), while overexpression of MHCK causes myosin to distribute primarily to the cytosol and blocks formation of cell polarity in response to chemoattractant (80). All of these perturbations severely impair chemotaxis (78–80). It is unlikely that myosin II phosphorylation represents the only important response to cGMP, however, because mutations of the myosin II heavy chain show almost normal chemotaxis (81). So far, a role for cGMP in leucocyte chemotaxis has not been reported; perhaps myosin regulation by cGMP in *Dicytostelium* plays a role similar to Rho-mediated regulation of myosin in mammalian cells.

7. Co-ordination of actin polymerization, polarization, and directed movement

Both neutrophils and *Dicytostelium* undergo massive bursts of actin polymerization in response to chemotactic gradients, and this polymerization is necessary for chemotaxis: inhibition of actin polymerization by cell-permeable toxins (cytochalasin, which caps the barbed ends of actin filaments, or latrunculin, which sequesters actin monomers) prevents chemoattractants from inducing polar morphology and directed migration. How then is actin polymerization coupled to these responses? Where does chemoattractant-induced actin polymerization take place? This section will describe co-ordination of the spatial distribution of polymerizing actin filaments with cell polarity and directed migration in response to gradients of chemoattractant. We begin with a brief description of actin biochemistry and explain how addition of actin monomers to polymers probably produces protrusions of the plasma membrane. We then describe a highly informative model of actin polymerization, intracellular motility of *L. monocytogenes*, a pathogenic bacterium, and conclude by describing chemoattractant-induced foci of actin polymerization at the up-gradient edge of migrating cells.

7.1 Growing actin filaments and Brownian ratchets

Actin, one of the most highly conserved proteins known, is found in all eukaryotes. In the presence of physiological salt concentrations and ATP, monomeric actin assembles into actin filaments. An actin filament is a polar structure, the ends of which are designated as 'pointed' and 'barbed' (based on their appearance in electron micrographs after decoration by a myosin fragment). Monomers are added to the barbed end 10 times faster than to the pointed end (82). Because the cytosolic concentration of actin monomers far exceeds the critical concentration for their addition to either end of a pre-existing filament, cells use two kinds of proteins to prevent unregulated polymerization: monomeric actin-binding proteins, including thymosin-β4 and profilin, and capping proteins, including gelsolin and capping protein, which associate with barbed ends of actin filaments and prevent addition of monomers (83). Thus, cells can increase the formation of actin polymers in two ways—by generating nuclei for polymerization *de novo* (a process that can be accelerated by the Arp2/3 complex, as described above), or by generating an increased number of barbed (fast-growing) ends by uncapping or severing pre-existing actin filaments (Fig. 10).

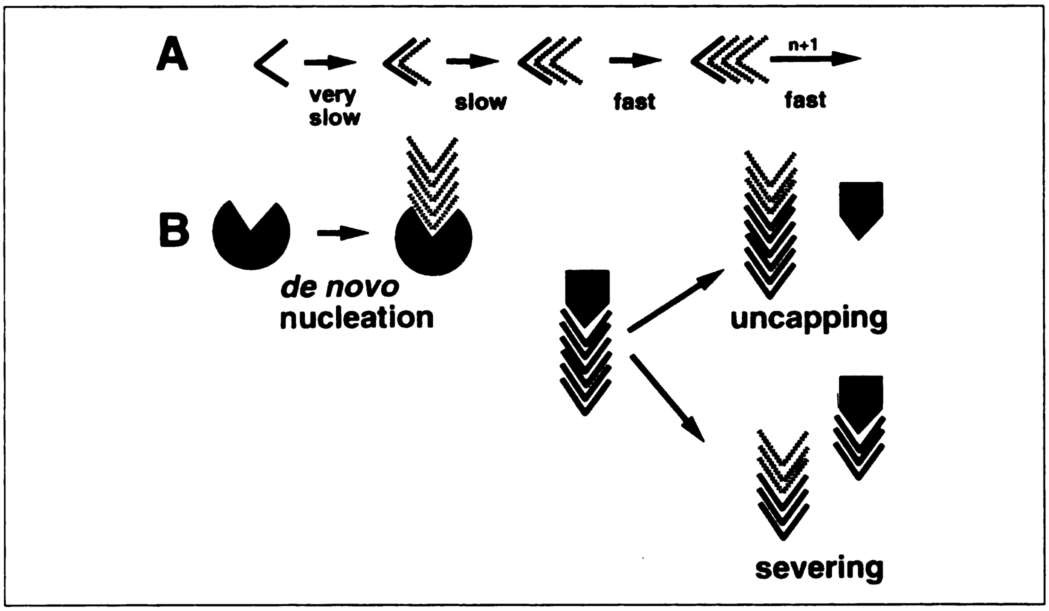

Fig. 10 Review of actin dynamics. (A) Polymerization of actin (black Vs) is limited by formation of actin trimers. Formation of actin dimers is a very slow event, formation of an actin trimers is also slow, but the addition of actin subunits to trimers or greater polymers proceeds much more rapidly. Actin polymerization (hatched Vs) proceeds in the barbed end (as opposed to pointed end) direction. (B) Means of generating nuclei for actin polymerization. Actin polymerization is limited in cells through actin sequestering proteins and proteins that cap the fast-growing barbed end of actin filaments. Actin polymerization can be induced in three basic ways. *De novo* nucleation of actin polymerization is accomplished through molecules that simulate actin dimers or trimers; the Arp2/3 complex is thought to act in this fashion. Alternatively, barbed ends can be generated from pre-existing capped actin filaments either by uncapping (such as PI(4,5)P_2-mediated uncapping of filaments) or severing (gelsolin and cofilin are thought to act in this fashion).

How might growth of an actin filament extend the plasma membrane toward a chemoattractant? Even in the absence of accessory proteins or signalling molecules, actin polymerization suffices to induce surface protrusions of a vesicle loaded with a high concentration of actin monomers; such protrusions extend at rates similar to those observed at leading edges of neutrophils and *Dicytostelium* (84). How does a growing actin polymer exert force on the membrane? According to one explanation, using a thermal Brownian ratchet (85), growth of actin polymers does not actively push the membrane, but instead makes Brownian motion of the membrane unidirectional: Brownian motion randomly pushes the membrane back and forth; movement in the forward direction allows a monomer to be added to the barbed end of a filament apposed to the membrane, and addition of a monomer to the filament opposes movement in the backward direction. A slightly more complex model, the 'elastic Brownian ratchet' (86), agrees somewhat better with experimental observations. In the latter model, elasticity of the actin filament increases the likelihood that thermal fluctuations will create gaps between the membrane and the filament large enough for addition of an actin monomer. The simple Brownian ratchet allows only the membrane to undergo thermal fluctuations because the filament itself is not elastic. In the elastic ratchet model, the filament's flexibility allows it to vibrate away from the membrane, providing additional opportunities for addition of monomer, and also allowing the filament to exert an active force on the membrane (in contrast to the simple Brownian ratchet) when the elongated filament bends back into its original position. As a result, the ratchet in this model can actively push the membrane forward. The elastic ratchet would generate force optimally when filaments are oriented at an angle of 48° relative to the plane of the membrane (86)—in close agreement with the angle (45°–55°) observed experimentally at leading edges of lamellipodia (87, 88).

7.2 Motility of *L. monocytogenes*

This bacterium evades the immune system by living in the cytoplasm of host cells and moves from one cell to another by virtue of its ability to move rapidly, exert force on the plasma membrane, and push itself into the cytosol of a second cell. Its rapid movement leaves in its wake a long tail of polymerized actin (89). Actin polymerization appears to provide the driving force for *Listeria* motility (Fig. 11), as suggested by the observation that these organisms move at the same rate at which an actin filament polymerizes, and by experiments in which prevention of actin polymerization also prevents *Listeria* motility (90, 91). This motility requires only one bacterial protein, ActA, but requires host factors in addition to G-actin. Testing biochemical fractions of cell extracts for proteins required for *Listeria*-induced actin polymerization led to isolation of the Arp2/3 complex; the ability of this complex to nucleate actin is greatly potentiated by the bacterial ActA protein (as described above) (57).

In the absence of other host factors, *Listeria* do not move in the presence of ActA and the Arp2/3 complex, although they form actin 'clouds' (rather than tails). Thus

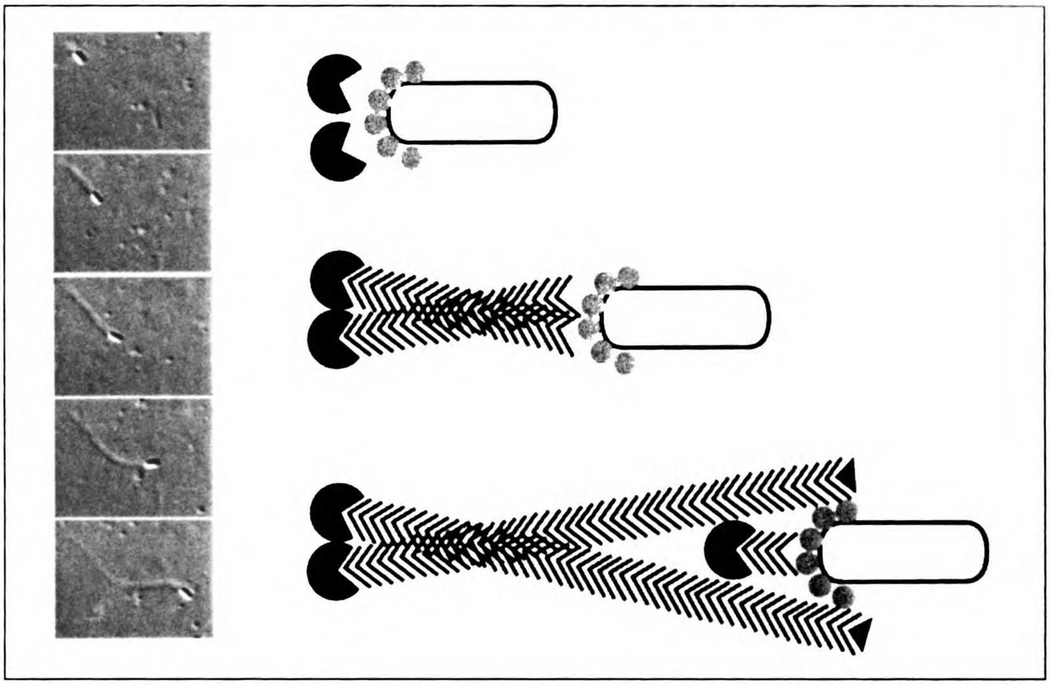

Fig. 11 Model for *Listeria* motility. The intracellular bacterial pathogen *Listeria monocytogenes* exhibits actin-based motility in the cytosol of infected cells (Nomarski image to the left of the figure shows moving *Listeria* leaving an comet-like actin tail in its wake). The bacterium expresses a protein, ActA (circles), on its surface. This recruits and activates the Arp2/3 complex (black 'Pacman' shapes), which stimulates *de novo* nucleation of actin polymerization (black Vs). The force of actin polymerization propels the bacterium by an elastic Brownian ratchet (see text), and actin filaments are capped (black triangles) after they leave the posterior region of the bacterium. For the sake of simplicity, other proteins also required for *Listeria* motility, such as VASP (104), are not represented.

motility probably requires additional proteins that act, in part, by controlling the orientation of filaments that push the bacterium forward. How might this occur? Normally, actin polymerizes only at the portion of the actin tail adjacent to that bacterial surface. Actin tails are composed of long, axial and short, randomly oriented filaments (92). Thus it is likely (92, 93) that actin filaments nucleated at the surface of *Listeria* stop polymerizing when they leave the zone of actin polymerization near the bacterial surface, and become capped at their barbed ends. Thus, normal motility requires other host factors, possibly including proteins that induce cross-linking of filaments in the actin tail, which may be required for action of the elastic Brownian ratchet.

7.3 Specifying *where* actin polymerizes during chemotaxis

Like motility of *Listeria* in the cytoplasm, directed movement during chemotaxis probably requires precise positioning of the sites of actin polymerization. Recently it has become possible to analyse the spatial distribution of filament nucleation and polymerization by assessing incorporation into the actin cytoskeleton of tagged (fluorescent) actin monomers introduced into cells by microinjection or permeabilization. This approach has shown that actin polymerizes preferentially at the leading edges of lamellipodia in fibroblasts and at the tips of filopodia in neuronal growth cones (94, 95).

Similar experiments in permeabilized neutrophils (96) suggest that exposure to chemoattractants causes polymerization foci to form at or just under the plasma membrane in multiple discrete sites located predominantly at the tips of ruffles that protrude from a cell's leading edge or pseudopodium. A gradient of chemoattractant biases spatial distribution of these foci to the up-gradient edge of the cell. Two observations (96) suggest that the Arp2/3 complex plays a crucial role in determining sites of polymerization:

(1) the complex dynamically redistributes to the up-gradient surface of neutrophils;

(2) a pool of the complex that preferentially resists methanol extraction co-localizes with sites of actin polymerization at the tips of finger-like actin bundles that project into the pseudopodium.

These data led to a model (96) in which stimulation of chemoattractant receptors leads to organization of polymerization foci, at or just under the plasma membrane, which are functionally equivalent to the zone of actin polymerization generated by the ActA protein at the posterior surface of *L. monocytogenes*. In this model (Fig. 12), actin polymerization at the surface of the polymerization focus propels it and the cell membrane forward, forming an actin 'finger', analogous to a *Listeria* tail. Polymerization takes place only in the zone of actin polymerization at the tip of the growing finger, and filaments are capped at their barbed ends after they leave this zone. Asymmetrical establishment and/or maintenance of polymerization foci produce the cytoskeletal and morphological rearrangements responsible for moving the cell up a chemotactic gradient. The model predicts that inhibiting the activity of the Arp2/3 complex will block chemotaxis and formation of actin fingers. A comprehensive test of the model, of course, will require reconstitution of the signal cascade from chemotactic GPCRs to the final effectors for actin polymerization.

7.4 Autonomous cell polarization and motility

The effects of chemoattractants on cell polarity, actin rearrangements, and motility are superimposed upon an *intrinsic ability of motile eukaryotic cells to establish and maintain polarity,* even in the absence of extracellular stimuli. Indeed, as described below, the actin cytoskeleton itself can exhibit an intrinsic capacity to establish and maintain polarity. It will be an important challenge to determine to how the chemotactic response harnesses these intrinsic abilities to generate directed polarity and movement.

Small cell fragments of keratocytes provide an instructive example of the cytoskeleton's ability to regulate itself (97). Such fragments are non-motile, and lack

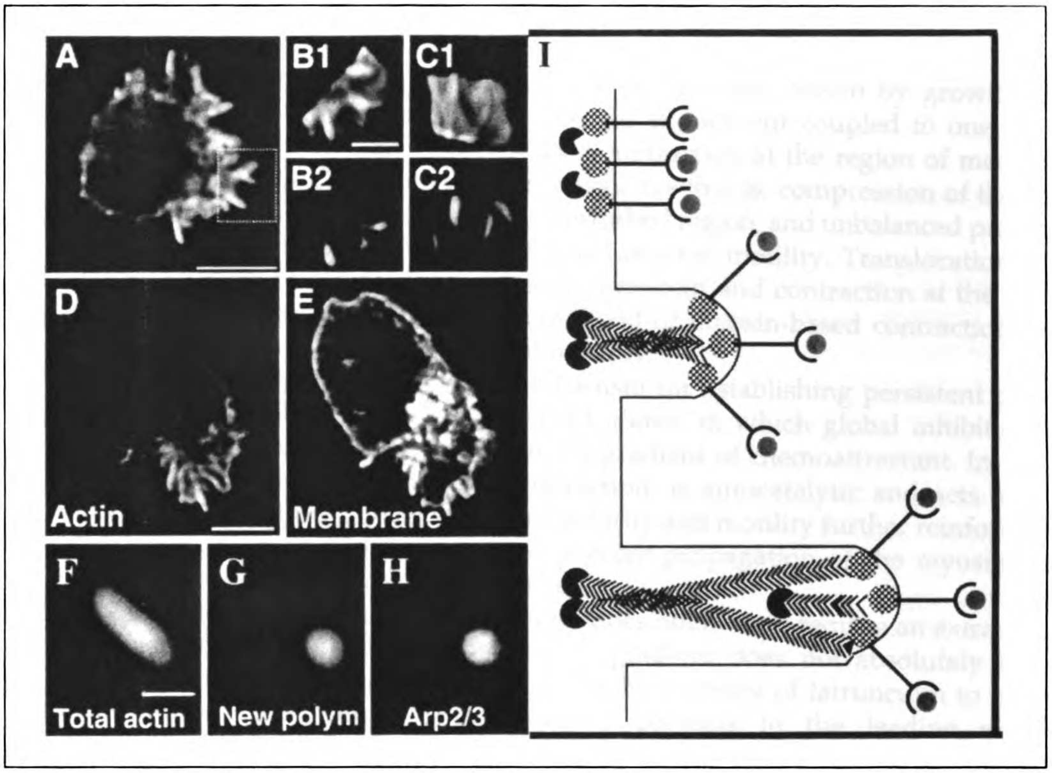

Fig. 12 Spatial control of actin polymerization during neutrophil chemotaxis. (A) Phalloidin staining of a neutrophil stimulated with uniform chemoattractant, representing total actin. Bar = 5 μm. (B, C) Three-dimensional reconstruction of the boxed region of pseudopodium from (A): (B) represents a top view of the pseudopodium and (C) represents a side view. (B1, C1) Phalloidin staining, representing total actin. Bar = 5 μm. (B2, C2) TMR-actin stain, representing newly polymerized actin. (D) Actin staining of a neutrophil stimulated with uniform chemoattractant. (E) The cell surface of the same neutrophil as (D), detected by virtue of GFP attached to a chemotactic receptor. Note that the cell surface perfectly corresponds to the morphology of the tips of the finger-like actin bundles. (F–H) Finger-like projection of a neutrophil stimulated with uniform chemoattractant, permeabilized in the presence of TMR-actin, and then fixed and stained for antibodies to the Arp2/3 complex. (F) Phalloidin stain, representing total actin. Bar = 0.5 μm. (G) Newly incorporated actin. (H) Arp2/3 complex. (I) Model for chemoattractant-stimulated actin polymerization during neutrophil chemotaxis (similar to the *Listeria* model from Fig. 11). Binding of ligand to GPCR chemoattractant receptor (grey circle in wineglass shape) leads to generation of internal signals (checkerboard circles) which locally recruit and activate the Arp2/3 complex (black 'Pacman' shapes). The Arp2/3 complex stimulates *de novo* nucleation of actin polymerization (black Vs). The force of actin polymerization propels the cell membrane by an elastic Brownian ratchet (see text), and actin filaments are capped (black triangle) after they leave the region of activated G proteins. A good candidate for recruitment of the Arp2/3 complex is activated Cdc42. Panels A–H reprinted from ref. 96 with permission from *Nature Cell Biology*.

polarity of actin and myosin until they are subjected to mechanical stimulation; the fragments then establish anisotropic arrays of actin and myosin and begin to move. Polarity and motility are maintained long after the external mechanical stimulation is removed, suggesting that an internal mechanism maintains polarity and motility. It is thought to do so by generating a positive feedback loop that reinforces polarity and motility (97). How might it do so? An unperturbed, non-polar cell or cell fragment represents a balance among multiple actin protrusions, driven by growing actin polymers and distributed over the entire cell surface but coupled to one another through membrane tension. Myosin-based contraction at the region of mechanical perturbation is thought to unbalance the system—that is, compression of the actin-myosin system inhibits protrusion in the perturbed region, and unbalanced protrusion at the other edge of the cell fragment generates net motility. Translocation of the fragment further reinforces accumulation of myosin and contraction at the back of the cell, and protrusions reduce the likelihood of myosin-based contraction at the front; both effects reinforce polarity and motility.

Note that this cytoskeletal-based mechanism for establishing persistent polarity somewhat resembles the model, described above, in which global inhibition and local activation allow the cell to interpret a gradient of chemoattractant. In the cell fragment one signal, myosin-based contraction, is autocatalytic and acts at short range, while subsequent development of polarity and motility further reinforces this signal and acts over a longer range to prevent propagation of the myosin-based contraction to other parts of the moving cell.

Just as induction of polarity and motility does not always require an extracellular stimulus, interpretation of the chemotactic gradient does not absolutely require rearrangement of the cytoskeleton, as shown by inability of latrunculin to prevent GPCR-induced recruitment of GFP-tagged proteins to the leading edge of *Dicytostelium* and neutrophils (described above). It is likely that these potentially independent functions co-operate with one another in a cell moving toward a source of chemoattractant. A challenge for the future is to unravel the connections that mediate such co-operation.

8. Perspectives and future directions

Recent advances in studies of eukaryotic chemotaxis furnish tantalizing glimpses into specific signalling pathways and cytoskeletal rearrangements. We still do not know, however, how the cell choreographs the vast congeries of regulatory events to produce the dance of chemotaxis. Closer approaches to this central mystery will follow several roads; here we sketch approaches to questions that we find especially provocative.

8.1 G_i-coupled receptors

To mediate chemotaxis, must the GPCR do more than simply link binding of a chemoattractant to activation of a trimeric G-protein? G_i-linked GPCRs are required for chemotaxis of mammalian cells, while α_i itself is not (5); these observations suggest that we should search for a unique property of G_i-coupled receptors, distinct from their selectivity for G_i. Such properties might include the following:

1. G_i-coupled receptors serve as docking sites for RGS or other proteins that enhance a cell's ability to interpret the chemotactic gradient.

2. G_i-coupled receptors signal directly to chemotactic effectors distinct from the G-trimer, as reported (98) for certain GPCRs in *Dicytostelium*.
3. G_i-coupled receptors activate G-trimers containing a structurally specific subset of $\beta\gamma$ subunits.
4. By associating with one another or with other membrane proteins, G_i-coupled receptors are targeted specifically to membrane subdomains specialized for chemotactic signalling.

Some of these possibilities could be tested by analysing phenotypes of GPCR chimeras that combine amino-acid sequences of a chemotactic G_i-coupled receptor with complementary sequences derived from a GPCR that does not mediate chemotaxis.

8.2 G-protein $\beta\gamma$ versus α subunits

Since $G\beta\gamma$ appears to couple directly to chemotactic effectors, what are the functions of the α subunit? Does it merely provide a 'handle' for the GPCR to trigger release of $\beta\gamma$, or does it transmit a separate signal? Experiments in HEK293 cells (5), described above, suggest that the GTP-bound α_i subunit may not play a necessary role in chemotaxis. It is likely that chemotactic GPCRs activate G-trimers in addition to G_i, and other α subunits may carry messages crucial for chemotaxis. For instance, activation of G_{13} (or G_{12}) can activate Rho by interacting with p115 RhoGEF (47), and loss of α_{13} produces knockout mice whose embryonic fibroblasts show severely impaired migratory responses to thrombin (99), which stimulates a GPCR coupled to both G_i and G_{13} (100). In addition, as noted above, G-protein α subunits could perform a key role by serving as substrates for regulation by RGS and other proteins, thereby regulating the half-life of $\beta\gamma$ release upon receptor activation. These issues may be most effectively addressed by genetic approaches in *Dicytostelium* and mammalian cells—that is, by knocking out specific α subunits and/or expressing α subunits with point mutations analogous to $G\beta$ mutations used to dissect the signalling role of $\beta\gamma$ (9).

8.3 Inhibitory signals that may help to interpret the gradient

Exposure of a neutrophil or *Dicytostelium* cell to a chemotactic gradient rapidly induces inhibition of the GPCR-mediated signal, manifested in two ways, asymmetry of the signal and generalized adaptation (also termed densitization): the first produces a specific decrease in the intensity of signals transmitted at the back of the cell, relative to the front, while the second reversibly diminishes the cell's overall responsiveness to the stimulus. At present we do not know how—or even whether—the two kinds of inhibition relate to one another, although both are likely to play essential roles in chemotaxis. As noted above, we do know that chemotaxis is *not* likely to depend on certain well-established adaptation/desensitization mechanisms (including phosphorylation or internalization of the GPCR, or a decrease of its ability to bind ligand).

None the less, identifying the inhibitor(s) required for chemotaxis represents a crucial challenge. One difficulty is that inhibitors may act by distinct mechanisms at multiple stages of the signal cascade. When sensitive genetic screens, *in vitro* assays, or biochemical fractionation do identify an inhibitor, it will be necessary to identify both the substrate(s) for inhibition and the signalling protein(s) that generate the inhibitor; candidates for all these roles include ligand-occupied GPCRs, G-protein α subunits, released $\beta\gamma$ subunits, RGS proteins, and many others.

8.4 Spatial readouts for GPCR-dependent signals

We can usually distinguish between mutations or pharmacological manipulations that impair a cell's general ability to move from those that prevent it from moving in the right direction. Within the latter class, however, we must learn to better distinguish between mutations and drugs that prevent primary interpretation of the chemotactic gradient and those that transmit polarized signals to downstream effectors. Recent observations (29; 105) that latrunculin fails to prevent asymmetrical recruitment of GFP-tagged receptor activity markers to the plasma membrane are promising first efforts in this direction. These results have not yet specified precisely where the amplification occurs in the signalling cascade, for reasons noted above. In this regard, it will be important to design assays that can determine the spatial distribution of other GPCR-dependent signals, including ligand-induced conformational change of the GPCR itself, free $\beta\gamma$, α–GTP, and others.

8.5 Effectors for chemoattractant-mediated actin polymerization

Many of the effectors that link chemotactic receptor activation with actin polymerization remain unknown. Extract systems have proven powerful for elucidating signalling events downstream of the Rho-GTPases or immediately upstream of the Arp2/3 complex, but permeabilized cell systems or genetic analyses will probably be required to link these processes with receptor activation. Actin polymerization mutants have generally been poorly represented in most *Dictyostelium* chemotaxis screens because of redundancy of the genes involved, necessity of these genes for cell viability, or a selection bias for the screens. Recent evidence for the final possibility comes from the observation that general chemotaxis mutants, such as Gβ null mutants, also exhibit a defect in bacterial phagocytosis. Mutants defective in phagocytosis would be overlooked in traditional screens because selection is typically performed by seeding individual clones on bacterial lawns. A recent screen designed to isolate mutants defective in chemotaxis and phagocytosis has yielded 10 mutants defective in chemoattractant-induced actin polymerization, suggesting that this approach will prove valuable in elucidating the signal transduction cascade from the chemotactic receptor to the actin polymerization machinery (107).

8.6 Signal cascades mediated by Rho-GTPases

Despite the key roles of Rho-GTPases as polarity effectors for chemotaxis, we know little of the specific biochemical mechanisms that regulate their activation or mediate their effects on polarity. Assessing changes in morphology represents an indirect and potentially incomplete strategy for identifying such mechanisms. For instance, the ability of Cdc42 to induce formation of filopodia, and the loss of both filopodia and directed motility in macrophages lacking Cdc42 function, are proposed (43) to indicate a role of filopodia in sensing the chemotactic gradient. Alternatively, Cdc42 could play morphologically 'invisible' roles in chemotaxis (e.g. by directly regulating other Rho-GTPases). Similarly, the successive appearance of filopodia, lamellipodia, and stress fibres after activation of Cdc42 is proposed (101) to represent a hierarchy of GTPase regulation, but the order of events in time does not constitute direct, compelling evidence. More precise dissection of the chemotactic signalling cascade will require assays for other activities, including robust methods for measuring the fraction of a cell's complement of a particular Rho-GTPase that is bound to GTP. One such strategy, recently developed as a means for measuring activated Cdc42 (102), Rac (102), and Rho (103) is to co-immunoprecipitate the GTPase with an appropriate downstream effector. Applied to other second messengers whose effectors preferentially recognize the second messenger's activated state, this approach should prove valuable in ordering signalling events.

8.7 Spatial readouts for signals mediated by Rho-GTPases

Determining the roles of Rho-GTPases will also require new tools for assaying and manipulating their activities in space. For instance, dominant-negative and dominant-active mutants of several Rho-GTPases produce similar defects in chemotaxis. Do these G proteins play a rather permissive role, fulfilled by cycling between active and inactive forms (and prevented by mutations that abrogate their abilities to bind or hydrolyse GTP)? Alternatively, and perhaps more likely, do these mutations prevent a specific spatial distribution, required for normal chemotaxis, of the Rho-family protein's effector-stimulating activity? To distinguish between permissive and spatially instructive roles of a Rho-GTPase (or any other signalling protein) in rearranging the cytoskeleton, two kinds of assays will be useful:

1. assays that determine the distribution of the protein's activity in space (e.g. a GFP-tagged effector protein that binds preferentially to the GTP-bound form of a Rho-GTPase);
2. methods that restrict the spatial distribution of the activated Rho-GTPase (e.g. localizing a protein that recruits or otherwise targets an activated version of the Rho-GTPase to a specific region of the plasma membrane).

In sum, because chemotaxis is an inherently spatial function, we can fully understand it only by resolving and reconstituting its components and their activities in the three-dimensional space of the cell.

Acknowledgements

We thank H. Meinhardt, R. D. Mullins, D. Kalman, and members of the Bourne, Devreotes, and Sedat labs for helpful discussion and J. Hartwig, L. Ma, R. Rohatgi, and S. van Es for communicating data prior to publication. O. Weiner is a Howard Hughes Medical Institute Predoctoral Fellow.

References

1. Devreotes, P. N. and Zigmond, S. H. (1988) Chemotaxis in eukaryotic cells: a focus on leukocytes and Dictyostelium. *Annu. Rev. Cell Biol.*, **4**, 649–86.
2. Berg, H. C. (1988) A physicist looks at bacterial chemotaxis. *Cold Spring Harbor Symp. Quant. Biol.*, **53**, (Pt 1), 1–9.
3. Neptune, E. R. and Bourne, H. R. (1997) Receptors induce chemotaxis by releasing the betagamma subunit of Gi, not by activating Gq or Gs. *Proc. Natl Acad. Sci., USA*, **94**, 14489–94.
4. Arai, H., Tsou, C. L., and Charo, I. F. (1997) Chemotaxis in a lymphocyte cell line transfected with C-C chemokine receptor 2B: evidence that directed migration is mediated by betagamma dimers released by activation of Gαi-coupled receptors. *Proc. Natl Acad. Sci., USA*, **94**, 14495–9.
5. Neptune, E. R., Iiri, T., and Bourne, H. R. (1999) Gαi is not required for chemotaxis mediated by Gi-coupled receptors. *J. Biol. Chem.*, **274**, 2824–8.
6. Kumagai, A., Hadwiger, J. A., Pupillo, M., and Firtel, R. A. (1991) Molecular genetic analysis of two G alpha protein subunits in *Dictyostelium*. *J. Biol. Chem.*, **266**, 1220–8.
7. Hadwiger, J. A., Lee, S., and Firtel, R. A. (1994) The G alpha subunit G alpha 4 couples to pterin receptors and identifies a signaling pathway that is essential for multicellular development in *Dictyostelium*. *Proc. Natl Acad. Sci., USA*, **91**, 10566–70.
8. Wu, L., Valkema, R., Van Haastert, P. J., and Devreotes, P. N. (1995) The G protein beta subunit is essential for multiple responses to chemoattractants in *Dictyostelium*. *J. Cell. Biol.*, **129**, 1667–75.
9. Jin, T., Amzel, M., Devreotes, P. N., and Wu, L. (1998) Selection of Gβ subunits with point mutations that fail to activate specific signaling pathways *in vivo*: dissecting cellular responses mediated by a heterotrimeric G protein in *Dictyostelium discoideum*. *Mol. Biol. Cell*, **9**, 2949–61.
10. Lefkowitz, R. J., Inglese, J., Koch, W. J., Pitcher, J., Attramadal, H., and Caron, M. G. (1992) G-protein-coupled receptors: regulatory role of receptor kinases and arrestin proteins. *Cold Spring Harbor Symp. Quant. Biol.*, **57**, 127–33.
11. Goodman, O. B. Jr, Krupnick, J. G., Santini, F., Gurevich, V. V., Penn, R. B., Gagnon, A. W., Keen, J. H., and Benovic, J. L. (1996) Beta-arrestin acts as a clathrin adaptor in endocytosis of the β_2-adrenergic receptor. *Nature*, **383**, 447–50.
12. Kim, J. Y., Soede, R. D., Schaap, P., Valkema, R., Borleis, J. A., Van Haastert, P. J., Devreotes, P. N., and Hereld, D. (1997) Phosphorylation of chemoattractant receptors is not essential for chemotaxis or termination of G protein-mediated responses. *J. Biol. Chem.*, **272**, 27313–18.
13. Arai, H., Monteclaro, F. S., Tsou, C. L., Franci, C., and Charo, I. F. (1997) Dissociation of chemotaxis from agonist-induced receptor internalization in a lymphocyte cell line transfected with CCR2B. Evidence that directed migration does not require rapid modulation of signaling at the receptor level. *J. Biol. Chem.*, **272**, 25037–42.
14. Hsu, M. H., Chiang, S. C., Ye, R. D., and Prossnitz, E. R. (1997) Phosphorylation of the N-formyl peptide receptor is required for receptor internalization but not chemotaxis. *J. Biol. Chem.*, **272**, 29426–9.

15. Segall, J. E. (1993) Polarization of yeast cells in spatial gradients of alpha mating factor. *Proc. Natl Acad. Sci., USA*, **90**, 8332–6.
16. Dorer, R., Pryciak, P. M., and Hartwell, L. H. (1995) *Saccharomyces cerevisiae* cells execute a default pathway to select a mate in the absence of pheromone gradients. *J. Cell Biol.*, **131**, 845–61.
17. Dohlman, H. G., Apaniesk, D., Chen, Y., Song, J., and Nusskern, D. (1995) Inhibition of G-protein signaling by dominant gain-of-function mutations in Sst2p, a pheromone desensitization factor in *Saccharomyces cerevisiae*. *Mol. Cell Biol.*, **15**, 3635–43.
18. Bowman, E. P., Campbell, J. J., Druey, K. M., Scheschonka, A., Kehrl, J. H., and Butcher, E. C. (1998) Regulation of chemotactic and proadhesive responses to chemoattractant receptors by RGS (regulator of G-protein signaling) family members. *J. Biol. Chem.*, **273**, 28040–8.
19. Lan, K. L., Sarvazyan, N. A., Taussig, R., Mackenzie, R. G., DiBello, P. R., Dohlman, H. G., and Neubig, R. R. (1998) A point mutation in Gαo and Gαi1 blocks interaction with regulator of G protein signaling proteins. *J. Biol. Chem.*, **273**, 12794–7.
20. Spain, B. H., Koo, D., Ramakrishnan, M., Dzudzor, B., and Colicelli, J. (1995) Truncated forms of a novel yeast protein suppress the lethality of a G protein alpha subunit deficiency by interacting with the beta subunit. *J. Biol. Chem.*, **270**, 25435–44.
21. Whiteway, M. S., Wu, C., Leeuw, T., Clark, K., Fourest-Lieuvin, A. ,Thomas, D. Y., and Leberer, E. (1995) Association of the yeast pheromone response G protein beta gamma subunits with the MAP kinase scaffold Ste5p. *Science*, **269**, 1572–5.
22. Kao, L. R., Peterson, J., Ji, R., Bender, L., and Bender, A. (1996) Interactions between the ankyrin repeat-containing protein Akr1p and the pheromone response pathway in *Saccharomyces cerevisiae*. *Mol. Cell. Biol.*, **16**, 168–78.
23. Pryciak, P. M. and Hartwell, L. H. (1996) AKR1 encodes a candidate effector of the G beta gamma complex in the *Saccharomyces cerevisiae* pheromone response pathway and contributes to control of both cell shape and signal transduction. *Mol. Cell. Biol.*, **16**, 2614–26.
24. Richardson, R. M., Ali, H., Tomhave, E. D., Haribabu, B., and Snyderman, R. (1995) Cross-desensitization of chemoattractant receptors occurs at multiple levels. Evidence for a role for inhibition of phospholipase C activity. *J. Biol. Chem.*, **270**, 27829–33.
25. Xiao, Z., N. Zhang, D. B. Murphy, and P. N. Devreotes. (1997) Dynamic distribution of chemoattractant receptors in living cells during chemotaxis and persistent stimulation. *J Cell Biol*, 139, p. 365–74.
26. Servant, G., Weiner, O. D., Neptune, E. R., Sedat, J. W., and Bourne, H. R. (1999) Dynamics of a chemoattractant receptor in living neutrophils during chemotaxis. *Molec. Biol. Cell*, **10**, 1163–78.
27. Insall, R., Kuspa, A., Lilly, P. J., Shaulsky, G., Levin, L. R., Loomis, W. F., and Devreotes, P. (1994) CRAC, a cytosolic protein containing a pleckstrin homology domain, is required for receptor and G protein-mediated activation of adenylyl cyclase in *Dictyostelium*. *J. Cell Biol.*, **126**, 1537–45.
28. Lilly, P. J. and Devreotes, P. N. (1995) Chemoattractant and GTP gamma S-mediated stimulation of adenylyl cyclase in *Dictyostelium* requires translocation of CRAC to membranes. *J. Cell Biol.*, **129**, 1659–65.
29. Parent, C. A., Blacklock, B. J., Froehlich, W. M., Murphy, D. B., and Devreotes, P. N. (1998) G protein signaling events are activated at the leading edge of chemotactic cells. *Cell*, **95**, 81–91.
30. Ruedi Meili, C. E., Lee, S., Reddy, T. B. K., Hui Ma, and Firtel, R. A. (1999) Chemoattractant-mediated transient activation and membrane localization of Akt/PKB is required for efficient chemotaxis to cAMP in *Dictyostelium*. *EMBO J.*, **18**, (8), 2092–105.
31. Fisher, P. R. (1990) Pseudopodium activation and inhibition signals in chemotaxis by *Dictyostelium discoideum* amoebae. *Semin. Cell Biol.*, **1**, 87–97.

32. Turing, A. M. (1990) The chemical basis of morphogenesis. 1953 [classical article]. *Bull. Math. Biol.*, **52**, 153–97; discussion 119–52.
33. Gierer, A. and Meinhardt, H. (1972) A theory of biological pattern formation. *Kybernetik*, **12**, 30–9.
34. Meinhardt, H. and Gierer, A. (1974) Applications of a theory of biological pattern formation based on lateral inhibition. *J. Cell Sci.*, **15**, 321–46.
35. Gerisch, G. and Keller, H. U. (1981) Chemotactic reorientation of granulocytes stimulated with micropipettes containing fMet–Leu–Phe. *J. Cell Sci.*, **52**, 1–10.
36. Zigmond, S. H. (1974) Mechanisms of sensing chemical gradients by polymorphonuclear leukocytes. *Nature*, **249**, 450–2.
37. Ayscough, K. R. and Drubin, D. G. (1998) A role for the yeast actin cytoskeleton in pheromone receptor clustering and signalling. *Curr. Biol.*, **8**, 927–30.
38. Zigmond, S. H., Joyce, M.,Borleis, J., Bokoch, G. M., and Devreotes, P. N. (1997) Regulation of actin polymerization in cell-free systems by GTPγS and Cdc42. *J. Cell Biol.*, **138**, 363–74.
39. Katanaev, V. L. and Wymann, M. P. (1998) GTPγS-induced actin polymerisation *in vitro*: ATP- and phosphoinositide-independent signalling via Rho-family proteins and a plasma membrane-associated guanine nucleotide exchange factor. *J. Cell Sci.*, **111**, 1583–94.
40. Ma, L., Cantley, L. C., Janmey, P. A., and Kirschner, M. W. (1998) Corequirement of specific phosphoinositides and small GTP-binding protein Cdc42 in inducing actin assembly in *Xenopus* egg extracts. *J. Cell Biol.*, **140**, 1125–36.
41. Johnson, D. I. and Pringle, J. R. (1990) Molecular characterization of CDC42, a *Saccharomyces cerevisiae* gene involved in the development of cell polarity. *J. Cell Biol.*, **111**, 143–52.
42. Hall, A. (1998) Rho GTPases and the actin cytoskeleton. *Science*, **279**, 509–14.
43. Allen, W. E., Zicha, D., Ridley, A. J., and Jones, G. E. (1998) A role for Cdc42 in macrophage chemotaxis. *J. Cell Biol.*, **141**, 1147–57.
44. Butty, A. C., Pryciak, P. M., Huang, L. S., Herskowitz, I., and Peter, M. (1998) The role of Far1p in linking the heterotrimeric G protein to polarity establishment proteins during yeast mating. *Science*, **282**, 1511–16.
45. Nern, A. and Arkowitz, R. A. (1998) A GTP-exchange factor required for cell orientation. *Nature*, **391**, 195–8.
46. Nern, A. and Arkowitz, R. A. (1999) A Cdc24p–Far1p–Gβγ protein complex required for yeast orientation during mating. *J. Cell Biol.*, **144**, 1187–202.
47. Kozasa, T., Jiang, X., Hart, M. J., Sternweis, P. M., Singer, W. D., Gilman, A. G., Bollag, G., and Sternweis, P. C. (1998) p115 RhoGEF, a GTPase activating protein for Gα12 and Gα13. *Science*, **280**, 2109–11.
48. Roberts, A. W., *et al.* (1999) Deficiency of the hematopoietic cell-specific Rho family GTPase Rac2 is characterized by abnormalities in neutrophil function and host defense. *Immunity*, **10**, 183–96.
49. Ma, L., Rohatgi, R., and Kirschner, M. W. (1998) The Arp2/3 complex mediates actin polymerization induced by the small GTP-binding protein Cdc42. *Proc. Natl Acad. Sci., USA*, **95**, 15362–7.
50. Machesky, L. M., Atkinson, S. J., Ampe, C., Vandekerckhove, J., and Pollard, T. D. (1994) Purification of a cortical complex containing two unconventional actins from *Acanthamoeba* by affinity chromatography on profilin-agarose. *J. Cell Biol.*, **127**, 107–15.
51. Welch, M. D., DePace, A. H., Verma, S., Iwamatsu, A., and Mitchison, T. J. (1997) The human Arp2/3 complex is composed of evolutionarily conserved subunits and is localized to cellular regions of dynamic actin filament assembly. *J. Cell Biol.*, **138**, 375–84.

52. Winter, D., Podtelejnikov, A. V., Mann, M., and Li, R. (1997) The complex containing actin-related proteins Arp2 and Arp3 is required for the motility and integrity of yeast actin patches. *Curr. Biol.*, **7**, 519–29.
53. Kelleher, J. F., Atkinson, S. J., and Pollard, T. D. (1995) Sequences, structural models, and cellular localization of the actin-related proteins Arp2 and Arp3 from *Acanthamoeba*. *J. Cell Biol.*, **131**, 385–97.
54. Welch, M. D., Iwamatsu, A., and Mitchison, T. J. (1997) Actin polymerization is induced by Arp2/3 protein complex at the surface of *Listeria monocytogenes*. *Nature*, **385**, 265–9.
55. Yarar, D., To, W., Abo, A., and Welch, M. D. (1999) The Wiskott–Aldrich syndrome protein directs actin-based motility by stimulating actin nucleation with the Arp2/3 complex. *Curr. Biol.*, **9**, 555–8.
56. Mullins, R. D., Heuser, J. A., and Pollard, T. D. (1998) The interaction of Arp2/3 complex with actin: nucleation, high affinity pointed end capping, and formation of branching networks of filaments. *Proc. Natl Acad. Sci., USA*, **95**, 6181–6.
57. Welch, M. D., Rosenblatt, J., Skoble, J., Portnoy, D. A., and Mitchison, T. J. (1998) Interaction of human Arp2/3 complex and the *Listeria monocytogenes* ActA protein in actin filament nucleation. *Science*, **281**, 105–8.
58. McCollum, D., Feoktistova, A., Morphew, M., Balasubramanian, M., and Gould, K. L. (1996) The *Schizosaccharomyces pombe* actin-related protein, Arp3, is a component of the cortical actin cytoskeleton and interacts with profilin. *EMBO J.*, **15**, 6438–46.
59. Moreau, V., Madania, A., Martin, R. P., and Winsor, B. (1996) The *Saccharomyces cerevisiae* actin-related protein Arp2 is involved in the actin cytoskeleton. *J. Cell Biol.*, **134**, 117–32.
60. Mullins, R. D. and Pollard, T. D. (1999) Rho-family GTPases require the Arp2/3 complex to stimulate actin polymerization in *Acanthamoeba* extracts. *Curr. Biol.*, **9**, 405–15.
61. Machesky, L. M. and Insall, R. H. (1998) Scarl and the related Wiskott–Aldrich syndrome protein, WASP, regulate the actin cytoskeleton through the Arp2/3 complex. *Curr. Biol.*, **8**, 1347–56.
62. Rohatgi, R., Ma, L., Miki, H., Lopez, M., Kirchhausen, T., Takenawa, T., and Kirschner, M. W. (1999) The interaction between N-WASP and the Arp2/3 complex links Cdc42-dependent signals to actin assembly. *Cell*, **97**, 221–31.
63. Machesky, L. M., Mullins, R. D., Higgs, H. N., Kaiser, D. A., Blanchoin, L., May, R. C., Hall, M. E., and Pollard, T. D. (1999) Scar, a WASP-related protein, activates nucleation of actin filaments by the Arp2/3 complex. *Proc. Natl Acad. Sci., USA*, **96**, 3739–44.
64. Bear, J. E., Rawls, J. F., and Saxe, C. L. R. (1998) SCAR, a WASP-related protein, isolated as a suppressor of receptor defects in late *Dictyostelium* development. *J. Cell Biol.*, **142**, 1325–35.
65. Zicha, D., Allen, W. E., Brickell, P. M., Kinnon, C., Dunn, G. A., Jones, G. E., and Thrasher, A. J. (1998) Chemotaxis of macrophages is abolished in the Wiskott–Aldrich syndrome. *Br. J. Haematol.*, **101**, 659–65.
66. Symons, M., Derry, J. M., Karlak, B., Jiang, S., Lemahieu, V., McCormick, F., Francke, U., and Abo, A. (1996) Wiskott–Aldrich syndrome protein, a novel effector for the GTPase CDC42Hs, is implicated in actin polymerization. *Cell*, **84**, 723–34.
67. Miki, H., Sasaki, T., Takai, Y., and Takenawa, T. (1998) Induction of filopodium formation by a WASP-related actin-depolymerizing protein N-WASP. *Nature*, **391**, 93–6.
68. Hartwig, J. H., Bokoch, G. M., Carpenter, C. L. Janmey, P. A., Taylor, L. A., Toker, A., and Stossel, T. P. (1995) Thrombin receptor ligation and activated Rac uncap actin filament barbed ends through phosphoinositide synthesis in permeabilized human platelets. *Cell*, **82**, 643–53.

69. Janmey, P. A., Iida, K., Yin, H. L., and Stossel, T. P. (1987) Polyphosphoinositide micelles and polyphosphoinositide-containing vesicles dissociate endogenous gelsolin–actin complexes and promote actin assembly from the fast-growing end of actin filaments blocked by gelsolin. *J. Biol. Chem.*, **262**, 12228–36.
70. Miki, H., Suetsugu, S., and Takenawa, T. (1998) WAVE, a novel WASP-family protein involved in actin reorganization induced by Rac. *EMBO J.*, **17**, 6932–41.
71. Stasia, M. J., Jouan, A., Bourmeyster, N., Boquet, P., and Vignais, P. V. (1991) ADP-ribosylation of a small size GTP-binding protein in bovine neutrophils by the C3 exoenzyme of *Clostridium botulinum* and effect on the cell motility. *Biochem. Biophys. Res. Commun.*, **180**, 615–22.
72. Kimura, K. *et al.* (1996) Regulation of myosin phosphatase by Rho and Rho-associated kinase (Rho-kinase). *Science*, **273**, 245–8.
73. Chrzanowska-Wodnicka, M. and Burridge, K. (1996) Rho-stimulated contractility drives the formation of stress fibers and focal adhesions. *J. Cell Biol.*, **133**, 1403–15.
74. Sanders, L. C., Matsumura, F., Bokoch, G. M., and de Lanerolle, P. (1999) Inhibition of myosin light chain kinase by p21-activated kinase. *Science*, **283**, 2083–5.
75. Zigmond, S. H., Slonczewski, J. L., Wilde, M. W., and Carson, M. (1988) Polymorphonuclear leukocyte locomotion is insensitive to lowered cytoplasmic calcium levels. *Cell Motil. Cytoskeleton*, **9**, 184–9.
76. Marks, P. W. and Maxfield, F. R. (1990) Transient increases in cytosolic free calcium appear to be required for the migration of adherent human neutrophils. *J. Cell Biol.*, **110**, 43–52.
77. Kuwayama, H., Ishida, S., and Van Haastert, P. J. (1993) Non-chemotactic *Dictyostelium discoideum* mutants with altered cGMP signal transduction. *J. Cell Biol.*, **123**, 1453–62.
78. Liu, G., Kuwayama, H., Ishida, S., and Newell, P. C. (1993) The role of cyclic GMP in regulating myosin during chemotaxis of *Dictyostelium*: evidence from a mutant lacking the normal cyclic GMP response to cyclic AMP. *J. Cell Sci.*, **106**, 591–5.
79. Dembinsky, A., Rubin, H., and Ravid, S. (1996) Chemoattractant-mediated increases in cGMP induce changes in *Dictyostelium* myosin II heavy chain-specific protein kinase C activities. *J. Cell Biol.*, **134**, 911–21.
80. Abu-Elneel, K., Karchi, M., and Ravid, S. (1996) *Dictyostelium* myosin II is regulated during chemotaxis by a novel protein kinase C. *J. Biol. Chem.*, **271**, 977–84.
81. De Lozanne, A. and Spudich, J. A. (1987) Disruption of the *Dictyostelium* myosin heavy chain gene by homologous recombination. *Science*, **236**, 1086–91.
82. Pollard, T. D. (1986) Rate constants for the reactions of ATP- and ADP-actin with the ends of actin filaments. *J. Cell Biol.*, **103**, 2747–54.
83. Pantaloni, D. and Carlier, M. F. (1993) How profilin promotes actin filament assembly in the presence of thymosin beta 4. *Cell*, **75**, 1007–14.
84. Miyata, H., Nishiyama, S., Akashi, K., and Kinosita, K. Jr (1999) Protrusive growth from giant liposomes driven by actin polymerization. *Proc. Natl Acad. Sci., USA*, **96**, 2048–53.
85. Peskin, C. S., Odell, G. M., and Oster, G. F. (1993) Cellular motions and thermal fluctuations: the Brownian ratchet. *Biophys. J.*, **65**, 316–24.
86. Mogilner, A. and Oster, G. (1996) Cell motility driven by actin polymerization. *Biophys. J.*, **71**, 3030–45.
87. Small, J. V., Herzog, M., and Anderson, K. (1995) Actin filament organization in the fish keratocyte lamellipodium. *J. Cell Biol.*, **129**, 1275–86.
88. Svitkina, T. M., Verkhovsky, A. B., McQuade, K. M., and Borisy, G. G. (1997) Analysis of the actin–myosin II system in fish epidermal keratocytes: mechanism of cell body translocation. *J. Cell Biol.*, **139**, 397–415.

89. Dabiri, G. A., Sanger, J. M., Portnoy, D. A., and Southwick, F. S. (1990) *Listeria monocytogenes* moves rapidly through the host-cell cytoplasm by inducing directional actin assembly. *Proc. Natl Acad. Sci., USA,* **87**, 6068–72.
90. Sanger, J. M., Sanger, J. W., and Southwick, F. S. (1992) Host cell actin assembly is necessary and likely to provide the propulsive force for intracellular movement of *Listeria monocytogenes. Infect. Immun.,* **60**, 3609–19.
91. Theriot, J. A., Mitchison, T. J., Tilney, L. G., and Portnoy, D. A. (1992) The rate of actin-based motility of intracellular *Listeria monocytogenes* equals the rate of actin polymerization. *Nature,* **357**, 257–60.
92. Sechi, A. S., Wehland, J., and Small, J. V. (1997) The isolated comet tail pseudopodium of *Listeria monocytogenes*: a tail of two actin filament populations, long and axial and short and random. *J. Cell Biol.,* **137**, 155–67.
93. Marchand, J. B., Moreau,P., Paoletti, A., Cossart, P.,Carlier, M. F., and Pantaloni, D. (1995) Actin-based movement of *Listeria monocytogenes*: actin assembly results from the local maintenance of uncapped filament barbed ends at the bacterium surface. *J. Cell Biol.,* **130**, 331–43.
94. Symons, M. H. and Mitchison, T. J. (1991) Control of actin polymerization in live and permeabilized fibroblasts. *J. Cell Biol.,* **114**, 503–13.
95. Okabe, S. and Hirokawa, N. (1991) Actin dynamics in growth cones. *J. Neurosci.,* **11**, 1918–29.
96. Weiner, O. D., Servant, G., Welch, M. D., Mitchision, T. J., Sedat, J. W., and Bourne, H. R. (1999) Spatial control of actin polymerization during neutrophil chemotaxis. *Nature Cell Biol.,* **1**, 75–81.
97. Verkhovsky, A. B., Svitkina, T.M., and Borisy, G. G. (1999) Self-polarization and directional motility of cytoplasm. *Curr. Biol.,* **9**, 11–20.
98. Chen, M. Y., Insall, R. H., and Devreotes, P. N. (1996) Signaling through chemoattractant receptors in *Dictyostelium. Trends Genet.,* **12**, 52–7.
99. Offermanns, S., Mancino, V., Revel, J.P., and Simon, M. I. (1997) Vascular system defects and impaired cell chemokinesis as a result of Gα13 deficiency. *Science,* **275**, 533–6.
100. Offermanns, S., Laugwitz, K. L., Spicher, K., and Schultz, G. (1994) G proteins of the G12 family are activated via thromboxane A2 and thrombin receptors in human platelets. *Proc. Natl Acad. Sci., USA,* **91**, 504–8.
101. Nobes, C. D. and Hall, A. (1995) Rho, rac, and cdc42 GTPases regulate the assembly of multimolecular focal complexes associated with actin stress fibers, lamellipodia, and filopodia. *Cell,* **81**, 53–62.
102. Benard, V., Bohl, B. P., and Bokoch, G. M. (1999) Characterization of Rac and Cdc42 activation in chemoattractant-simulated human neutrophils using a novel assay for active GTPases. *J. Biol. Chem.,* **274**, 13198–204.
103. Ren, X. D., Kiosses, W. B., and Schwartz, M. A. (1999) Regulation of the small GTP-binding protein Rho by cell adhesion and the cytoskeleton. *EMBO J.,* **18**, 578–85.
104. Laurent, V., Loisel, T. P., Harbeck, B., Wehman, A., Grobe, L., Jockusch, B. M., Wehland, J., Gertler, F. B., and Carlier M. F. (1999) Role of proteins of the Ena/VASP family in actin-based motility of *Listeria monocytogenes. J. Cell Biol.,* **144**, 1245–58.
105. Servant, G., Weiner, O. D., Herzmark, P., Bhalla, T., Sedat, J. W., and Bourne, H. R. (2000) Neutrophil chemotaxis: Rho GTPases are required for polarized signals. *Science,* in press.
106. Meinhardt, H. (1999) Orientation of chemotactic cells and growth cones: models and mechanisms. *J. Cell Sci.,* **112**, 2867–2874.
107. van Es S, and Devreotes, P. N. (1999) Molecular basis of localized responses during chemotaxis in amoebae and leukocytes. *Cell Mol. Life Sci.,* **55**, 1341–51.

CHAPTER THREE

Chemokine Receptors are Uniformly Distributed during Neutrophil Chemotaxis

Reprinted from *Molecular Biology of the Cell* (1999, volume 10, 1163-1178), with permissions by the American Society for Cell Biology.

Molecular Biology of the Cell
Vol. 10, 1163–1178, April 1999

Dynamics of a Chemoattractant Receptor in Living Neutrophils during Chemotaxis[V]

Guy Servant,* Orion D. Weiner,*† Enid R. Neptune,* John W. Sedat,† and Henry R. Bourne*‡

*Departments of Cellular and Molecular Pharmacology and of †Biochemistry and Biophysics, University of California San Francisco, San Francisco, California 94143

Submitted October 29, 1998; Accepted February 2, 1999
Monitoring Editor: J. Richard McIntosh

Persistent directional movement of neutrophils in shallow chemotactic gradients raises the possibility that cells can increase their sensitivity to the chemotactic signal at the front, relative to the back. Redistribution of chemoattractant receptors to the anterior pole of a polarized neutrophil could impose asymmetric sensitivity by increasing the relative strength of detected signals at the cell's leading edge. Previous experiments have produced contradictory observations with respect to receptor location in moving neutrophils. To visualize a chemoattractant receptor directly during chemotaxis, we expressed a green fluorescent protein (GFP)-tagged receptor for a complement component, C5a, in a leukemia cell line, PLB-985. Differentiated PLB-985 cells, like neutrophils, adhere, spread, and polarize in response to a uniform concentration of chemoattractant, and orient and crawl toward a micropipette containing chemoattractant. Recorded in living cells, fluorescence of the tagged receptor, C5aR–GFP, shows no apparent increase anywhere on the plasma membrane of polarized and moving cells, even at the leading edge. During chemotaxis, however, some cells do exhibit increased amounts of highly folded plasma membrane at the leading edge, as detected by a fluorescent probe for membrane lipids; this is accompanied by an apparent increase of C5aR–GFP fluorescence, which is directly proportional to the accumulation of plasma membrane. Thus neutrophils do not actively concentrate chemoattractant receptors at the leading edge during chemotaxis, although asymmetrical distribution of membrane may enrich receptor number, relative to adjacent cytoplasmic volume, at the anterior pole of some polarized cells. This enrichment could help to maintain persistent migration in a shallow gradient of chemoattractant.

INTRODUCTION

Chemotaxis, or directed cell movement up a chemical gradient, plays a central role in the accumulation of leukocytes at sites of infection and inflammation (Baggiolini, 1998). This motility is thought to depend on many cellular functions, including 1) protrusion and adhesion of the front end, driven by actin assembly; 2) contraction, probably driven by myosin-based motors, which moves nucleus and bulk cytoplasm in a forward direction; and 3) deadhesion of the trailing edge, thought to be partly mediated by the Ca^{2+}-sensitive enzymes, calcineurin and calpain (Cassimeris and Zigmond, 1990; Downey, 1994; Huttenlocher *et al.*, 1997). These processes are initiated in a coordinated manner by activation of chemoattractant receptors, members of the G protein-coupled receptor superfamily, located at the cell surface.

Neutrophilic leukocytes (neutrophils) can crawl up a chemotactic gradient that corresponds to a difference in chemoattractant concentration as low as 1% across the length of the cell (Zigmond, 1977), indicating that these cells can compare and efficiently amplify small differences in concentrations of the extracellular stim-

---

[V] Online version of this article contains video material for Figures 1, 2, 4, and 5. Online version available at www.molbiolcell.org.

‡ Corresponding author. E-mail address: h_bourne@quickmail.ucsf.edu.

© 1999 by The American Society for Cell Biology

ulus. Moreover, in a homogeneous solution or in a shallow gradient of chemoattractant, locomoting neutrophils tend to move persistently in a given direction, turning only at small angles (Zigmond, 1977; Zigmond *et al.*, 1981). Higher density of chemoattractant receptors at the leading edge of a polarized neutrophil could account for the asymmetrically distributed sensitivity underlying the ability to respond to a shallow gradient (Zigmond *et al.*, 1981). Such an asymmetric distribution of receptors would enhance the intensity of signal detected at the anterior pole of a moving neutrophil, relative to the rest of its surface. By steepening the apparent chemotactic gradient across the cell, asymmetrically distributed receptors would reinforce the cell's polarity and persistent forward motion (Zigmond, 1977; Zigmond *et al.*, 1981).

The lack of methods for direct observation of cell-surface proteins on living, moving neutrophils has led most investigators to rely on approaches that localize chemoattractant receptors on cells fixed after random polarization in a uniform concentration of chemoattractant. Such approaches, including the use of labeled ligands (Sullivan, *et al.*, 1984; Walter and Marasco, 1984, 1987) or anti-receptor antibodies (Gray, *et al.*, 1997), have led investigators to conclude that chemoattractant receptors are concentrated at the front (Walter and Marasco, 1984) or midregion (Sullivan, *et al.*, 1984) or are uniformly dispersed over the neutrophil surface (Walter and Marasco, 1987; Gray *et al.*, 1997). These discrepancies reflect different techniques and experimental conditions for localizing receptors, but might also result from fixing the cells at different times after application of the stimulus (Sullivan *et al.*, 1984; Walter and Marasco, 1984). The latter possibility would suggest that receptors may be distributed differently in different stages of the neutrophil response. Two groups have reported greater amounts of fluorescently labeled *N*-formyl-Met-Leu-Phe (fMLP),[1] a chemoattractant ligand, at the front of living polarized neutrophils, suggesting enrichment of the fMLP receptor at the leading edge (Schmitt and Bultmann, 1990; McKay *et al.*, 1991). These reports (Schmitt and Bultmann, 1990; McKay, *et al.*, 1991) did not indicate whether the increased fluorescence resulted from an increased concentration of receptor molecules per unit area of plasma membrane or from the increased folding of membranes that is seen (Davis, *et al.*, 1982; Cassimeris and Zigmond, 1990) at the leading edge of motile neutrophils.

To observe receptors directly and in real time during chemotaxis, we sought to express in neutrophils a receptor linked to a fluorescent tag, green fluorescent protein (GFP). Neutrophils, however, are terminally differentiated, short lived in vitro, and refractory to most methods of transfection. Accordingly, we elected to use a cultured myeloid leukemia cell line, PLB-985, which can be induced by treatment with DMSO to differentiate into cells that display histochemical, morphological, and biochemical features of neutrophils (Tucker *et al.*, 1987; Dana *et al.*, 1998). Here we show that on a glass coverslip these cells also behave strikingly like neutrophils, adhering, spreading, orienting, and moving in response to a chemotactic gradient. Using a retroviral vector, we transduced PLB-985 cells with a GFP-tagged version of a receptor for C5a (hereafter termed the C5aR), a component of complement that is well established as a chemoattractant for neutrophils (Gerard and Gerard, 1991). This approach allows, for the first time, direct observation of a chemoattractant receptor during migration of living neutrophils.

MATERIALS AND METHODS

Materials

[^{125}I]-C5a was from New England Nuclear (Boston, MA). The polyclonal anti-C5aR antibody (Morgan *et al.*, 1993), raised against an amino acid sequence (residues 9–29) near the amino terminus of the human C5aR, was a gift from J.A. Ember and T.E. Hugli (Scripps, San Diego, CA). The Flag-tagged human C5aR cDNA in pCDM8 was a gift from C. Gerard (Harvard Medical School, Boston, MA). CalPhos Maximizer and the GFP fusion vector pEGFP-N3 were from CLONTECH (Palo Alto, CA). 1,1′-Dioctadecyl-3,3,3′,3′-tetramethyllindodicarbocyanine perchlorate (DiD) was from Molecular Probes (Eugene, OR). Texas Red-conjugated goat anti-rabbit IgG was from Jackson Immunoresearch Laboratories (West Grove, PA). Monoclonal GFP antibody was from CLONTECH. Vectashield antifade mounting medium was from Vector Laboratories (Burlingame, CA). Immersion oil (n = 1.518) was from R.P. Cargille Laboratories (Cedar Grove, NJ). Photoetched grid coverslips 1916–92525 were from Bellco Glass (Vineland, NJ). The amphotropic packaging cell line PA317 was from the American Type Culture Collection (Manassas, VA). The myeloid leukemia cell line PLB-985 was a gift from Arie Abo (Onyx Pharmaceuticals, Richmond, CA). The Ψ2 packaging cell line and the pLNCX retroviral vector were gifts from J. Michael Bishop (University of California San Francisco, San Francisco, CA). Polybrene, human recombinant complement C5a, and fMLP were from Sigma Chemical (St. Louis, MO). The carboxy-terminal agonist analogue of C5a, *N*-Met-Phe-Lys-Prod-Cha-Cha-dArg (ChaCha) (Konteatis *et al.*, 1994) was a gift from Josh Trueheart (Cadus Pharmaceuticals, Tarrytown, NY). G-418 was from Grand Island Biological (Grand Island, NY). All other cell culture reagents were from the Cell Culture Facility (University of San Francisco, San Francisco, CA).

Cell Culture

HEK293 cells and PA317 cells were grown in DMEM supplemented with 10% FBS, 100 U/ml penicillin, and 100 μg/ml streptomycin G. For Ψ2 cells, calf serum was used. PLB-985 cells were grown in RPMI 1640 supplemented with 25 mM HEPES, 10% FBS, 100 U/ml penicillin, 100 μg/ml streptomycin G, 50 μg/ml gentamicin and 2.5

---

[1] Abbreviations used: C5aR, C5a receptor; ChaCha, *N*-Met-Phe-Lys-ProdCha-Cha-dArg; CRAC, cytosolic regulator of adenylyl cyclase; DiD, 1,1′-dioctadecyl-3,3,3′,3′-tetramethylindodicarbocyanine perchlorate; FACS, fluorescence-activated cell sorting; fMLP, *N*-formyl-Met-Leu-Phe; GFP, green fluorescent protein; mHBSS, modified HBSS.

μg/ml fungizone. For differentiation, PLB-985 cells were plated at a density of 0.1×10^6 cells/ml and grown for 4 d until they reached a density of ~1. 5×10^6 cells/ml. Cells (2 ml) were then diluted with 16 ml fresh medium (lacking G-418, gentamicin, and fungizone), and 2 ml of a 13% stock solution of DMSO was added to the cell suspension. Cells were propagated for 6 or 7 d without changing the medium. Under these conditions, cells remained subconfluent, and differentiation was optimal, as determined by superoxide production (Iiri *et al.*, 1995). Conditioned medium was collected from PLB-985 cells plated at a density of 1×10^5 cells/ml and grown for 3 d until they reached a density of $\sim 8 \times 10^5$ cells/ml. Cells were spun down, and the medium was harvested and filtered though a 0.22-μm filter.

C5aR–GFP

To create a C5aR–GFP fusion protein, the whole C5aR cDNA in pCDM8 was amplified by PCR between a T7 primer and a C5aR cDNA carboxy-terminal primer, 5′-CGCGATACCGGTACCCACT-GCCTGGGTCTTCTGGGCCATAGTGTC-3′, designed to remove the stop codon and create a *Kpn*I site (underlined bases) for in-frame ligation with the *Kpn*I site of pEGFP-N3, located at the 5′- end of the GFP DNA. The PCR product was cut with *Hin*dIII/*Kpn*I and subcloned into the pEGFP-N3 fusion vector also cut with *Hin*dIII/*Kpn*I. A *Hin*dIII/*Fse*I fragment of the PCR-generated product was replaced by a *Hin*dIII/*Fse*I fragment from the original C5aR cDNA in pCDM8 to circumvent possible mutations in the receptor sequence introduced by PCR. The final ligated product was sequenced though the remaining region generated by PCR.

Generation of Amphotropic Retroviruses

A retroviral approach was used to create a stable population of PLB-985 cells expressing GFP or C5aR–GFP. The C5aR–GFP and GFP DNAs were subcloned into the pLNCX retroviral vector (Miller and Rosman, 1989) under the control of the cytomegalovirus promoter. The retroviral plasmids were transfected into Ψ2 ecotropic packaging cells by calcium/phosphate precipitation. Transiently produced virus was harvested after 48 h and used to transduce amphotropic PA317 packaging cells. Infections were carried out in 8 μg/ml polybrene for 4 h, infected medium was then diluted 1:1 with fresh PA317 culture medium, and cells were incubated an additional 48 h. Transduced PA317 cells were then selected in 0.5 mg/ml of active G-418. After 8–10 d, stable populations of G-418–resistant PA317 cells were established.

Transduction of PLB-985 Cells

PLB-985 cells were cocultured with retrovirally expressing PA317 cells and 8 μg/ml polybrene for 24 h, removed from the PA317 cell monolayer, and plated for 4 h on a new 100-mm culture dish, to separate the PLB-985 cells, which remain in suspension, from contaminating PA317 cells, which adhere to the dish. Transduced PLB-985 cells were selected by incubating an initial concentration of 1×10^5 cells/ml in conditioned medium containing 1.0 mg/ml G-418. Cell medium was changed every other week until confluency was reached ($\sim 1.5 \times 10^6$ cells/ml). Homogeneous populations of GFP- or GFP–C5aR-positive cells were obtained by fluorescence-activated cell sorting (FACS).

Chemotaxis Assays

HEK293 clones expressing the C5aR and C5aR–GFP were generated as described (Neptune and Bourne, 1997). Chemotaxis assays using these cells were performed in 48-well Boyden chambers as described (Neptune and Bourne, 1997).

Binding Assays

PLB-985 cells (2×10^5 cells) were incubated at 4°C for 5 h with various concentrations of [^{125}I]-C5a (400 Ci/mmol, 0.06–3.6 nM) in 200 μl binding buffer containing HBSS, 25 mM HEPES pH 7.4 and 0.1% (wt/vol) bovine serum albumin. Nonspecific binding was defined as the radioactivity bound in the presence of 100 nM nonradioactive C5a. Incubations were terminated by vacuum filtration though presoaked GF/C glass fiber filters (Whatman, Clifton, NJ), followed by rapid washing with 6 ml of ice-cold binding buffer. To determine binding affinities and capacities (K_d and B_{max}), binding data were subjected to nonlinear regression analysis using Prism software (GraphPad Software, San Diego, CA).

Microscopy

Differentiated PLB-985 cells were washed once with 10 ml RPMI 1640/25 mM HEPES and resuspended at a concentration of 3×10^6 cells/ml in modified HBSS (mHBSS) containing 150 mM NaCl, 4 mM KCl, 1.2 mM $MgCl_2$, 10 mg/ml glucose, and 20 mM HEPES, pH 7.2. Cells (3×10^5 in 100 μl) were plated on the center of a sterile no. 1.5 coverslip rimmed with a square agarose spacer 10 mm in length and 1 mm in height. The coverslip was incubated in a humid chamber at 37°C with 5% CO_2 for 20 min, and nonadherent cells were removed by two washes with mHBSS. Cells were stimulated at room temperature, either uniformly or from a point source of chemoattractant delivered with a micropipette. In the latter case, micropipettes were prepared from a borosilicate capillary with an outer diameter of 1.0 mm and an inner diameter of 0.58 mm using a model P-80/PC Flamming Brown Micropipet Puller (Sutter Instruments, Novato, CA) with step 1: heat = 635; velocity = 20; time = 1; step 2: heat = 605; pull = 160; velocity = 75; time = 25. Under these pulling conditions, the tip of the micropipette is sealed. The micropipette was back-filled with a solution of 10 μM fMLP or 100 μM ChaCha in mHBSS and lowered in focus into the center of the microscope's field of view with a micromanipulator (Narishige USA, Greenvale, NY). The micropipette's tip was broken by touching the side of a broken coverslip. When necessary, air bubbles were pushed out of the micropipette tip by applying a small pressure using a microinjection device. Under these conditions, the broken tip of the micropipette was 0.2 μm or less in diameter and produced more dramatic and more reproducible neutrophil chemotaxis toward the micropipette than did commercially available micropipettes with 0.5-μm tips (Eppendorf Femtotips).

All images were acquired with a scientific-grade cooled charged-coupled device on a multiwavelength wide-field three-dimensional microscopy system (Hiraoka *et al.*, 1991) in which the shutters, filter wheels, focus movement, and data collection were all computer driven. Cells were imaged using a 60 × 1.4 N.A. lens (Olympus, Lake Success, NY) and n = 1.518 immersion oil. Differential interference contrast images were acquired with a Nomarski system optimally aligned for our microscope system. For fluorescence imaging of living cells, the GFP and DiD signals were acquired in the FITC and Texas Red channels, respectively, on single optical sections (0.25 μm) near the bottom of cells. These conditions, at our microscope setting, produce partial confocal images of the samples (Hiraoka *et al.*, 1990). For fluorescence imaging of fixed cells, data stacks of immunofluorescent samples were acquired in the FITC and Texas Red channels by moving the stage in successive 0.25-μm focal planes through the sample. Out-of-focus light was removed with a constrained iterative deconvolution algorithm (Agard *et al.*, 1989).

To quantify the relative distribution of receptors within the plasma membrane, DiD and GFP signals were digitally recorded in their respective channels, and total fluorescence intensity of each was determined in five polygons of fixed area, placed at the front and sides of four separate cells. Fluorescence values were divided by the number of pixels, basal fluorescence (based on fluorescence outside the cell) subtracted, and values for the two probes normalized relative to the maximum fluorescence observed in an individual cell for GFP or DiD. Then the ratio of fluorescence intensity of GFP to that of DiD was calculated for each polygon. Mean ± SEM of the ratios for the 20 polygons (4 cells, 5 polygons in each) was calculated.

Immunoblotting

Cells (5×10^6) were lysed in 500 μl SDS sample buffer, and cell extracts were resolved on 8% polyacrylamide gel and transferred onto polyvinylidene difluoride membranes. GFP and C5aR–GFP were detected by immunoblotting with a monoclonal GFP antibody.

Immunostaining of Cell-Surface Receptors

Differentiated PLB-985 cells were plated as already described on etched grid coverslips, stimulated with a point source of chemoattractant, and fixed for 20 min by flooding with an excess of 3.7% paraformaldehyde in cytoskeleton buffer containing 10 mM HEPES, pH 7.2, 138 mM KCl, 3 mM $MgCl_2$, 2 mM EGTA, and 0.32 M sucrose. The location of cells responding to the micropipette was then recorded on the grid coverslip, which contains 520 alphanumeric coded squares. Cells were then washed twice in phosphate buffered saline, incubated for 20 min in a blocking solution (blotto) containing 50 mM Tris-HCl, pH 7.5, 1 mM $CaCl_2$, and 3% dry milk, followed by a 45-min incubation with a polyclonal anti-C5aR antibody (5 μg/ml in blotto). This antibody competes against C5a for binding to its receptor but not against carboxy-terminal analogues of C5a (Morgan *et al.*, 1993). After three successive washes in a solution containing 25 mM Tris-HCl, pH 7.4, 140 mM NaCl, 2.5 mM KCl, and 1 mM $CaCl_2$, the cells were incubated with Texas Red-conjugated goat anti-rabbit IgG (1:100 dilution in blotto) for 20 min. They were then washed three times, mounted in Vectashield, and sealed on a slide with clear nail polish.

Plasma Membrane Labeling with DiD

Differentiated PLB-985 cells were washed as already described. DiD (5 mg/ml in ethanol) was added to the cell suspension (in mHBSS) to a final concentration of 3.3 μg/ml. Cells were thoroughly mixed with the dye, and 3×10^5 cells (in 100 μl) were plated on each glass coverslip. After an incubation of 20 min at 37°C, cells were washed twice with mHBSS and kept in the dark at room temperature until analysis. After long incubations, DiD labels intracellular membranes to some degree (including pinocytotic vesicles). However, we quantified DiD:GFP ratios (see above) only for fluorescent signals at the plasma membrane.

RESULTS

Responses of PLB-985 Cells to Chemoattractant

Morphological and behavioral responses of differentiated PLB-985 cells to chemoattractant closely resemble those of blood neutrophils. In the experiment shown in Figure 1, a micropipette filled with 10 μM fMLP is positioned in front of three polarized cells. Within 30 sec, cell *a* shows intense ruffling at its leading edge (Figure 1A, arrows; a video of the experiment described in this figure is available on the internet version of this paper, at http://www.molbiolcell.org). In response to successive movements of the pipette (Figure 1, B–F), cell *a* extends new pseudopodia (arrowheads), reorients, and crawls toward the pipette. Repositioning the micropipette near cells *b* and *c* (Figure 1, G and H) causes these cells to respond and extend pseudopodia toward the micropipette, while cell *a* continues to follow. Upon removal of the chemoattractant source (Figure 1I), the three cells retract their pseudopodia but keep their polarized morphology.

After differentiation, 50–75% of the PLB-985 cells are unpolarized in the absence of chemoattractant (Figure 1J) but polarize rapidly in response to a pipette containing chemoattractant (Figure 1, K and L). Some cells in the differentiated population, unlike neutrophils, retract their uropods ineffectively, resulting in the formation of long membrane extensions at their back (Figure 1, cell *a*, panels C–D). In addition, some cells (our unpublished data) show no morphological response to uniform or pipette-delivered chemoattractant; we suspect that such cells are not fully differentiated.

Expression of recombinant genes in PLB-985 cells does not affect the response to a chemotactic gradient (Figure 2; a video of the experiment described in this figure is available on the internet version of this paper, at http://www.molbiolcell.org). Using a retroviral vector, DNA-encoding GFP was transferred into undifferentiated PLB-985 cells. A population of transduced cells, selected for resistance to G-418 (see MATERIALS AND METHODS), was further selected (by FACS) for expression of GFP. GFP expression in this population is robust but varies significantly from cell to cell (compare cells *b*, *d*, and *e*, Figure 2A). In the experiment depicted in Figure 2, five GFP-expressing cells (previously induced to differentiate by exposure to DMSO; see MATERIALS AND METHODS) rapidly extend pseudopodia toward the micropipette delivering fMLP (Figure 2B, arrowheads) and crawl toward it until they meet in the center of the field (Figure 2, C–F).

A Functioning C5aR–GFP Chimera Is Expressed at the Cell Surface

To observe the subcellular distribution of a chemoattractant receptor in living cells, we attached GFP to the carboxy terminus of the human C5aR. Figure 3 shows that the C5aR–GFP chimera can mediate chemotaxis in HEK293 cells and is targeted to the plasma membrane of PLB-985 cells. Because the C5aR is normally present in neutrophils (Gerard and Gerard, 1991), we chose to test the ability of the chimera to mediate chemotaxis in stably transfected HEK293 cells; the C5aR–GFP and the wild-type C5aR mediate chemotaxis over the same range of C5a concentrations (Figure 3, A and B). The C5aR–GFP also supports chemotaxis in stably transfected avian DT-40 pre-B cells (our unpublished data). In PLB-985 cells, immunoblots with anti-GFP antibody show a major 70-kDa band, the size expected for the C5aR–GFP chimera (Figure 3B, lanes 2 and 3). Anti-GFP antibody does not reveal smaller proteins corresponding to the size of free GFP (27 kDa) (Figure 3B).

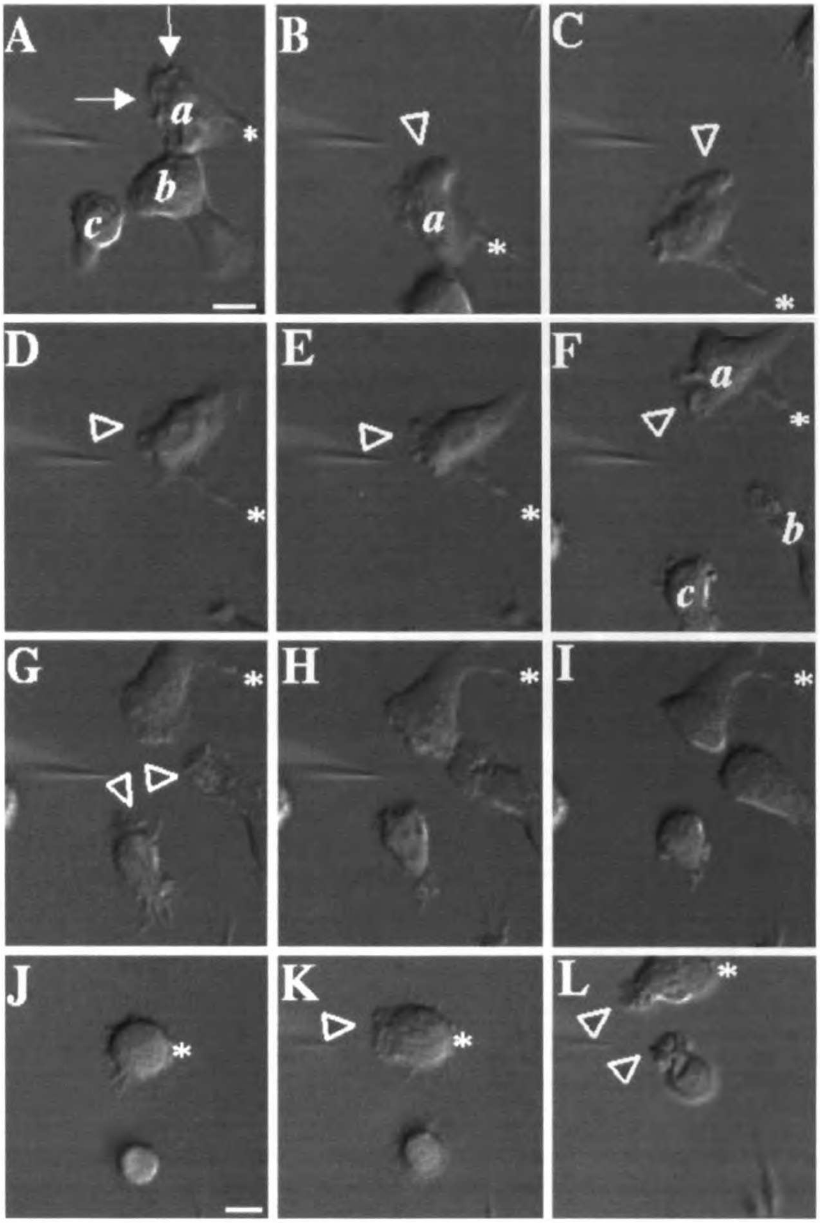

Figure 1. Responses of differentiated PLB-985 cells to a point source of chemoattractant. PLB-985 cells were differentiated by treatment with 1.3% DMSO for 7 d and plated on glass coverslips. Cells were then stimulated with fMLP (10 μM) delivered from a micropipette, and images were recorded every 5 s as described in MATERIALS AND METHODS. Panels A–I show morphological responses after (A) 30, (B) 90, (C) 150, (D) 210, (E) 240, (F) 270, (G) 300, and (H) 360 s of micropipette stimulation; panel I shows the same cells 90 s after removal of the micropipette. Panels J–L show responses of nonpolarized cells after (K) 30 and (L) 140 s exposure to fMLP in the micropipette. Arrows point to chemoattractant-stimulated membrane ruffles. Arrowheads point to newly formed or reorienting pseudopodia. Asterisks indicate stable points of reference in panels A–I and J–L, respectively, to allow the reader to appreciate movement of the micropipette. This session is representative of three similar observations. Bar, 10 μm. A video of the experiment described in this figure is available on the internet version of this paper, at http://www.molbiolcell.org.

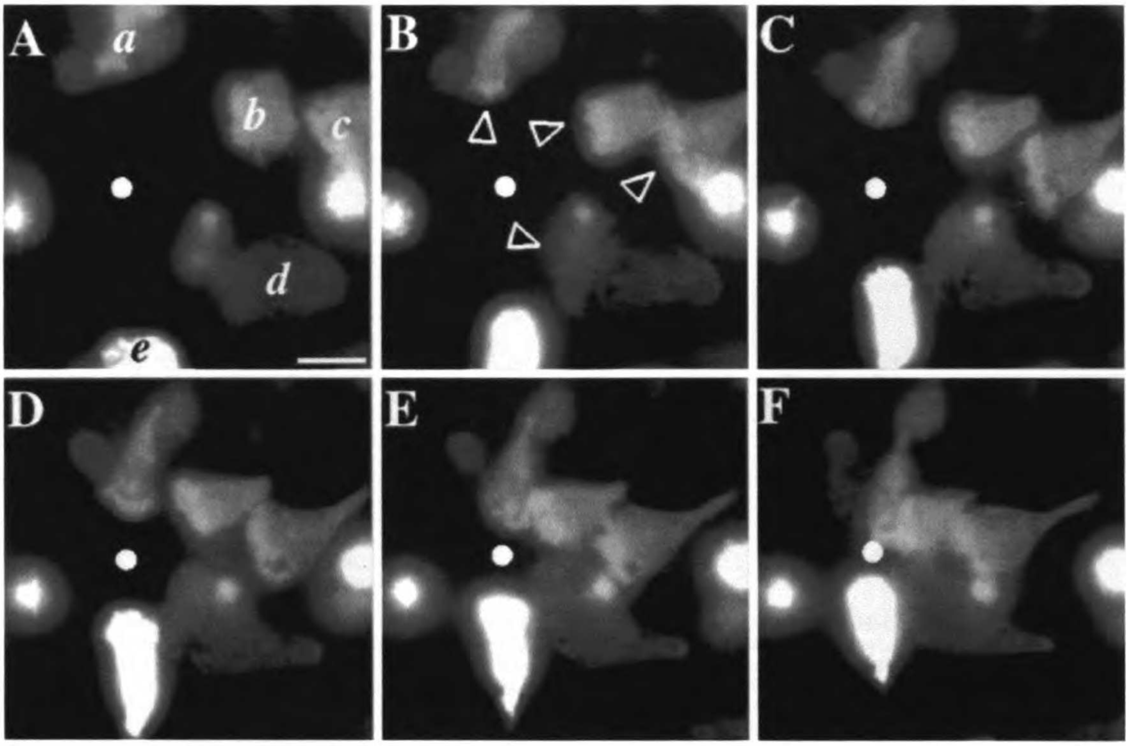

Figure 2. Chemotactic behavior of PLB-985 cells stably expressing GFP introduced by a retroviral vector. Cells were infected, selected in G-418, and sorted by FACS for GFP fluorescence, as described in MATERIALS AND METHODS. GFP-expressing cells were differentiated in 1.3% DMSO for 7 d and plated on glass coverslips. Cells were then stimulated with fMLP (10 μM) delivered from a micropipette (white dot), and images were recorded every 5 s, under pseudoconfocal conditions, as described in MATERIALS AND METHODS. Panels A–F show responses after (A) 0, (B) 60, (C) 120, (D) 180, (E) 240, and (F) 300 s. Arrowheads point to pseudopodia advancing in response to the agonist. This session is representative of two similar observations. Bar, 10 μm. A video of the experiment described in this figure is available on the internet version of this paper, at http://www.molbiolcell.org.

The C5aR–GFP chimera is expressed on the plasma membrane of PLB-985 cells. Using a retroviral vector, the gene encoding C5aR–GFP was transferred into nondifferentiated PLB-985 cells. Transduced cells were then selected and GFP-positive cells sorted by FACS (see MATERIALS AND METHODS). As expected for a membrane-bound protein, the C5aR–GFP fluorescent signal in differentiated cells is enriched at the cell periphery (Figure 4, A and A'). Saturation-binding experiments performed with [^{125}I]-C5a reveal that expression of the C5aR–GFP chimera increased maximal binding of C5a at the cell surface by ~60%, relative to cells expressing the endogenous C5aR (Figure 3C): K_d and B_{max} values (mean ± SD of 3 determinations) were 0.51 ± 0.06 nM and 63,900 ± 7500 sites/cell for C5aR-GFP–expressing cells, and 0.57 ± 0.23 nM and 40,900 ± 6100 sites/cell for cells expressing GFP alone (not fused to the C5aR). Both B_{max} values are within the range previously reported for the C5aR of neutrophils (Huey and Hugli, 1985; Drapeau *et al.*, 1993). Fluorescence intensities of individual cells, however, vary by as much as 10-fold, as determined by FACScan analysis (our unpublished data). Thus the number of C5aR–GFP molecules in the PLB-985 cells we examined ranges from ~8000 to ~80,000 per cell. Nonetheless, the cell-surface location of the C5aR–GFP protein on moving PLB-985 cells does not depend on the level of its expression (see Figure 5, compare cells *a* and *d*).

Distribution of the C5aR-GFP in PLB-985 Cells

Exposure of PLB-985 cells to a uniform concentration of C5a causes agonist-induced internalization of a portion of some C5aR-GFP molecules, but the distribution of receptors at the cell surface remains uniform even when the cells polarize in response to the chemoattractant. In the experiment summarized in Figure 4,

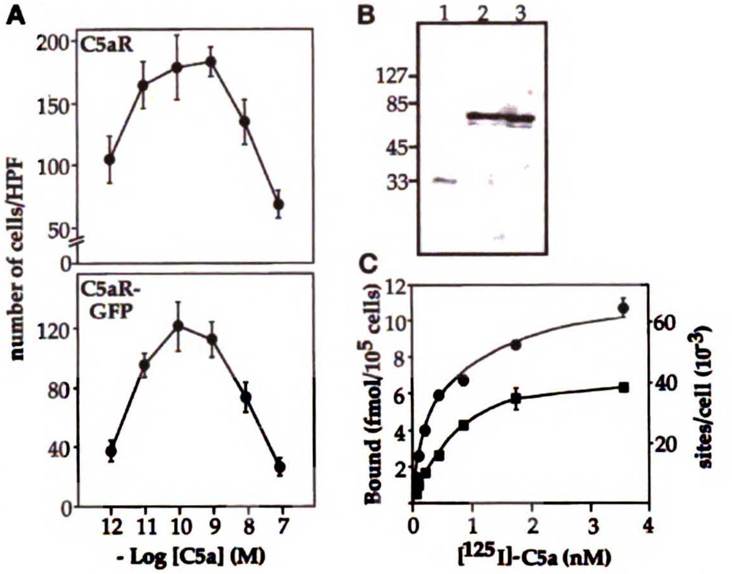

Figure 3. Characterization of the C5aR-GFP chimera. (A) C5aR–GFP can mediate chemotaxis. HEK293 cells stably expressing either the C5aR or the C5aR–GFP fusion protein were subjected to a migration assay in a 48-well Boyden chamber, as described previously (Neptune and Bourne, 1997). At the end of the assay, cells adhering to the lower side of the porous filter were fixed, stained, and counted using a microscope. Results are expressed as the number of cells counted in a high-power field (HPF) (200×) and correspond to the mean ± SD of four determinations. Similar results were obtained in four other experiments. Absolute numbers of migrated cells in the experiment shown do not reflect different abilities of the two cell types to migrate toward C5a; instead, the absolute numbers reflect the numbers of each cell type used in each well (22,500 and 37,500 cells expressing the C5aR–GFP or the C5aR, respectively). (B) Integrity of the C5aR–GFP fusion protein in differentiated PLB-985 cells. PLB-985 cells were transduced with a retrovirus carrying C5aR–GFP as described in MATERIALS AND METHODS. Transduced cells were selected and GFP-positive cells were sorted by FACS. Cell extracts were prepared from 5 × 10^6 differentiated cells as described in MATERIALS AND METHODS, resolved on 8% polyacrylamide, and transferred onto a polyvinylidene difluoride membrane. GFP and the C5aR–GFP were then revealed with a monoclonal GFP antibody. Lane 1, extract from 10^5 GFP-expressing cells; lanes 2 and 3, extracts from two different aliquots, each representing 3 × 10^5 C5aR-GFP–expressing cells. (C) Binding of [^{125}I]-C5a to PLB-985 cells. Differentiated GFP-expressing cells (squares) and C5aR-GFP–expressing cells (circles) were incubated at 4°C for 5 h with the indicated concentrations of [^{125}I]-C5a (0.06–3.6 nM). Nonspecific binding was evaluated in the presence of 100 nM nonradioactive C5a. Incubations were terminated by rapid filtration though GF/C filters. In the experiment shown, nonlinear regression analysis of the binding data yielded B_{max} values of 68,400 sites/cell and 47,600 sites/cell for C5aR–GFP and GFP-expressing PLB-985 cells, respectively. Similar results were obtained in two additional experiments.

receptor distribution in five cells is recorded in living cells under pseudoconfocal conditions (Hiraoka *et al.*, 1990) (a video of the experiment described in this figure is available on the internet version of this paper, at http://www.molbiolcell.org). Within 56 s of C5a treatment, clusters of C5aR–GFP begin to form at the plasma membrane (Figure 4, C and C′, arrows). Later time points (Figure 4, D and E) reveal considerable internalization of C5aR–GFP, in addition to a dramatic change in cell morphology. Cells increase in size, owing to agonist-induced spreading and increased adhesion on the glass coverslip (Figure 4, D and E). After exposure to C5a for 3 min, four of the five cells clearly exhibit front-tail polarity, and internalized receptors are concentrated in their uropods (Figure 4, F and F′, arrowheads). C5aR–GFP remaining at the cell surface, however, remains uniformly distributed through the plasma membrane, qualitatively (Figure 4, F and F′) and as indicated by a scan of fluorescence intensity (Figure 4G).

Expression of the C5aR–GFP does not impair the ability of PLB-985 cells to respond to chemoattractant (Figure 5; a video of the experiment described in this figure is available on the internet version of this paper, at http://www.molbiolcell.org). In this experiment, visualized under pseudoconfocal conditions, cells orient and move toward a point source of a C5aR agonist, ChaCha (Konteatis *et al.*, 1994), delivered by micropipette. Their behavior mimics in detail that described for neutrophils under similar circumstances (Zigmond, 1974; Gerisch and Keller, 1981). The micropipette is first positioned in the middle of a field containing five cells (Figure 5A). Within 44–110 s, all cells in the field show clear responses to the ChaCha gradient (Figure 5, B and C). Cell *a*, which was already polarized toward the center of the cell cluster before stimulation (Figure 5A), now exhibits extensive ruffling at its front; cells *c* and *d* are clearly polarized and also exhibit ruffling at their fronts (Figure 5B, arrowheads). The back of cell *b*, characterized by its retraction fibers (Figure 5A, filled arrowhead), transforms into a new leading edge that moves toward the micropipette, while cell *e* turns its front toward the micropipette (Figure 5B). At later time points, all cells in the field converge and crawl toward the micropipette (Figure 5, D–F); additional cells, not in the field at the beginning of the experiment, also make their way up the ChaCha gradient (Figure 5D).

Figure 5 also shows that C5aR–GFP fluorescence remains uniformly distributed on the surface of cells

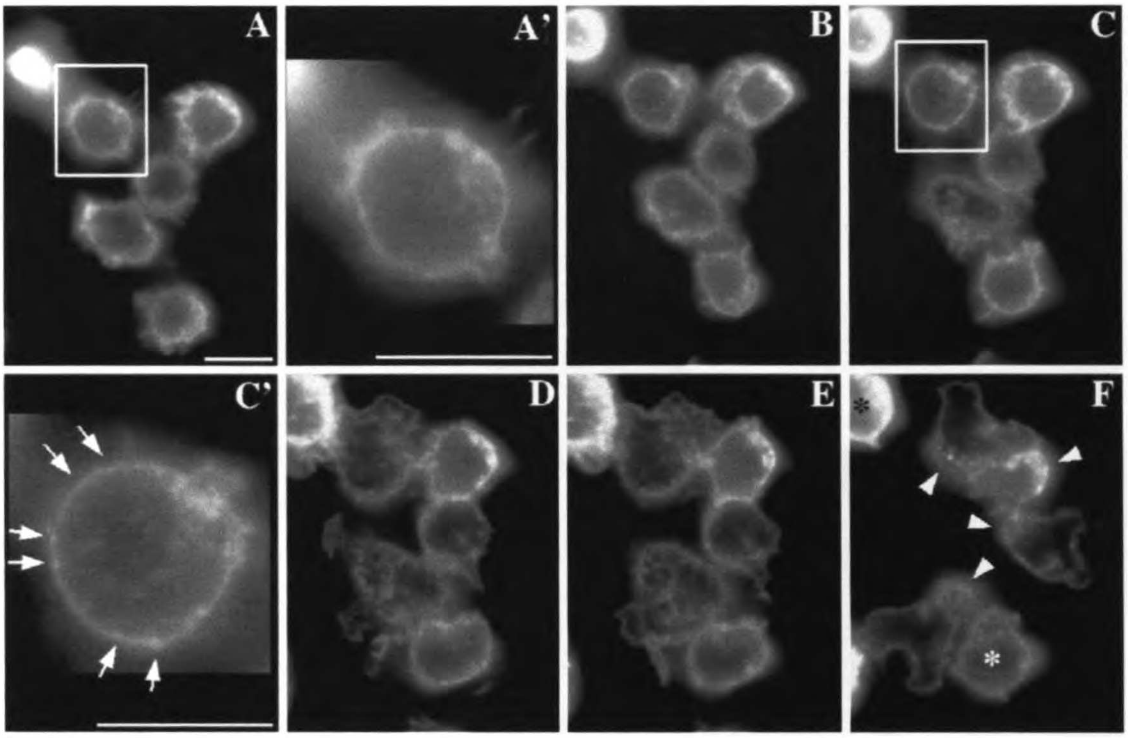

Figure 4. C5aR–GFP dynamics after stimulation of PLB-985 cells with a uniform concentration of C5a. C5aR-GFP–expressing PLB-985 cells were differentiated with 1.3% DMSO, plated on glass coverslips, and exposed to a uniform concentration (20 nM) of C5a in mHBSS; images were recorded every 2 s, under pseudoconfocal conditions, as described in MATERIALS AND METHODS. Responses are shown after (A) 0, (B) 28, (C) 56, (D) 140, (E) 168, and (F) 308 s. Panels A' and C' show magnifications of the cells indicated in panels A and C, respectively. Panel F' shows a magnification of panel F. Panel G shows a fluorescence intensity scan analysis of the cell in the lower left corner in panels F and F'. Arrows point to agonist-stimulated receptor patches. Arrowheads (in F and F') point to internalized receptors located in the uropod of polarized cells. The asterisks in panel F indicate cells that spread but did not clearly develop a polarized morphology after stimulation. This session is representative of three similar observations. Bar, 10 μm. A video of the experiment described in this figure is available on the internet version of this paper, at http://www.molbiolcell.org.

orienting and moving toward the ChaCha-containing micropipette, just as in the case of cells exposed to a uniform concentration of chemoattractant (see Figure 4). The agonist delivered by micropipette also induces accumulation of internalized C5aR–GFP in the uropods of polarized cells (Figure 5F, red arrowheads) within a time scale similar to that seen in uniformly stimulated cells (Figure 4). Nonetheless, most cells show no relative increase of fluorescence intensity anywhere on the cell surface, not even at the leading edge. Trailing portions of certain cells show an apparent decrease in fluorescent signal (Figure 5, C and E, arrows), but focusing up and down showed that this appearance reflects a difference in cell shape at the trailing edge, where the cell flattens and terminates in retraction fibers (see Figure 1A, cells *a* and *b*). Consequently, focusing on the front and midregion of cells causes a loss of fluorescence intensity at the back.

C5aR–GFP Fluorescence Is Proportional to Membrane Surface

By itself, the C5aR–GFP fluorescent signal may not reflect with precision the density of receptor molecules per unit area of plasma membrane. For example, we sometimes observed an apparent enrichment of C5aR–GFP fluorescence at the anterior poles of moving cells (see Figure 5C, cells *b* and *c*), and therefore asked whether this resulted from an increased density of receptors or from an increased amount of plasma membrane, which might be folded more extensively at a cell's leading edge. The experiments shown in Figures 6 and 7 indicate that the latter explanation is correct.

In the three cells shown in Figure 6, each stimulated by a point source of ChaCha, plasma membranes are labeled with a membrane probe, DiD. C5aR–GFP and DiD signals are alternatively recorded, in the FITC and

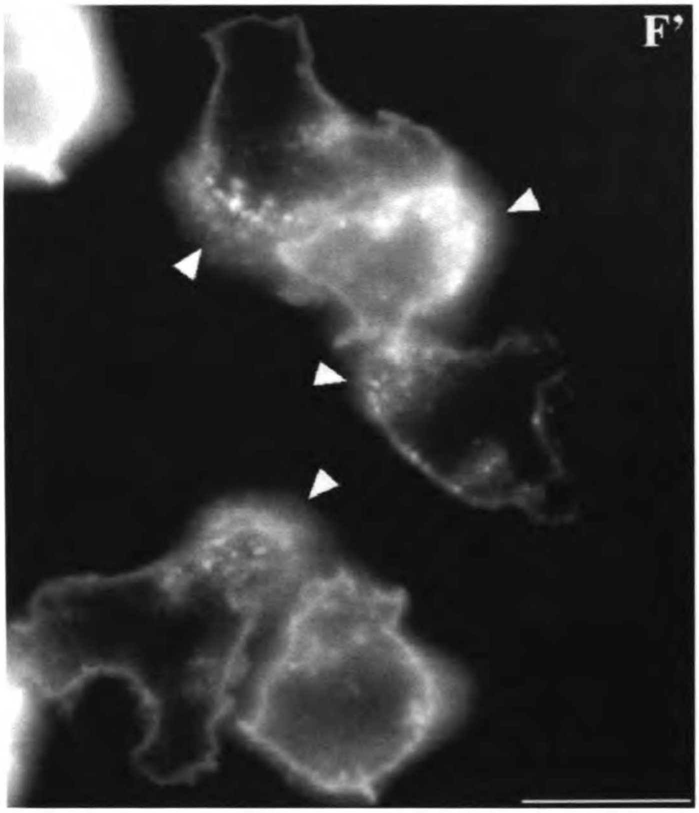

Figure 4 (cont).

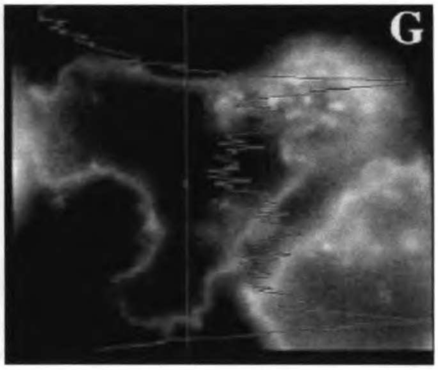

Texas Red channels, respectively. The cells in panels A and C crawl toward the micropipette (shown by the white dot) while the cell in panel B polarizes toward it. At this magnification it is possible to appreciate the complexity of the fluorescent signal at the leading edge (Figure 6, arrows), which reflects ruffles or folds of the plasma membrane caused by dramatic reorganization of the actin cytoskeleton beneath it (Weiner, Servant, Sedat, and Bourne, manuscript in preparation). Under these conditions, the cell in panel A and (to a lesser extent) cells in panels B and C exhibit greater C5aR–GFP fluorescence at their anterior poles where the membrane folds are more complex. DiD fluorescence is also higher at the anterior poles of the cells; indeed, distributions of the C5aR–GFP and DiD signals are superimposable. We infer that the apparent increases in C5aR–GFP concentration reflect increases in relative abundance of plasma membranes, rather than preferential accumulation of receptors, at the leading edge. Quantification of the GFP and DiD signals in 20 patches of membrane (see MATERIALS AND METHODS) revealed a ratio of fluorescence intensities for the two probes (GFP:DiD) of 1.08 ± 0.05 (mean ± SEM of 20 determinations performed in 4 separate cells migrating toward chemoattractant). This ratio does not differ significantly from 1.0; we cannot, however, rule out a very small change ($< 8\%$) in receptor distribution.

To test this inference more stringently, we examined C5aR–GFP and DiD distribution in a different way (Figure 7). In this experiment, the C5aR–GFP and DiD signals are acquired on a fixed cell in successive 0.25-μm focal planes through the sample, and out-of-focus light is removed with a constrained iterative deconvolution algorithm (Agard *et al.*, 1989). Maximum intensity projections of all the three-dimensional data stacks from a polarized cell clearly show membrane enrichment and concomitant enrichment of receptor density at the leading edge (Figure 7A, arrow). Figure 7B shows a single focal plane of the cell in panel A. Once again, the leading edge shows parallel enrichment of DiD and C5aR–GFP fluorescence in a pattern that suggests the existence of complex folds even within a thin section. Together these results indicate that asymmetric distribution of plasma membrane folds can alter the apparent distribution of a mem-

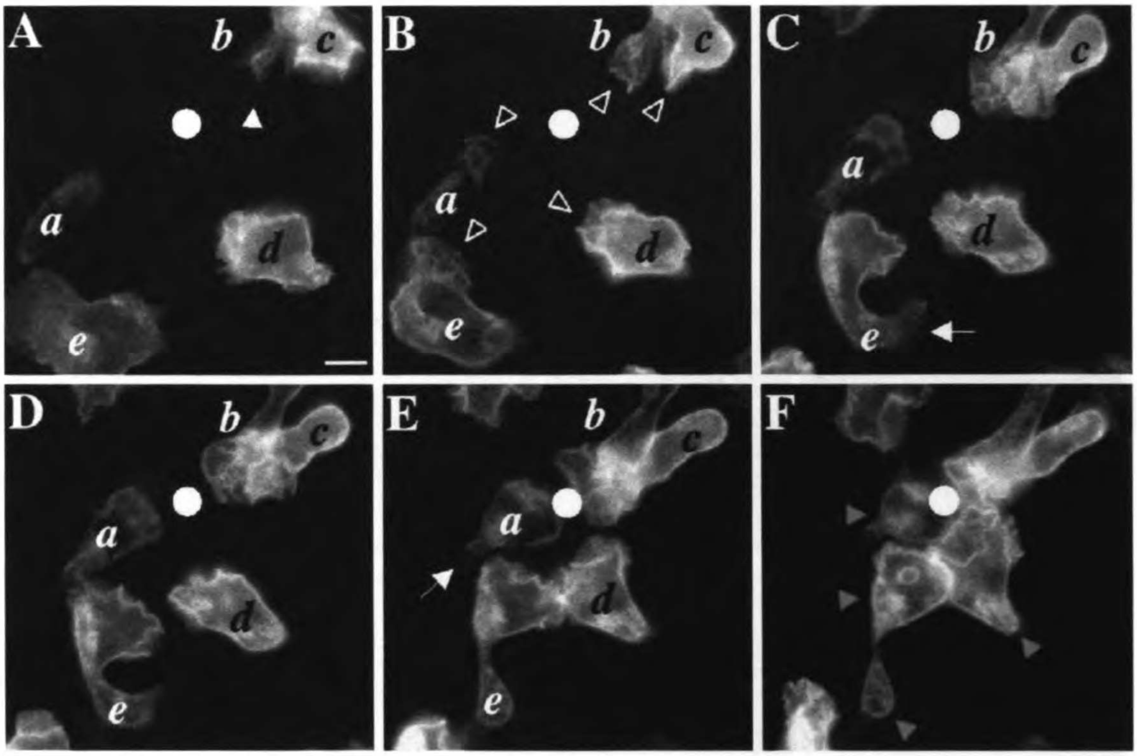

Figure 5. C5aR-GFP dynamics after stimulation of PLB-985 cells with a point source of ChaCha delivered from a micropipette. C5aR-GFP-expressing cells were differentiated with 1.3% DMSO and plated on glass coverslips. Cells were then stimulated with ChaCha (100 μM) delivered from a micropipette, and images were recorded every 2 s, under pseudoconfocal conditions, as described in MATERIALS AND METHODS. Responses are shown after (A) 0, (B) 44, (C) 110, (D) 154, (E) 176, and (F) 220 s of micropipette stimulation (white dot). The closed arrowhead in panel A points to the retraction fibers of cell *b*. Open arrowheads (panel B) point to ruffles at the leading edges of locomoting cells. Arrows in panels C and E point at the back of polarized cells. Red arrowheads (panel F) point to internalized C5aR–GFP. This session is representative of three similar observations. Bar, 10 μm. A video of the experiment described in this figure is available on the internet version of this paper, at http://www.molbiolcell.org.

brane protein detected by fluorescence microscopy, which has been extensively utilized to localize chemoattractant receptors on leukocytes (Schmitt and Bultmann, 1990; McKay *et al.*, 1991; Nieto *et al.*, 1997). The results also point to a potential limitation of confocal microscopy: apparent enrichment of a protein may reflect tight folds of the plasma membrane, rather than changes in concentration of the protein per square micron of membrane.

Receptors Accessible to the Ligand Are Also Uniformly Distributed

The experiment shown in Figure 8 rules out an alternative mechanism that neutrophils might use to amplify a chemotactic gradient. In this hypothetical mechanism, intensity of the extracellular signal is increased at the front because receptors at the back of the cell are sequestered in a compartment not accessible to ligand, but located just under the plasma membrane; if so, C5aR–GFP would appear uniformly distributed, even though a larger fraction of the receptors at the front of the cell would be able to detect the chemoattractant. To test the hypothesis, C5aR-GFP–expressing cells are stimulated with a point source of ChaCha and fixed, and receptors are assessed both by the C5aR-GFP fluorescent signal and with an antibody raised against a peptide corresponding to the extracellular amino terminus of the C5aR (Morgan *et al.*, 1993). Because this antibody does not compete against C5a analogues for binding to the C5aR (Morgan *et al.*, 1993), it is possible to localize cell surface receptors after stimulation with ChaCha. Figure 8 shows a C5aR-GFP–expressing cell fixed while crawling toward ChaCha, delivered by a micropipette (the arrow-

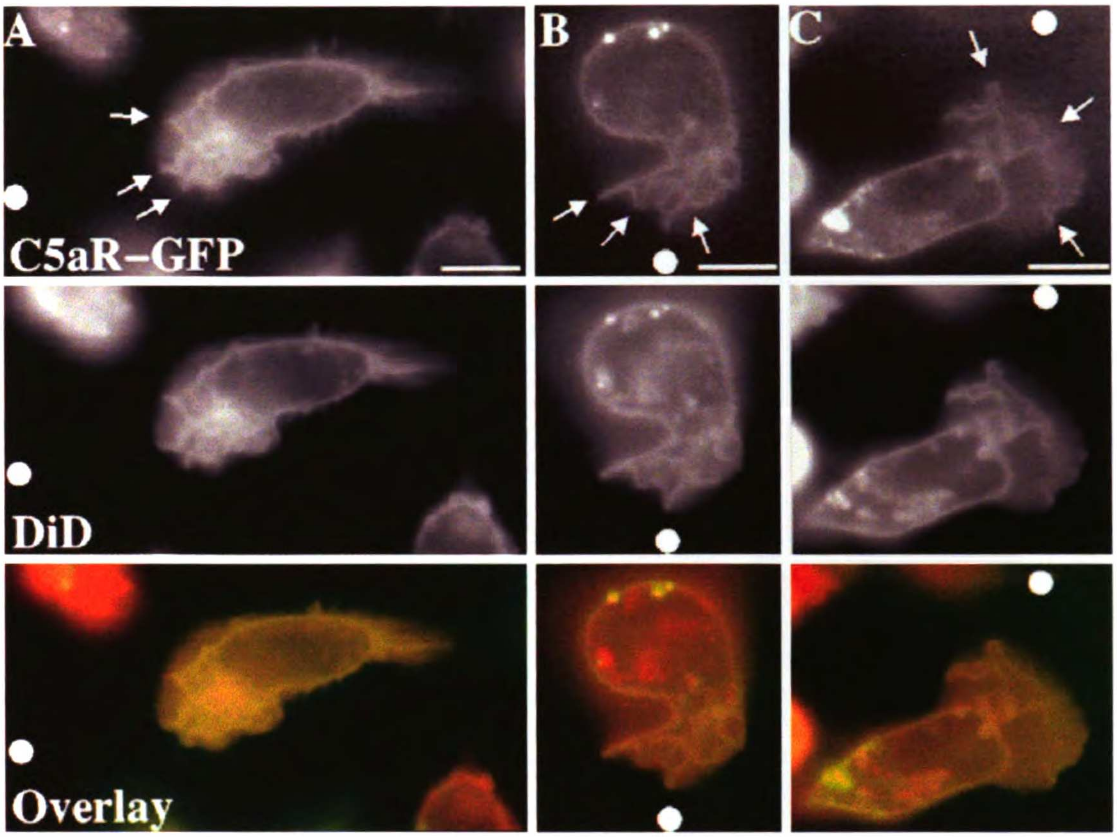

Figure 6. Localization of C5aR–GFP relative to the plasma membrane of moving PLB-985 cells. C5aR-GFP–expressing cells were differentiated with DMSO 1.3%, labeled with DiD, and plated on glass coverslips. Cells were then stimulated with ChaCha (100 μM) delivered from a micropipette. Under pseudoconfocal conditions, the GFP and DiD signals were alternatively recorded in the FITC and Texas Red channels, respectively, as described in MATERIALS AND METHODS. Single cells, from three different experiments, are shown crawling toward the source of ChaCha (white dot). Arrows point to the ruffling fronts of the cells. Bar, 10 μm.

head indicates the direction of migration). Neither the fluorescence specific for the anti-C5aR antibody nor that emitted by C5aR–GFP is enriched at the surface of the cell's leading edge, compared with the back. The C5aR–GFP and the antibody signals overlap, with the exception of the intracellular pool of internalized C5aR–GFP (overlay, arrows).

DISCUSSION

Many investigators have sought to identify and dissect the working parts of the sophisticated guiding system that neutrophils use to find bacteria at sites of infection (Devreotes and Zigmond, 1988; Downey, 1994; Perez, 1994; Bokoch, 1995; Prossnitz and Ye, 1997). Two kinds of observations suggest that this system depends, in part, upon relatively enhanced sensitivity to chemoattractant of the crawling neutrophil's leading edge. First, such cells tend to preserve the same leading edge, often preferring—like cell *e* in Figure 5, above—to turn toward an incoming new chemotactic gradient rather than to form a new front (Zigmond, 1977; Zigmond *et al.*, 1981). Second, neutrophils crawl up a very shallow gradient with little apparent deviation from a straight course, even when the concentration of chemoattractant at the leading edge is only 1% greater than that at the cell's trailing edge. Together, these findings indicate that asymmetric sensitivity of the guidance system itself accompanies the polarized morphology of a neutrophil. An attractive explanation (Zigmond, *et al.*,

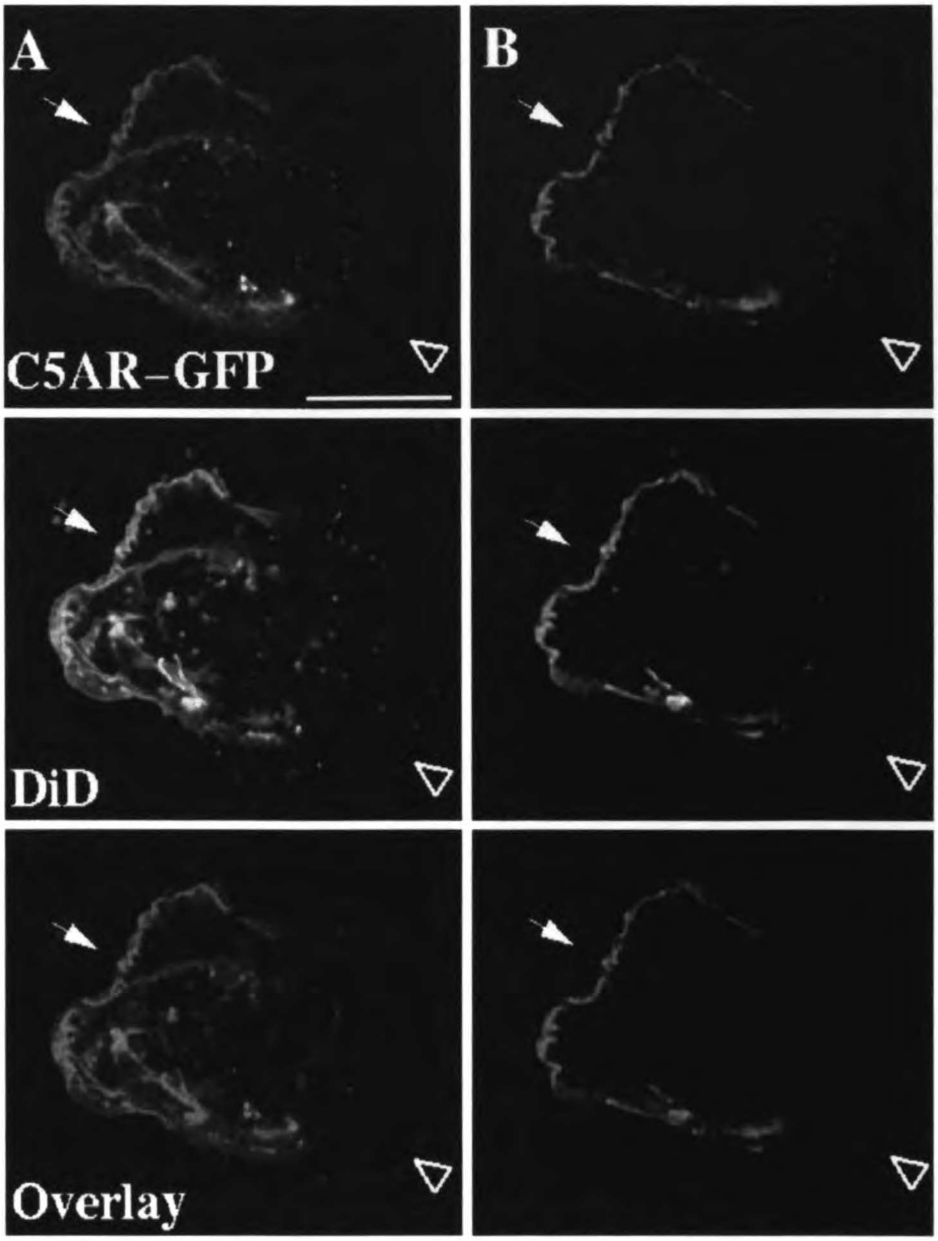

Figure 7. Localization of C5aR–GFP relative to the plasma membrane of fixed PLB-985 cells. C5aR-GFP–expressing cells were differentiated with 1.3% DMSO, labeled with DiD, and plated on glass coverslips. Cells were then stimulated with a uniform concentration (20 nM) of C5a for 3 min at room temperature and fixed. The GFP and DiD signals were acquired alternatively in the FITC and Texas Red channels, respectively, as described in MATERIALS AND METHODS in successive 0.25-μm focal planes through the sample; out-of-focus light was removed with a constrained iterative deconvolution algorithm (Agard et al., 1989). (A) Maximum intensity projections of three-dimensional data stacks from a polarized DiD-stained, C5aR-GFP–expressing-cell. (B) A single focal plane of the cell in panel A. The arrow and arrowhead point to the front and the back of the cell, respectively. Bar, 10 μm.

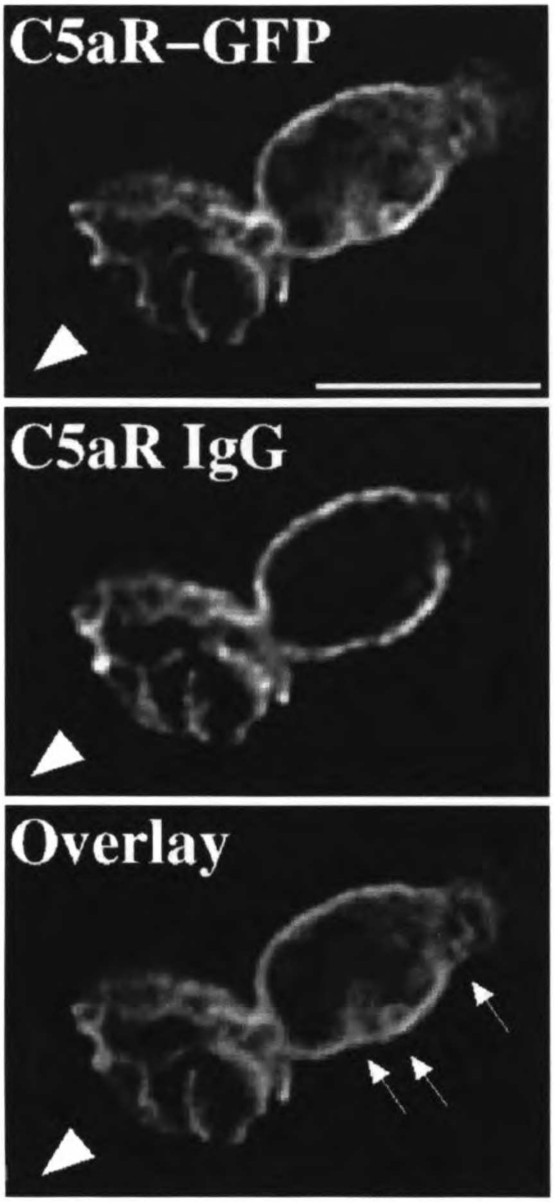

Figure 8. Immunostaining of cell-surface C5aRs. C5aR-GFP–expressing cells were differentiated with 1.3% DMSO and plated on glass-etched grid coverslips. Cells were stimulated with a point source of ChaCha (100 μM) delivered by a micropipette and fixed. Locations of cells responding to the micropipette were recorded, and immunofluorescence of surface C5aR was assessed as described in MATERIALS AND METHODS. The GFP and IgG signals were acquired alternatively in the FITC and Texas Red channels, respectively, as described in MATERIALS AND METHODS, in successive 0.25-μm focal planes through the sample; out-of-focus light was

Figure 8 (cont). removed with a constrained iterative deconvolution algorithm (Agard *et al.*, 1989). Images represent a single 0.25-μm focal plane near the bottom of the cell. The arrowhead indicates the direction of migration. Arrows point to internalized clusters of C5aR–GFP. These results were reproduced in one additional independent experiment. Bar, 10 μm.

1981; Cassimeris and Zigmond, 1990) for increased sensitivity and persistence of the neutrophil's leading edge is that the chemoattractant receptors themselves accumulate at a higher concentration at the front of the cell. To our knowledge, the present study is the first to test this hypothesis in living neutrophils engaged in chemotaxis. Our results, with differentiated PLB-985 cells expressing a GFP-tagged C5aR, indicate that this hypothesis is not correct. Instead, our results agree with observations in cells of a unicellular organism, *Dictyostelium discoideum*: receptors for cAMP, a chemoattractant for this organism, maintain an even distribution throughout the cell surface during chemotaxis toward a pipette containing cAMP (Xiao *et al.*, 1997).

Here we discuss the relevance of PLB-985 cells for understanding neutrophil chemotaxis, discrepancies between our findings and previous reports, and potential mechanisms that could explain increased sensitivity of the leading edge to chemoattractant, without invoking differential distribution of receptors.

PLB-985 Cells as a Model for Neutrophil Behavior

The PLB-985 cell line was established from cells in the peripheral blood of a patient with acute nonlymphocytic leukemia (Tucker *et al.*, 1987). Growth of these cells in the presence of DMSO induces granulocytic maturation, indicated by morphology, histochemical staining, production of superoxide anions, and increased synthesis of the primary granule proteinases, elastase and cathepsin G (Dana *et al.*, 1998). PLB-985 cells differentiated in the presence of DMSO provide an accurate model for studying neutrophil chemotaxis, as indicated by the following evidence: first, such cells behave like neutrophils when challenged with either a uniform concentration or a gradient of chemoattractant (Figures 1, 2, 4, and 5). Exposed to a uniform concentration of chemoattractant, PLB-985 cells adhere and spread on glass coverslips; some cells then polarize in random directions, much like neutrophils (Davis, *et al.*, 1982; Sullivan, *et al.*, 1984; Walter and Marasco, 1984; Cassimeris and Zigmond, 1990; McKay *et al.*, 1991; Gray *et al.*, 1997). In contrast—again like neutrophils—differentiated PLB-985 cells orient themselves toward and then crawl up the gradient of chemoattractant delivered by micropipette, and retract their pseudopodia when the source is removed.

Several observations indicate that our fluorescent receptor probe, the C5aR–GFP protein, accurately reflects behavior of endogenous receptors for C5a and other chemoattractants on the neutrophil surface. The fluorescent protein, GFP, has been fused to many proteins, including G protein-coupled receptors, as a tool for assessing their localization and fate in living cells (Sengupta, *et al.*, 1996; Barak *et al.*, 1997a,b; Tarasova, *et al.*, 1997; Xiao *et al.*, 1997). C5aR–GFP functions indistinguishably from the wild-type C5aR in stably transfected HEK293 cells, where it mediates chemotaxis over the same range of C5a concentrations (Figure 3). C5aR–GFP functions normally in PLB-985 cells also, at least with respect to its ability to undergo rapid agonist-induced internalization (Figures 4, 5, 7, and 8), as is the case in other cells for a number of G protein-coupled receptors fused to GFP (Barak *et al.*, 1997b; Tarasova, *et al.*, 1997). Moreover, C5aR-GFP is targeted to its appropriate location at the plasma membrane of PLB-985 cells, producing a peripheral fluorescent signal that coincides perfectly with that of the fluorescent signal of a plasma membrane probe, DiD (Figures 6 and 7). Finally, it is unlikely that expression of the recombinant C5aR substantially alters sensitivity of PLB-985 cells to C5a ligands, because cell surfaces of these cells display only 60% more C5a-binding sites than do those of control cells expressing GFP alone (Figure 3).

Behavior of C5aR–GFP Compared with Other Chemoattractant Receptors

Before discussing differences between our findings and those of others, we should first note that in several respects the C5aR–GFP fusion protein precisely mimics behavior reported for several other chemoattractant receptors. To infer behavior of chemoattractant receptors in living neutrophils, previous investigations used fluorescently modified ligands, including *N*-formyl peptides and C5a (Janeczek *et al.*, 1989; Schmitt and Bultmann, 1990; Van Epps, *et al.*, 1990; Johansson *et al.*, 1993). Before receptors are internalized, these fluorescent ligands aggregate into patches on the neutrophil membrane (Janeczek, *et al.*, 1989; Van Epps, *et al.*, 1990; Johansson, *et al.*, 1993); similarly, C5aR–GFP forms clusters at the plasma membrane shortly after stimulation with C5a (Figure 4C′). After clustering at the plasma membrane, fluorescent *N*-formyl peptides are internalized and accumulate in the uropods of polarized neutrophils (Schmitt and Bultmann, 1990); similarly, after plasma membrane clusters are observed, C5aR–GFP internalizes and accumulates in uropods (Figure 4, F and F′). Finally, fluorescent fMLP ligands accumulated in the uropods of polarized cells translocate from the uropods to the perinuclear region of neutrophils (Schmitt and Bultmann, 1990); similarly, some internalized C5aR-GFP eventually moves to the perinuclear region of PLB-985 cells (Figure 5F, cell E, red arrowheads and our unpublished data). Thus behavior of the C5aR–GFP molecule closely resembles receptor behavior inferred from studies with fluorescent ligands.

Our observation that the C5aR remains uniformly distributed on the surface of neutrophils during chemotaxis is not in accord with several previous reports that chemoattractant receptors cluster at the leading edge of neutrophils (Walter and Marasco, 1984; Schmitt and Bultmann, 1990; McKay *et al.*, 1991) or T lymphocytes (Nieto *et al.*, 1997). Unlike our experiments, these investigations either tracked fluorescently tagged ligand (rather than the receptors themselves) in real time or used antibodies or radiolabeled ligands to detect receptors in fixed cells. Moreover, none of these studies asked whether the increased fluorescent or radioactive signal at the anterior pole of a polarized cell represents an increased number of receptor molecules per unit area of membrane or simply reflects complex membrane folding at the front. An increased "concentration" of plasma membrane at the leading edge, probably produced by complex membrane folds, could produce the illusion of a higher concentration of membrane receptors, even in confocal microscopy, as suggested by comparing the C5aR-GFP and DiD patterns of Figures 6 and 7. Instead, our observations suggest that during chemotaxis C5aR–GFP behaves very like an inert probe of membrane concentration, and is not concentrated, per unit of cell surface, at the leading edge or anywhere else. In keeping with this inference, two studies (McKay *et al.*, 1991; Nieto *et al.*, 1997) showed that the apparent redistribution of chemoattractant receptors to the leading edge of leukocytes correlated strictly with the acquisition of a polarized morphology; in one of these cases (Nieto *et al.*, 1997), moreover, the redistribution was observed for receptors other than those whose activation induced the cell polarization.

Our conclusion that receptors do not accumulate preferentially at the leading edge of migrating neutrophils should be qualified, because of the relatively low resolution of the data. Indeed, some images (e.g., Figure 8) suggest that receptor density may be very much higher on a few membrane projections at the cell's leading edge. These localized increases in receptor density may represent fixation artifact, because they were seen only in images made from fixed cells. Whether or not the increases of C5aR–GFP on membrane projections represent artifacts, we see them in cells responding to fMLP, indicating that they are not agonist specific (our unpublished result).

Possible Mechanisms for Amplifying the Chemotactic Gradient

If receptor redistribution does not amplify the chemotactic gradient, we must conclude that neutrophils use some other mechanism to detect a concentration difference as small as 1% from front to back. How might such an apparent amplification come about? At what level of the signaling pathway does amplification take place? One straightforward possibility is that increased complexity and folding of plasma membrane, which we observed at the leading edge (Figures 6 and 7), increases the sensitivity of the cell's anterior pole simply because the absolute number of receptor molecules is higher there. Tight membrane folds could also induce a significant increase in ratio of cell surface to *local* volume of cytoplasm (just beneath the membrane); an increase in this ratio would increase the intensity of the cytoplasmic signals (second messengers or activated proteins) that trigger polymerization of actin. Such mechanisms could make the cell sense an apparently steeper gradient of chemoattractant from front to back, reinforcing the cell's polarity and its persistent forward motion.

This scenario cannot be the whole story; however, as indicated by recent observations, indicating that actin-induced complex folding of plasma membrane in a pseudopod is not necessary for asymmetric detection of a chemotactic gradient by *D. discoideum* cells (Parent *et al.*, 1998). In these experiments, a cAMP gradient produced an asymmetric intracellular signal, much greater at the front than the back, even when actin polymerization was completely blocked by latrunculin, a toxin that sequesters G-actin. Assessment of the intracellular signal depended upon ligand-induced recruitment to the plasma membrane of a GFP-tagged cytoplasmic protein, the cytoplasmic regulator of adenylyl cyclase (CRAC). After latrunculin treatment, a cAMP gradient caused no apparent morphological polarity, because actin was not polymerized; in the same cells, however, the cAMP gradient caused recruitment of CRAC-GFP to surfaces of the cells facing the pipette, rather than the side away from the pipette. Thus actin-induced membrane folds may facilitate directional motility, but are probably not required for asymmetric detection of a gradient, at least in so far as neutrophils use detection mechanisms similar to those of *D. discoideum*.

If this inference applies to the chemotactic-signaling mechanisms of neutrophils and other eukaryotic cells, it will be necessary to look for other molecular mechanisms that may amplify asymmetry of the chemotactic signal. Does amplification of the signal depend upon asymmetric activity or ligand affinity of receptors, or does it take place at a downstream site, involving concentrations, recruitment, or activities of G proteins, RGS (regulators of G protein signaling) (Dohlman and Thorner, 1997; Berman and Gilman, 1998), or effector molecules? Many scenarios have been suggested (Walter and Marasco, 1987; Devreotes and Zigmond, 1988), but none so far is supported by real evidence. Answers will come from a combination of genetic analysis, real-time observations of chemotaxis in model systems like the PLB-985 cell, and biochemical dissection of the signals that link receptors and G proteins to polymerization of actin.

ACKNOWLEDGMENTS

We thank members of the Bourne laboratory for valuable discussion, and the following individuals for their gifts: A. Abo for the PLB-985 cell line; J.M. Bishop for the Ψ2 packaging cell line and the pLNCX retroviral vector; J.A. Ember and T.E. Hugli for the polyclonal anti-C5aR antibody; and C. Gerard for the C5aR cDNA. We also thank William Hyun and Jane Gordon of the Laboratory for Cell Analysis for their help with FACS. This work was supported in part by National Institutes of Health grants GM-27800 and CA-54427 (H.R.B.) and GM-25101 (J.W.S.). G.S. is a Medical Research Council of Canada Postdoctoral Fellow, and O.D.W. is a Howard Hughes Medical Institute Predoctoral Fellow.

REFERENCES

Agard, D.A., Hiraoka, Y., Shaw, P., and Sedat, J.W. (1989). Fluorescence microscopy in three dimensions. Methods Cell Biol. *30*, 353–377.

Baggiolini, M. (1998). Chemokines and leukocyte traffic. Nature *392*, 565–568.

Barak, L.S., Ferguson, S.S., Zhang, J., and Caron, M.G. (1997a). A β-arrestin/green fluorescent protein biosensor for detecting G protein-coupled receptor activation. J. Biol. Chem. *272*, 27497–27500.

Barak, L.S., Ferguson, S.S., Zhang, J., Martenson, C., Meyer, T., and Caron, M.G. (1997b). Internal trafficking and surface mobility of a functionally intact β2-adrenergic receptor-green fluorescent protein conjugate. Mol. Pharmacol. *51*, 177–184.

Berman, D.M., and Gilman, A.G. (1998). Mammalian RGS proteins: barbarians at the gate. J. Biol. Chem. *273*, 1269–1272.

Bokoch, G.M. (1995). Chemoattractant signaling and leukocyte activation. Blood *86*, 1649–1660.

Cassimeris, L., and Zigmond, S.H. (1990). Chemoattractant stimulation of polymorphonuclear leukocyte locomotion. Semin. Cell Biol. *1*, 125–134.

Dana, R., Leto, T.L., Malech, H.L., and Levy, R. (1998). Essential requirement of cytosolic phospholipase A2 for activation of the phagocyte NADPH oxidase. J. Biol. Chem. *273*, 441–445.

Davis, B.H., Walter, R.J., Pearson, C.B., Becker, E.L., and Oliver, J.M. (1982). Membrane activity and topography of F-Met-Leu-Phe-treated polymorphonuclear leukocytes. Acute and sustained responses to chemotactic peptide. Am. J. Pathol. *108*, 206–216.

Devreotes, P.N., and Zigmond, S.H. (1988). Chemotaxis in eukaryotic cells: a focus on leukocytes and *Dictyostelium*. Annu. Rev. Cell Biol. *4*, 649–686.

Dohlman, H.G., and Thorner, J. (1997). RGS proteins and signaling by heterotrimeric G proteins. J. Biol. Chem. *272*, 3871–3874.

Downey, G.P. (1994). Mechanisms of leukocyte motility and chemotaxis. Curr. Opin. Immunol. *6*, 113–124.

Drapeau, G., Brochu, S., Godin, D., Levesque, L., Rioux, F., and Marceau, F. (1993). Synthetic C5a receptor agonists. Pharmacology, metabolism and in vivo cardiovascular and hematologic effects. Biochem. Pharmacol. *45*, 1289–1299.

Gerard, N.P., and Gerard, C. (1991). The chemotactic receptor for human C5a anaphylatoxin. Nature *349*, 614–617.

Gerisch, G., and Keller, H.U. (1981). Chemotactic reorientation of granulocytes stimulated with micropipettes containing fMet-Leu-Phe. J. Cell Sci. *52*, 1–10.

Gray, G.D., Hasslen, S.R., Ember, J.A., Carney, D.F., Herron, M.J., Erlandsen, S.L., and Nelson, R.D. (1997). Receptors for the chemoattractants C5a and IL-8 are clustered on the surface of human neutrophils. J. Histochem. Cytochem. *45*, 1461–1467.

Hiraoka, Y., Sedat, J.W., and Agard, D.A. (1990). Determination of three-dimensional imaging properties of a light microscope system. Partial confocal behavior in epifluorescence microscopy. Biophys. J. *57*, 325–333.

Hiraoka, Y., Swedlow, J.R., Paddy, M.R., Agard, D.A., and Sedat, J.W. (1991). Three-dimensional multiple-wavelength fluorescence microscopy for the structural analysis of biological phenomena. Semin. Cell Biol. *2*, 153–165.

Huey, R., and Hugli, T.E. (1985). Characterization of a C5a receptor on human polymorphonuclear leukocytes (PMN). J. Immunol. *135*, 2063–2068.

Huttenlocher, A., Palecek, S.P., Lu, Q., Zhang, W., Mellgren, R.L., Lauffenburger, D.A., Ginsberg, M.H., and Horwitz, A.F. (1997). Regulation of cell migration by the calcium-dependent protease calpain. J. Biol. Chem. *272*, 32719–32722.

Iiri, T., Homma, Y., Ohoka, Y., Robishaw, J.D., Katada, T., and Bourne, H.R. (1995). Potentiation of Gi-mediated phospholipase C activation by retinoic acid in HL-60 cells. Possible role of G gamma 2. J. Biol. Chem. *270*, 5901–5908.

Janeczek, A.H., Marasco, W.A., van Alten, P.J., and Walter, R.J. (1989). Autoradiographic analysis of formylpeptide chemoattractant binding, uptake and intracellular processing by neutrophils. J. Cell Sci. *94*, 155–168.

Johansson, B., Wymann, M.P., Holmgren-Peterson, K., and Magnusson, K.E. (1993). N-formyl peptide receptors in human neutrophils display distinct membrane distribution and lateral mobility when labeled with agonist and antagonist. J. Cell Biol. *121*, 1281–1289.

Konteatis, Z.D., Siciliano, S.J., Van Riper, G., Molineaux, C.J., Pandya, S., Fischer, P., Rosen, H., Mumford, R.A., and Springer, M.S. (1994). Development of C5a receptor antagonists. Differential loss of functional responses. J. Immunol. *153*, 4200–4205.

McKay, D.A., Kusel, J.R., and Wilkinson, P.C. (1991). Studies of chemotactic factor-induced polarity in human neutrophils. Lipid mobility, receptor distribution and the time-sequence of polarization. J. Cell Sci. *100*, 473–479.

Miller, A.D., and Rosman, G.J. (1989). Improved retroviral vectors for gene transfer and expression. Biotechniques *7*, 980–982, 984–9866, 989–990.

Morgan, E.L., Ember, J.A., Sanderson, S.D., Scholz, W., Buchner, R., Ye, R.D., and Hugli, T.E. (1993). AntiC5a receptor antibodies. Characterization of neutralizing antibodies specific for a peptide, C5aR-(9–29), derived from the predicted amino-terminal sequence of the human C5a receptor. J. Immunol. *151*, 377–388.

Neptune, E.R., and Bourne, H.R. (1997). Receptors induce chemotaxis by releasing the betagamma subunit of Gi, not by activating Gq or Gs. Proc. Natl. Acad. Sci. USA *94*, 14489–14494.

Nieto, M., Frade, J.M., Sancho, D., Mellado, M., Martinez, A.C., and Sanchez-Madrid, F. (1997). Polarization of chemokine receptors to the leading edge during lymphocyte chemotaxis. J. Exp. Med. *186*, 153–158.

Parent, C.A., Blacklock, B.J., Froehlich, W.M., Murphy, D.B., and Devreotes, P.N. (1998). G protein signaling events are activated at the leading edge of chemotactic cells. Cell *95*, 81–91.

Perez, H.D. (1994). Chemoattractant receptors. Curr. Opin. Hematol. *1*, 40–44.

Prossnitz, E.R., and Ye, R.D. (1997). The N-formyl peptide receptor: a model for the study of chemoattractant receptor structure and function. Pharmacol. Ther. *74*, 73–102.

Schmitt, M., and Bultmann, B. (1990). Fluorescent chemotactic peptides as tools to identify the f-Met-Leu-Phe receptor on human granulocytes. Biochem. Soc. Trans. *18*, 219–222.

Sengupta, P., Chou, J.H., and Bargmann, C.I. (1996). odr-10 Encodes a seven transmembrane domain olfactory receptor required for responses to the odorant diacetyl. Cell *84*, 899–909.

Sullivan, S.J., Daukas, G., and Zigmond, S.H. (1984). Asymmetric distribution of the chemotactic peptide receptor on polymorphonuclear leukocytes. J. Cell Biol. *99*, 1461–1467.

Tarasova, N.I., Stauber, R.H., Choi, J.K., Hudson, E.A., Czerwinski, G., Miller, J.L., Pavlakis, G.N., Michejda, C.J., and Wank, S.A. (1997). Visualization of G protein-coupled receptor trafficking with the aid of the green fluorescent protein. Endocytosis and recycling of cholecystokinin receptor type A. J. Biol. Chem. *272*, 14817–14824.

Tucker, K.A., Lilly, M.B., Heck, L., Jr., and Rado, T.A. (1987). Characterization of a new human diploid myeloid leukemia cell line (PLB-985) with granulocytic and monocytic differentiating capacity. Blood *70*, 372–378.

Van Epps, D.E., Simpson, S., Bender, J.G., and Chenoweth, D.E. (1990). Regulation of C5a and formyl peptide receptor expression on human polymorphonuclear leukocytes. J. Immunol. *144*, 1062–1068.

Walter, R.J., and Marasco, W.A. (1984). Localization of chemotactic peptide receptors on rabbit neutrophils. Exp. Cell Res. *154*, 613–618.

Walter, R.J., and Marasco, W.A. (1987). Direct visualization of formylpeptide receptor binding on rounded and polarized human neutrophils: cellular and receptor heterogeneity. J. Leukocyte Biol. *41*, 377–391.

Xiao, Z., Zhang, N., Murphy, D.B., and Devreotes, P.N. (1997). Dynamic distribution of chemoattractant receptors in living cells during chemotaxis and persistent stimulation. J. Cell Biol. *139*, 365–374.

Zigmond, S.H. (1974). Mechanisms of sensing chemical gradients by polymorphonuclear leukocytes. Nature *249*, 450–452.

Zigmond, S.H. (1977). Ability of polymorphonuclear leukocytes to orient in gradients of chemotactic factors. J. Cell Biol. *75*, 606–616.

Zigmond, S.H., Levitsky, H.I., and Kreel, B.J. (1981). Cell polarity: an examination of its behavioral expression and its consequences for polymorphonuclear leukocyte chemotaxis. J. Cell Biol. *89*, 585–592.

CHAPTER FOUR

Actin Polymerization and a Nucleator of Actin Polymerization, the Arp2/3 Complex, are Polarized During Neutrophil Chemotaxis

Reprinted by permission from *Nature Cell Biology* Vol. 1 No.2 pp 75-81.

Copyright 1999 Macmillan Magazines Limited.

Spatial control of actin polymerization during neutrophil chemotaxis

Orion D. Weiner*†, Guy Servant†, Matthew D. Welch†‡, Timothy J. Mitchison†§, John W. Sedat* and Henry R. Bourne†¶

**Department of Biochemistry and Biophysics, University of California, San Francisco, California 94143-0554, USA*
†Department of Cellular and Molecular Pharmacology, University of California, San Francisco, California 94143-0450, USA
‡Present address: Department of Molecular and Cell Biology, University of California, Berkeley, California 94720, USA
§Present address: Department of Cell Biology, Harvard Medical School, 240 Longwood Avenue, Boston, Massachusetts 02115, USA
¶e-mail: h_bourne@quickmail.ucsf.edu

Neutrophils respond to chemotactic stimuli by increasing the nucleation and polymerization of actin filaments, but the location and regulation of these processes are not well understood. Here, using a permeabilized-cell assay, we show that chemotactic stimuli cause neutrophils to organize many discrete sites of actin polymerization, the distribution of which is biased by external chemotactic gradients. Furthermore, the Arp2/3 complex, which can nucleate actin polymerization, dynamically redistributes to the region of living neutrophils that receives maximal chemotactic stimulation, and the least-extractable pool of the Arp2/3 complex co-localizes with sites of actin polymerization. Our observations indicate that chemoattractant-stimulated neutrophils may establish discrete foci of actin polymerization that are similar to those generated at the posterior surface of the intracellular bacterium *Listeria monocytogenes*. We propose that asymmetrical establishment and/or maintenance of sites of actin polymerization produces directional migration of neutrophils in response to chemotactic gradients.

Neutrophils, cells of the innate immune system, hunt and kill bacteria, which they find by reading chemotactic gradients of formylated peptides released from the bacteria. Neutrophils respond to chemotactic stimuli by increasing the nucleation and polymerization of actin filaments[1]. They respond to a gradient of chemoattractant by extending actin-rich pseudopodia preferentially in the direction of the highest concentration of chemotactic molecules[2]. Although actin polymerization is necessary for this morphological polarity and for migration of the neutrophils in response to chemotactic gradients[3,4], the spatial distribution of actin polymerization in response to chemotactic gradients is not well understood. A knowledge of this distribution will be crucial in understanding how neutrophils and other chemoattactant-responsive cells spatially rearrange their actin cytoskeletons during chemotaxis.

The Arp2/3 complex, a strong candidate for the regulation of actin polymerization in chemotaxis, has not been studied during chemotaxis. This complex stimulates the nucleation of actin filaments[5,6] in a regulatable fashion[6,7], and conditional Arp2 and

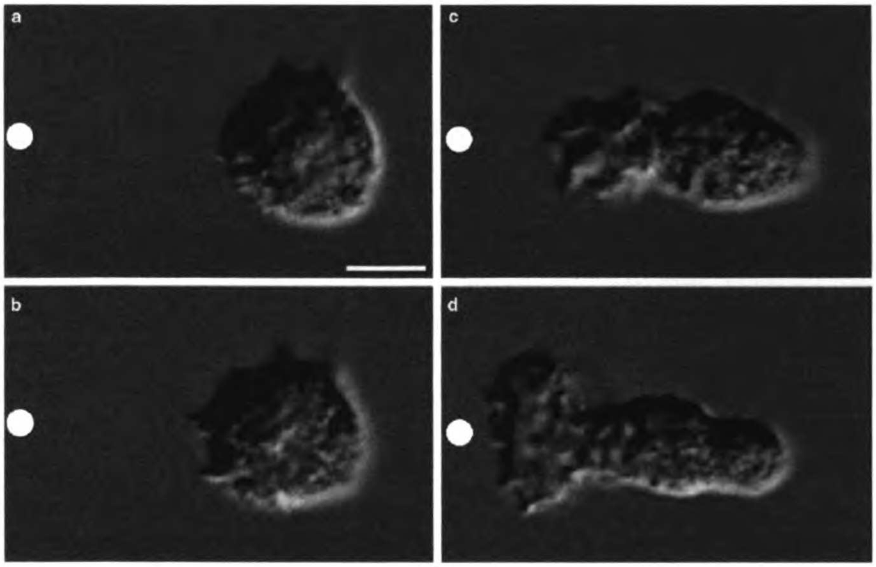

Figure 1 **Polarization of a neutrophil in response to a gradient of chemoattractant. a–d**, Nomarski images of an unpolarized neutrophil responding to a micropipette containing 10μM FMLP (white circle) at **a**, 5 s, **b**, 30 s, **c**, 81 s, and **d**, 129 s.

© 1999 Macmillan Magazines Ltd

Arp3 mutations in yeast produce several defects in actin function[9,10].

Neutrophils would seem to represent an ideal model system for the study of the spatial control of actin polymerization during chemotaxis. However, standard techniques for determining the subcellular localization of actin polymerization, through incorporation of fluorescently labelled actin into microinjected[11,12] or permeabilized[12,13] cells, have proven difficult or impossible to use when studying neutrophils. It would be useful to express GFP-tagged proteins in neutrophils to analyze protein dynamics in living cells during chemotaxis. However, it has not been possible to express recombinant proteins in neutrophils because they are short-lived terminally differentiated cells.

We have now overcome these difficulties, and report that chemoattractant-stimulated neutrophils establish discrete sites of actin polymerization whose distribution is biased towards the cell surface that is directed towards the highest concentration of chemoattractant. The least-extractable pool of the Arp2/3 complex co-localizes with these sites of actin polymerization, and this complex dynamically redistributes to the region of living neutrophils that receives maximal chemotactic stimulation. We propose that asymmetrical establishment and/or maintenance of these sites of actin polymerization mediates the directional migration of neutrophils in response to gradients of chemoattractant.

Results

Actin distribution and polymerization. Before stimulation by chemoattractant, neutrophils lack obvious polarity. Between 5 s (Fig. 1a) and 30s (Fig. 1b) of exposure to a point source of *N*-formyl-methionyl-leucyl-phenylalanine (FMLP), supplied through a micropipette (Fig. 1a–d, white circle), neutrophils begin to extend their surface toward the chemotactic pipette. Only the neutrophil surface directed up the chemotactic gradient ruffles and extends as neutrophils become polarized in the direction of the micropipette (Fig. 1b–d; see Supplementary Information). Microspikes constantly project from the leading edge towards the micropipette (Fig. 1b–d; see Supplementary Information), some continuing to extend for more than 1 minute if the direction of chemotactic stimulation remains constant. How do neutrophils control actin polymerization to generate these complex, polarized morphologies in response to chemoattractant?

To identify sites of actin polymerization accurately in permeabilized neutrophils, we used fluorescently labelled actin (tetramethylrhodamine–actin (TMR–actin)), but first we had to minimize potential damage to the native cytoskeleton caused by the many neutral proteases of neutrophils. We first treated neutrophils with the membrane-permeable serine-protease inhibitor diisopropyl fluorophosphate (DFP), exposed them to chemoattractant, and then permeabilized them in the presence TMR–actin (procedure modified from refs 12,14). DFP does not alter the cytoskeletal morphology of fixed neutrophils or the ability of neutrophils to undergo chemotaxis. In permeabilized neutrophils polarized by exposure to uniform chemoattractant (that is, chemoattractant was present in the buffer surrounding the cells, rather than in a micropipette), exogenous actin incorporates at distinct sites on the pseudopodial surface and in a perinuclear fashion. The pseudopodial incorporation reflects actin polymerization, but the perinuclear incorporation does not, as shown by the latter's persistence when actin polymerization is inhibited (Fig. 2). Thus we can analyse actin incorporation in regions of the cell away from the nucleus, but cannot determine the total distribution of actin polymerization in polarized cells.

In neutrophils stimulated with uniform chemoattractant for 60 s, new actin incorporation occurs predominantly at the front surface of the pseudopodium. In horizontal cross-sections, new actin incorporation is concentrated at the tips of radially projecting actin bundles (Fig. 2a–c, arrows). If cells are permeabilized in the presence of cytochalasin D, which inhibits actin polymerization, only perinuclear actin incorporation is observed (Fig. 2d), with no incorporation at the tips of radial actin bundles (arrowheads).

To obtain a more complete picture of the organization of the actin polymerization in the neutrophil pseudopodium, we generated three-dimensional reconstructions of neutrophil pseudopodia (Fig. 3e,f). These reconstructions reveal that what appear to be finger-like actin bundles in horizontal cross-section correspond to radially projecting actin ruffles, that the crescent-like projecting tips of these actin ruffles represent the sites of maximal actin polymerization, and that the sites of actin polymerization are not contiguous with one another. Thus, although sites of actin polymerization are present in many locations throughout the leading edge of stimulated neutrophils, the leading surface of the cell does not polymerize actin uniformly. Instead, the complex ruffled pseudopodium is composed of many distinct sites of actin polymerization organized at the tips of radially distributed actin projections. To our knowledge, this is the first three-dimensional analysis of actin incorporation in a motile cell.

Neutrophils only transiently contain more than one pseudopodium; in neutrophils with two pseudopodia, one pseudopodium gains dominance and actively extends while the other pseudopodium is retracted (D.R. Soll, personal communication; O.D.W., unpublished observations). Of 25 randomly chosen neutrophils with multiple pseudopodia, 17 exhibited much more dramatic actin incorporation for one pseudopodial projection than the other(s), as shown for a single neutrophil in Fig. 3 (compare arrowhead and arrow in Fig. 3c). This indicates that actin polymerization does not depend solely on the pre-existing actin distribution and that two morphologically similar regions of the cell can differ in their abilities to polymerize F-actin.

To determine whether external chemotactic gradients bias the spatial distribution of sites of actin polymerization, we exposed neutrophils to a chemotactic micropipette and then permeabilized them in the presence of fluorescently labelled actin. Actin fingers showing polymerization at their tips are observed only on the up-gradient face of cells exposed to a point source of chemoattractant (data not shown).

Distribution and dynamics of the Arp2/3 complex. To study the dynamics of the Arp2/3 complex during neutrophil chemotaxis, it would be useful to follow the distribution of a green fluorescent protein (GFP)-tagged component of the complex. To overcome the difficulties of expressing a recombinant protein in short-lived neutrophils, we took advantage of the human promyelocytic cell line PLB-985. These cells can be cultured indefinitely, transfected using retroviruses, and then differentiated into cells that resemble human neutrophils in their signalling properties and response to chemoattractant.

Immediately after exposure to the chemotactic micropipette (Fig. 4, white circle), neutrophils either lack polarity and show a uniform distribution of Arp3–GFP (Fig. 4a, top left neutrophil), or exhibit a slight polarity with Arp3–GFP uniformly distributed throughout the cytosol and excluded from the nucleus (Fig. 4a, bottom right cell). Within about a minute of exposure to the chemotactic micropipette, Arp3–GFP concentrates in the region of neutrophils that is beginning to exhibit cell polarity (that is, the region of the cell that is facing up the gradient of chemoattractant; Fig. 4b, top left cell), or in the pseudopod of polarized cells that are starting to migrate towards the chemotactic micropipette (Fig. 4b, lower right cell; the two cells shown in the centre were unresponsive during this experiment). Arp3–GFP remains strongly concentrated in the pseudopod as the cells migrate towards the chemotactic micropipette (Fig. 4c–e; see Supplementary Information). In contrast, GFP is present throughout the cytosol of cells expressing GFP alone (data not shown). When the chemotactic micropipette (Fig. 4f–j) moves, Arp3–GFP dynamically redistributes with the moving pseudopod to concentrate on the surface of the cell nearest the chemoattractant (see Supplementary Information). To our knowledge, this is the first analysis of the dynamics of the Arp2/3 complex in a

© 1999 Macmillan Magazines Ltd

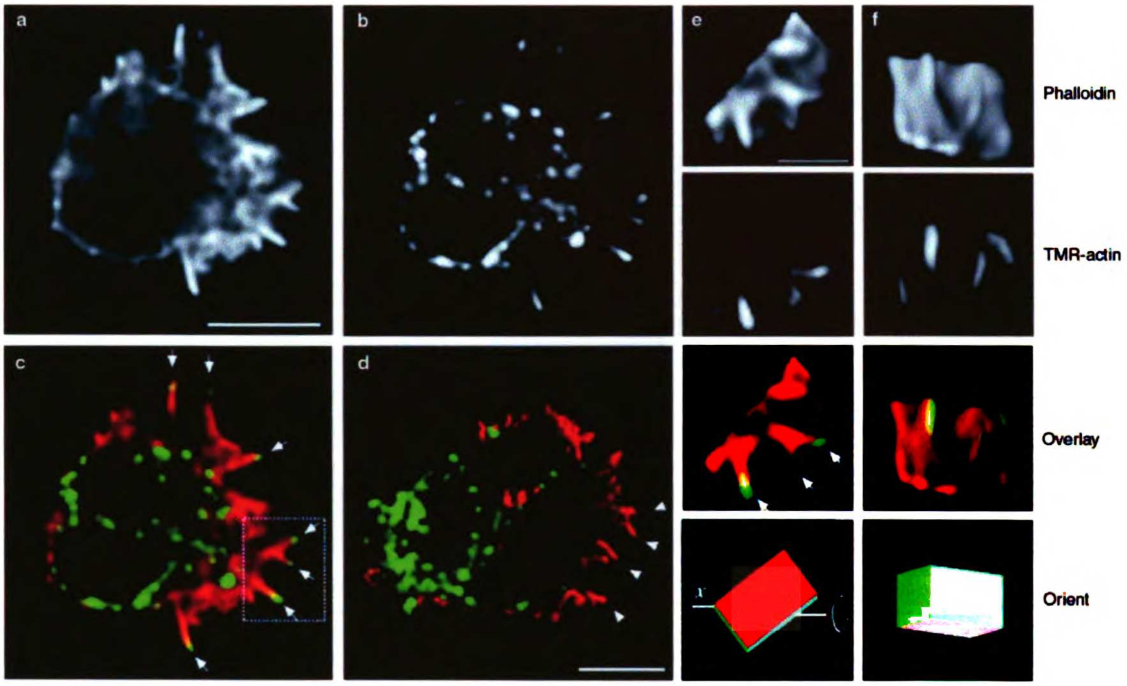

Figure 2 **Spatial distribution of incorporation of TMR–actin in a chemoattractant-stimulated permeabilized neutrophil. a–c**, Neutrophil exposed to a uniform concentration (20nM) of FMLP for 60s. Scale bar represents 5 μm. **a**, Phalloidin stain, representing pre-existing filaments and those that incorporated actin during the assay. Note that because phalloidin is excluded by some actin-binding proteins, such as cofilin, phalloidin staining does not necessarily represent all actin filaments. **b**, TMR–actin stain, representing newly incorporated TMR–actin only. **c**, Colour overlay, showing phalloidin stain in red and TMR–actin stain in green. Arrows in **c** indicate sites of new actin incorporation at the tips of finger-like actin bundles. **d**, A neutrophil stimulated and permeabilized as in **a–c** but in the presence of 0.2 μm cytochalasin D. Colour scheme is as in **c**. Arrowheads indicate the absence of TMR–actin incorporation at the tips of finger-like actin bundles. Perinuclear actin incorporation parallels the subcellular distribution of granules (data not shown). Because bright perinuclear but not pseudopodial TMR–actin incorporation is observed when cytochalasin D is present during the permeabilization reaction, we conclude that incorporation at the pseudopodial surface represents new actin polymerization and that perinuclear incorporation results from G-actin-binding proteins or structures, as has been reported for permeabilized fibroblasts[12]. **e, f**, Three-dimensional reconstruction of the boxed region of the pseudopodium shown in **c**. The bottom two panels indicate the relative orientation of the region of the pseudopodium from **c** as it is rotated along its x-axis. The scale bar in **e** represents 2 μm. Scale bar in **d** represents 5 μm.

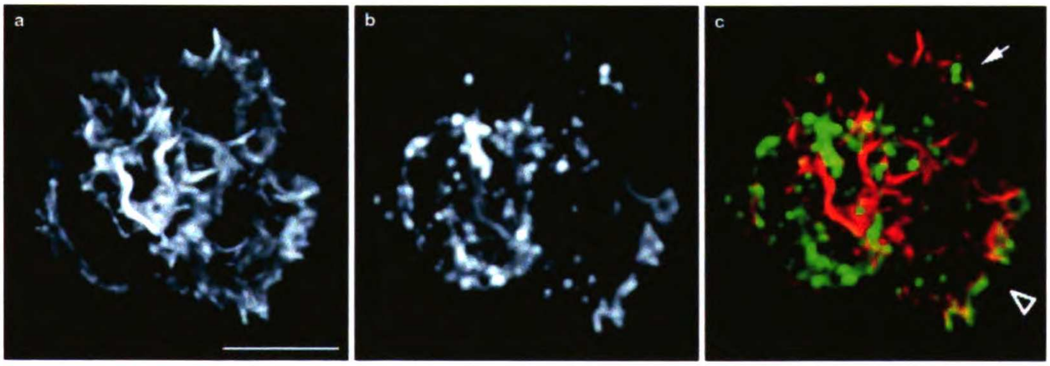

Figure 3 **Spatial distribution of TMR–actin incorporation in a neutrophil with two pseudopodia.** Images represent maximum-intensity projections of three-dimensional immunofluorescence data. **a**, Phalloidin staining, representing total actin. **b**, TMR–actin staining, representing newly incorporated actin. **c**, Colour overlay, with phalloidin staining in red and newly incorporated actin in green. Arrow indicates a pseudopodium with minimal new actin incorporation. Arrowhead indicates a pseudopodium that is predominant in terms of new actin incorporation. The intense perinuclear TMR–actin stain does not represent new actin polymerization (Fig. 2). Scale bar represents 5 μm.

© 1999 Macmillan Magazines Ltd

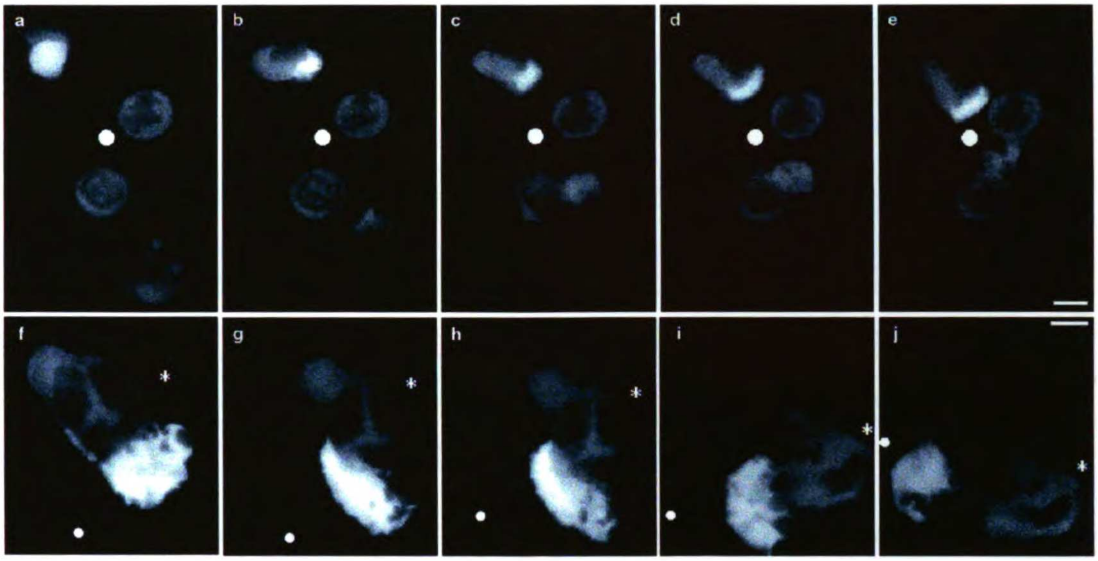

Figure 4 **Response of neutrophils expressing Arp3–GFP to a stationary or moving chemotactic micropipette. a–e,** Response to a stationary micropipette. **f–j,** Response to a motile micropipette. Images are single optical sections from near the bottom of a cell. **a,** Image taken immediately after exposing neutrophils to a chemotactic micropipette (white circle). **b–e,** Same group of neutrophils at **b,** 72 s, **c,** 166 s, **d,** 196 s, and **e,** 240 s of exposure to the chemotactic micropipette. **f,** A polarized neutrophil responding to a moving chemotactic micropipette (white circle). The white asterisk represents a fixed reference point. **g–h,** Same cell as that shown in **f** at **g,** 78 s, **h,** 109 s, **I,** 193 s, and **j,** 305 s of exposure to the micropipette. Scale bar represents 5 μm.

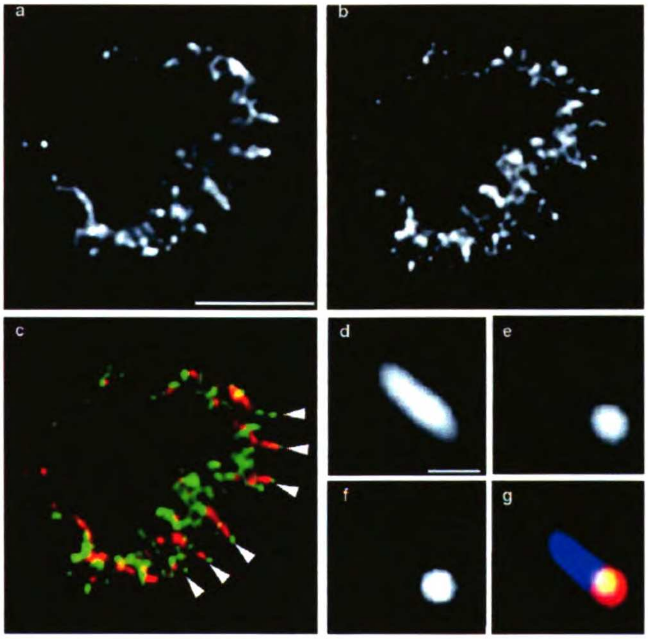

Figure 5 **Immunofluorescence localization of endogenous Arp2/3 complex and actin in human neutrophils and the relationship of Arp2/3 localization to sites of actin polymerization.** Images are single optical sections from near the midsection of cell. **a,** Actin immunostaining. Scale bar represents 5 μm. **b,** p21–Arc immunostaining. **c,** Colour overlay, showing actin in red and p21–Arc in green. Arrowheads indicate the localization of p21–Arc at the tips of actin fingers. **d–g,** Detail of an actin finger, from a cell permeabilized in the presence of TMR–actin to detect sites of actin polymerization and then processed for p21–Arc and actin immunostaining. **d,** Anti-actin staining, showing pre-existing and newly incorporated actin filaments. Scale bar represents 0.5 μm. **e,** TMR–actin staining, showing newly incorporated actin. **f,** p21–Arc staining. **g,** Triple overlay of **d–f,** showing total actin shown in light blue, newly incorporated actin in red, and p21–Arc in green. The green staining co-localizes with red and appears yellow.

© 1999 Macmillan Magazines Ltd

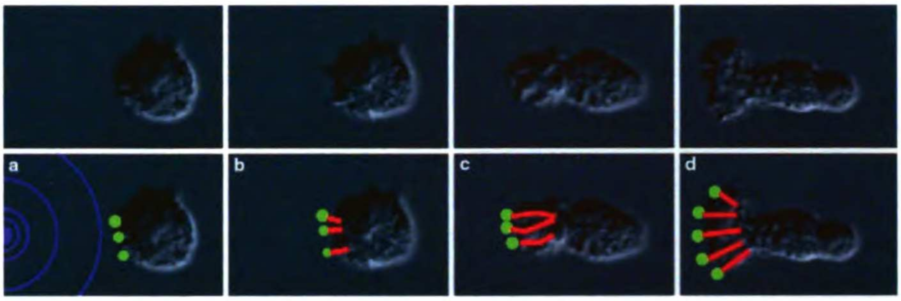

Figure 6 **Model of actin polymerization in response to a chemotactic signal.** Top, Nomarski images of an unpolarized neutrophil exposed to a chemotactic micropipette (just to left of field) for **a**, 5 s, **b**, 30 s, **c**, 81 s, and **d**, 129 s. Bottom, the model. **a**, A neutrophil exposed to a gradient of chemoattractant (purple concentric circles) generates an asymmetric distribution of polymerization foci. **b–d**, The force generated by polymerization of actin (red lines) propels the polymerization focus forward and pushes the membrane outwards. The preferential activation of polymerization foci nearest to the chemoattractant could result in directional migration of neutrophils in response to chemotactic gradients and would be consistent with the behaviour of the pseudopod in response to a changing direction of chemoattractant. Note that this figure represents a single optical section of a neutrophil responding to a chemotactic gradient; the three-dimensional organization of the sites of actin polymerization and actin projections is shown in Fig. 2e, f.

living cell in response to a directional chemoattractant.

To determine the subcellular distribution of the endogenous Arp2/3 complex in human neutrophils, we tested several affinity-purified rabbit polyclonal antibodies, raised against the p21–Arc, p34–Arc (for Arp complex) and Arp3 components of the human Arp2/3 complex[15], on chemoattractant-stimulated human neutrophils. Because all these antibodies showed similar distributions, we describe only the results obtained with the anti-p21–Arc antibody, which consistently produced the brightest staining. In neutrophils stimulated with uniform FMLP for 90 s, fixed with formaldehyde, extracted with methanol, and processed for immunocytochemistry with antibodies to actin (Fig. 5a) and p21–Arc (Fig. 5b), p21–Arc (green) is enriched at the tips of radially projecting actin fingers (red) (Fig. 5c). To determine the relationship between sites of actin polymerization and the Arp2/3 complex, we processed neutrophils permeabilized in the presence of tetramethylrhodamine–actin (TMR–actin) for p21–Arc immunocytochemistry. p21–Arc immunostaining co-localizes with sites of actin polymerization at the tip of actin fingers (Fig. 5d–g). This actin finger extends into the cell periphery, a region in which all exogenous actin incorporation is prevented by cytochalasin D (Fig. 2d).

Discussion

In our experiments with permeabilized neutrophils, chemoattractant-induced actin polymerization is restricted to the pseudopodial surface of stimulated cells and is concentrated at the tips of actin bundles that project into the plasma membrane. This pattern of actin incorporation resembles that seen in *in vivo* studies of the intracellular bacterium *Listeria monocytogenes*, a situation in which new actin polymerization occurs only at the most proximal portion of the actin tail, immediately adjacent to the posterior surface of the bacterium[16,17]. This pattern of actin polymerization differs from that seen previously in neutrophils[14], where incorporation of exogenous (fluorescently labelled) actin paralleled the distribution of endogenous F-actin. We attribute this discrepancy to the fact that here we protected the endogenous actin cytoskeleton from proteolysis. If neutrophils are not pretreated with DFP before permeabilization, extensive proteolysis of actin and actin-associated proteins is observed[18], possibly generating, through the severing and uncapping of pre-existing actin filaments, barbed actin ends, which can be elongated. When we omit DFP treatment before permeabilizing neutrophils, we typically observe incorporation of exogenous actin throughout the distribution of endogenous F-actin (data not shown).

Our results show that, in living neutrophils, a GFP-tagged Arp3 component of the Arp2/3 complex is uniformly distributed in unpolarized cells before stimulation, rapidly accumulates in pseudopodia following exposure of the neutrophils to chemoattractant, and dynamically redistributes in response to a moving source of chemoattractant. These data indicate that external spatial signals may modulate the behaviour of the Arp2/3 complex. The localization of Arp3–GFP throughout the newly polymerized pseudopod supports the hypothesis that the Arp2/3 complex acts as a nucleus for actin polymerization and is incorporated into growing actin filaments as a pointed-end cap. These data are consistent with the localization of Arp2/3 to the lamellipodia of fixed fibroblasts[15,19] and the pseudopodia of fixed *Acanthamoeba castellanii*[20–22]. In living, unstimulated neutrophils, the localization of GFP–Arp3 resembles that in living unstimulated fibroblasts[23], with diffuse cytoplasmic staining and a weak signal in the lamellipodia, although we do not observe dynamic Arp2/3 dots under any conditions. Upon chemotactic stimulation, neutrophils exhibit massive recruitment of the Arp2/3 complex to the pseudopodia; thus protrusive structures of resting cells contain a small amount of Arp2/3 complex and chemoattractant induces a marked recruitment of this complex to the growing pseudopod.

In unstimulated neutrophils expressing GFP–Arp3 that are fixed with formaldehyde and then permeabilized, the Arp2/3 complex is present throughout the actin cytoskeleton (data not shown). In contrast, after chemoattractant-stimulated neutrophils are permeabilized and then fixed and extracted with methanol, the Arp2/3 complex is predominantly associated with the sites of active actin polymerization. This enrichment of a 'less-extractable pool' of the Arp2/3 complex at sites of actin polymerization is observed only for stimulated neutrophils and is most dramatic for samples permeabilized before fixation. We suspect that our fixation and permeabilization conditions preferentially extract Arp2/3 complexes present in actin tails but stabilize Arp2/3 complexes that are associated with factors that induce its recruitment or activation. A reasonable candidate for recruitment of the Arp2/3 complex is the small GTPase Cdc42. Activated Cdc42 can induce actin polymerization in neutrophil, *Dictyostelium* and *Xenopus* extracts[24,25]. The Arp2/3 complex is biochemically downstream of Cdc42-mediated actin polymerization in cell extracts[7,26], and activated Cdc42 forms a stable complex with the Arp2/3 complex and other associated proteins[7], perhaps accounting for the behaviour of the least-extractable pool of the Arp2/3 complex in our permeabilized neutrophil system.

Chemoattractant-induced sites of actin polymerization in neutrophils are at the tips of actin fingers that extend into the plasma membrane; these sites co-localize with the least-extractable pool of

© 1999 Macmillan Magazines Ltd

the Arp2/3 complex, and the fingers correspond to radially protruding structures that extend from the neutrophil towards point sources of chemoattractant. On the basis of these data, we present a model for actin polymerization in response to chemotactic stimulation; this model is analogous to models proposed for actin-based motility of the intracellular bacterial pathogen *Listeria monocytogenes*.

Listeria monocytogenes can move rapidly in the cytoplasm of infected host cells[27,28]. The bacterially expressed protein ActA stimulates the ability of the host Arp2/3 complex to nucleate actin filaments[6] and this localized actin polymerization at the bacterial surface is thought to drive bacterial motility. In well preserved *Listeria* pseudopodial projections in macrophages, the actin tail consists of long axial filaments and short randomly orientated filaments[29], supporting the suggestion[29,30] that the actin filaments nucleated at the surface of *Listeria* continue to polymerize only while next to the bacterial surface; after the filaments have left the zone of actin polymerization adjacent to the bacterial surface, they are capped at their barbed ends and cease growing.

We propose that stimulation of neutrophil chemoattractant receptors leads to the organization of foci of actin polymerization, at or just under the plasma membrane, that are functionally equivalent to the zone of actin polymerization generated by the ActA protein at the posterior surface of *Listeria monocytogenes* (Fig. 6). In this model, each focus mediates actin polymerization at its surface by activating the nucleating ability of the Arp2/3 complex. Actin filaments continue to polymerize only while in the zone of actin polymerization at the surface of the polymerization focus, and filaments are capped at their barbed ends after they have left this zone. Actin polymerization at the surface of the polymerization focus propels it and the cell membrane forward, forming an actin finger similar to that of a *Listeria* tail, with polymerization taking place at the tip of the growing finger (Fig. 6).

How might neutrophils regulate the behaviour of these polymerization foci to mediate cell migration up chemotactic gradients? We have shown that neutrophils extend microspikes and radial actin ruffles towards a point source of chemoattractant, that the tips of these actin bundles represent the sites of maximum actin polymerization, and that the spatial distribution of actin polymerization does not depend solely on the distribution of pre-existing actin and can be biased by chemotactic gradients. On the basis of these data, we propose that asymmetric establishment and/or maintenance of sites of actin polymerization produce the cytoskeletal and morphological rearrangements that mediate cell migration up gradients of chemoattractants. ☐

Methods

Neutrophil preparation and stimulation.

A drop of healthy human blood, acquired by pinprick, was collected on the centre of a sterile coverslip and neutrophils were isolated as described. The cells were covered with mHBSS medium (150 mM NaCl, 4 mM KCl, 1.2 mM $CaCl_2$, 1 mM $MgCl_2$, 10 mg ml^{-1} glucose and 20 mM HEPES, pH 7.2) and incubated at 37 °C for 15 min before chemotactic stimulation. All subsequent steps were carried out at room temperature.

For uniform chemotactic stimulation, cells were incubated in mHBSS containing 20 nM FMLP (Sigma). For delivery of a point source of FMLP, we allowed a solution of 10 µM FMLP to diffuse passively out of the tip of a micropipette of diameter ~0.2 µm whose position relative the coverslip could be controlled with a Narishige micromanipulator (procedure modified from ref. 32).

Preparation of TMR–actin.

Actin was prepared from frozen rabbit muscle (Pel-Freez Biologicals, Rogers, AR), polymerized into filamentous form, and derivatized with *N*-hydroxysuccinimidyl-5-carboxytetramethylrhodamine (Molecular Probes) as described. TMR–actin was stored at a concentration of 100 µM at –80 °C after freezing aliquots in liquid nitrogen. Before use, TMR–actin was rapidly thawed from –80 °C, diluted ten times in G-buffer, sonicated using a Vibracell sonicator (Sonics and Materials, Danbury, CT), and clarified in a microfuge for 20 min at 4 °C.

Permeabilized cells.

Before permeabilization, neutrophils were treated for 5 min in mHBSS containing 1 mM DFP (Sigma). Neutrophils were then permeabilized (using a modification of the procedure in refs 12,14). For experiments involving uniform chemoattractant stimulation, neutrophils were stimulated for 60 s in mHBSS containing 20 nM FMLP and then permeabilized for 3 min in cytoskeleton buffer with sucrose (CBS; containing 10 mM MES, pH 6.1, 138 mM KCl, 3mM $MgCl_2$, 2 mM EGTA; refs 12,35) containing 0.2 mg ml^{-1} saponin or 1% NP40, 1 mM ATP, 20 nM FMLP and 0.35 µM TMR–actin, added immediately before use. For some experiments, 1 µg ml^{-1} fluorescein isothiocyanate (FITC)–phalloidin was used to stabilize the F-actin cytoskeleton during permeabilization.

Immunocytochemistry.

To visualize the actin cytoskeleton, cells were fixed for 20 min in a solution of 3.7% paraformaldehyde in CBS and then incubated with 10 units ml^{-1} Texas-Red-labelled X-phalloidin (Molecular Probes) for 20 min. For experiments involving affinity-purified rabbit anti-p21–Arc primary antibodies, neutrophils were fixed for 40 min in 3.7% paraformaldehyde, briefly washed in PBS containing 0.5% Triton-X100, and then incubated in methanol at –20 °C for 3 min before incubation with a 1:50 dilution of anti-p21–Arc antibody for 1 h. Mouse anti-actin antibodies (5 µg ml^{-1}; Boehringer Mannheim) were used to label the actin cytoskeleton for methanol-fixed samples. All secondary antibodies were from Jackson ImmunoResearch Laboratories.

Amphotropic retrovirus generation and PLB985-cell transduction.

For experiments involving the GFP-tagged construct, we used the human promyelocytic cell line PLB-985 (ref. 36). CDNAs encoding EGFP (Clontech) and Arp3–GFP were cloned into the pLNCX retroviral vector under the control of the CMV promoter. Retroviruses were produced and PLB-985 cells were stably transduced as described.

Microscopy and analysis.

All images were acquired with a scientific-grade, cooled, charge-coupled device on a multiwavelength wide-field three-dimensional microscopy system (ref. 39 and references therein) in which the shutters, filter wheels, focus movement, and data collection are all computer driven. Neutrophils were imaged using a ×60 1.4 NA lens (Olympus) and n=1.518 immersion oil (RP Cargille Laboratories, Cedar Grove, NJ). Immunofluorescent samples were imaged in successive 0.25-µm focal planes through the sample, and out-of-focus light was removed with a constrained iterative deconvolution algorithm. Maximum-intensity projections, side views and rotated reconstructions of the three-dimensional data stacks were generated using image-visualization environment software. Unless otherwise indicated, all images represent single optical sections of immunofluorescence data.

RECEIVED 11 FEBRUARY 1999; REVISED 7 APRIL 1999; ACCEPTED 10 APRIL 1999; PUBLISHED 15 MAY 1999.

---

1. Cano, M. L., Lauffenburger, D. A. & Zigmond, S. H. Kinetic analysis of F-actin depolymerization in polymorphonuclear leukocyte lysates indicates that chemoattractant stimulation increases actin filament number without altering the filament length distribution. *J. Cell Biol.* 115, 677–687 (1991).
2. Zigmond, S. H. Mechanisms of sensing chemical gradients by polymorphonuclear leukocytes. *Nature* 249, 450–452 (1974).
3. Zigmond, S. H. & Hirsch, J. G. Effects of cytochalasin B on polymorphonuclear leucocyte locomotion, phagocytosis and glycolysis. *Exp. Cell Res.* 73, 383–393 (1972).
4. Watts, R. G., Crispens, M. A. & Howard, T. H. A quantitative study of the role of F-actin in producing neutrophil shape. Cell Motil. *Cytoskeleton* 19, 159–168 (1991).
5. Mullins, R. D., Heuser, J. A. & Pollard, T. D. The interaction of Arp2/3 complex with actin: nucleation, high affinity pointed end capping, and formation of branching networks of filaments. *Proc. Natl Acad. Sci. USA* 95, 6181–6186 (1998).
6. Welch, M. D., Rosenblatt, J., Skoble, J., Portnoy, D. A. & Mitchison, T. J. Interaction of human Arp2/3 complex and the *Listeria monocytogenes* ActA protein in actin filament nucleation. *Science.* 281, 105–108 (1998).
7. Ma, L., Rohatgi, R. & Kirschner, M. W. The Arp2/3 complex mediates actin polymerization induced by the small GTP-binding protein Cdc42. *Proc. Natl Acad. Sci USA* 95, 15362–15367 (1998).
8. McCollum, D., Feoktistova, A., Morphew, M., Balasubramanian, M. & Gould, K. L. The *Schizosaccharomyces pombe* actin-related protein, Arp3, is a component of the cortical actin cytoskeleton and interacts with profilin. *EMBO J.* 15, 6438–6446 (1996).
9. Moreau, V., Madania, A., Martin, R. P. & Winson, B. The *Saccharomyces cerevisiae* actin-related protein Arp2 is involved in the actin cytoskeleton. *J. Cell Biol.* 134, 117–132 (1996).
10. Winter, D., Podtelejnikov, A. V., Mann, M. & Li, R. The complex containing actin-related proteins Arp2 and Arp3 is required for the motility and integrity of yeast actin patches. *Curr. Biol.* 7, 519–529 (1997).
11. Okabe, S. & Hirokawa, N. Actin dynamics in growth cones. *J. Neurosci.* 11, 1918–1929 (1991).
12. Symons, M. H. & Mitchison, T.J. Control of actin polymerization in live and permeabilized fibroblasts. *J. Cell Biol.* 114, 503–513 (1991).
13. Chan, A. Y. *et al.* EGF stimulates an increase in actin nucleation and filament number at the leading edge of the lamellipod in mammary adenocarcinoma cells. *J. Cell Sci.* 111, 199–211 (1998).
14. Redmond, T. & Zigmond, S. H. Distribution of F-actin elongation sites in lysed polymorphonuclear leukocytes parallels the distribution of endogenous F-actin. Cell Motil. *Cytoskeleton* 26, 7–18 (1993).
15. Welch, M. D., DePace, A. H., Verma, S., Iwamatsu, A. & Mitchison, T. J. The human Arp2/3 complex is composed of evolutionarily conserved subunits and is localized to cellular regions of dynamic actin filament assembly. *J. Cell Biol.* 138, 375–384 (1997).
16. Sanger, J. M., Sanger, J. W. & Southwick, F. S. Host cell actin assembly is necessary and likely to provide the propulsive force for intracellular movement of *Listeria monocytogenes*. *Infect. Immun.* 60, 3609–3619 (1992).
17. Theriot, J. A., Mitchison, T. J., Tilney, L. G. & Portnoy, D. A. The rate of actin-based motility of intracellular *Listeria monocytogenes* equals the rate of actin polymerization. *Nature.* 357, 257–260 (1992).
18. Amrein, P. C. & Stossel, T. P. Prevention of degradation of human polymorphonuclear leukocyte proteins by diisopropylfluorophosphate. *Blood* 56, 442–447 (1980).
19. Machesky, L. M. *et al.* Mammalian actin-related protein 2/3 complex localizes to regions of lamellipodial protrusion and is composed of evolutionarily conserved proteins. *Biochem. J.* 328, 105–112 (1997).
20. Machesky, L. M., Atkinson, S. J., Ampe, C., Vandekerckhove, J. & Pollard, T. D. Purification of a cortical complex containing two unconventional actins from *Acanthamoeba* by affinity chromatography on profilin-agarose. *J. Cell Biol.* 127, 107–115 (1994).

© 1999 Macmillan Magazines Ltd

21. Kelleher, J. F., Atkinson, S. J. & Pollard, T.D. Sequences, structural models, and cellular localization of the actin-related proteins Arp2 and Arp3 from *Acanthamoeba*. *J. Cell Biol.* **131**, 385–397 (1995).
22. Mullins, R. D., Kelleher, J. F., Xu, J. & Pollard, T. D. Arp2/3 complex from *Acanthamoeba* binds profilin and cross-links actin filaments. *Mol. Biol.Cell.* **9**, 841–852 (1998).
23. Schafer, D. A. *et al.* Visualization and molecular analysis of actin assembly in living cells. *J. Cell Biol.* **143**, 1919–1930 (1998).
24. Zigmond, S. H., Joyce, M., Borleis, J., Bokoch, G. M., & Devreotes, P. N. Regulation of actin polymerization in cell-free systems by GTP-γS and Cdc42. *J. Cell Biol.* **138**, 363–374 (1997).
25. Ma, L., Cantley, L. C., Janmey, P. A., & Kirschner, M. W. Corequirement of specific phosphoinositides and small GTP-binding protein Cdc42 in inducing actin assembly in *Xenopus* egg extracts. *J.Cell Biol.* **140**, 1125–1136 (1998).
26. Mullins, R. D. & Pollard, T. D. Rho-family G-proteins act through Arp2/3 complex to stimulate actin polymerization in *Acanthamoeba* extracts.*Curr. Biol.* (in the press).
27. Dabiri, G. A., Sanger, J. M., Portnoy, D. A. & Southwick, F. S. Listeria monocytogenes moves rapidly through the host-cell cytoplasm by inducing directional actin assembly. *Proc. Natl Acad. Sci. USA* **87**, 6068–6072 (1990).
28. Tilney, L. G. & Tilney, M. S. The wily ways of a parasite: induction of actin assembly by Listeria. *Trends Microbiol.* **1**, 25–31 (1993).
29. Sechi, A. S., Wehland, J. & Small, J. V. The isolated comet tail pseudopodium of *Listeria monocytogenes*: a tail of two actin filament populations, long and axial and short and random. *J. Cell Biol.* **137**, 155–167 (1997).
30. Marchand, J. B. *et al.* Actin-based movement of *Listeria monocytogenes*: actin assembly results from the local maintenance of uncapped filament barbed ends at the bacterium surface. *J. Cell Biol.* **130**, 331–343 (1995).
31. Cassimeris, L., McNeill, H. & Zigmond, S. H. Chemoattractant-stimulated polymorphonuclear leukocytes contain two populations of actin filaments that differ in their spatial distributions and relative stabilities. *J. Cell Biol.* **110**, 1067–1075 (1990).
32. Gerisch, G. & Keller, H. U. Chemotactic reorientation of granulocytes stimulated with micropipettes containing fMet-Leu-Phe. *J. Cell Sci.* **52**, 1–10 (1981).
33. Pardee, J. D. & Spudich, J. A. Purification of muscle actin. *Methods Enzymol.* **85B**, 164–181 (1982).
34. Kellogg, D. R., Mitchison, T. J. & Alberts, B. M. Behaviour of microtubules and actin filaments in living *Drosophila* embryos. *Development* **103**, 675–686 (1988).
35. Small, J. V. Organization of actin in the leading edge of cultured cells: influence of osmium tetroxide and dehydration on the ultrastructure of actin meshworks. *J. Cell Biol.* **91**, 695–705 (1981).
36. Tucker, K. A., Lilly, M. B., Heck, L. Jr & Rado, T. A. Characterization of a new human diploid myeloid leukemia cell line (PLB-985) with granulocytic and monocytic differentiating capacity. *Blood* **70**, 372–378 (1987).
37. Miller, A. D. & Rosman, G. J. Improved retroviral vectors for gene transfer and expression. *Biotechniques* **7**, 980–982, 984–986, 989–990 (1989).
38. Servant, G., Weiner, O. D., Neptune, E., Sedat, J. W. & Bourne, H. R. Dynamics of a chemoattractant receptor in living neutrophils during chemotaxis. *Mol. Biol. Cell* **10**, 1163-1178 (1999).
39. Hiraoka, Y., Swedlow, J. R., Paddy, M. R., Agard, D. A. & Sedat, J. W. Three-dimensional multiple-wavelength fluorescence microscopy for the structural analysis of biological phenomena. *Semin. Cell Biol.* **2**, 153–165 (1991).
40 Agard, D. A., Hiraoka, Y., Shaw, P. & Sedat, J. W. Fluorescence microscopy in three dimensions. *Methods Cell Biol.* **30**, 353–377 (1989).
41. Swedlow, J. R., Sedat, J. W. & Agard, D. A. *in Deconvolution of Images and Spectra* (ed. Jansson, P. A.) 284–307 (Academic, San Diego, 1997).
42. Chen, H., Hughes, D. D., Chan, T. A., Sedat, J. W. & Agard, D. A. IVE (Image Visualization Environment): a software platform for all three-dimensional microscopy applications. *J. Struct. Biol.* **116**, 56–60 (1996).

ACKNOWLEDGEMENTS

We thank A. Abo, D. Agard, C. Bargmann, D. Drubin, Z. Kam, C. Kenyon, R. Mullins, J. Taunton, J. Weissman, S. Zigmond and members of the Bourne and Sedat laboratories for discussions; A. Abo for the PLB-985 promyelocytic cell line; and C. Bargmann, C. Kenyon, J.V. Small, and S. Zigmond for critical reading of the manuscript. This work was supported in part by grants from the NIH (to H.R.B., J.W.S. and T.J.M.). M.D.W. is a Leukemia Society of America Special Fellow; G.S. is a Medical Research Council of Canada Postdoctoral Fellow; and O.D.W. is an HHMI Predoctoral Fellow.

Correspondence and requests for materials should be addressed to H.R.B.

Supplementary information is available on *Nature Cell Biology*'s World-Wide Web site (http://cellbio.nature.com).

© 1999 Macmillan Magazines Ltd

CHAPTER FIVE

PI(3,4,5)P3 Exhibits an Amplified Polarity During Neutrophil Chemotaxis

Reprinted with permission from Servant, G.*, O.D. Weiner*, P. Herzmark, T. Bhalla, J.W. Sedat, and H.R. Bourne (2000). Polarization of chemoattractant receptor signaling during neutrophil chemotaxis. *Science,* **287:** 1037-1040. (*co-first authors).

Copyright 2000, American Association for the Advancement of Science.

Polarization of Chemoattractant Receptor Signaling During Neutrophil Chemotaxis

Guy Servant,[1*] Orion D. Weiner,[1,2*] Paul Herzmark,[1]
Tamás Balla,[3] John W. Sedat,[2] Henry R. Bourne[1]†

Morphologic polarity is necessary for chemotaxis of mammalian cells. As a probe of intracellular signals responsible for this asymmetry, the pleckstrin homology domain of the AKT protein kinase (or protein kinase B), tagged with the green fluorescent protein (PHAKT-GFP), was expressed in neutrophils. Upon exposure of cells to chemoattractant, PHAKT-GFP is recruited selectively to membrane at the cell's leading edge, indicating an internal signaling gradient that is much steeper than that of the chemoattractant. Translocation of PHAKT-GFP is inhibited by toxin-B from *Clostridium difficile*, indicating that it requires activity of one or more Rho guanosine triphosphatases.

Neutrophils and other motile cells respond to a chemoattractant gradient by rapidly adopting a polarized morphology, with distinctive leading and trailing edges oriented with respect to the gradient (*1*). Actin is polymerized preferentially at the leading edge (*1, 2*), even in quite shallow chemoattractant gradients (∼1 to 2% change in concentration across one cell diameter) (*1*). The remarkable asymmetry of newly polymerized actin suggests that the neutrophil can greatly amplify the much smaller asymmetry of the extracellular signal detected by chemoattractant receptors. Amplification of the internal signaling asymmetry, relative to the external gradient of chemoattractant, must take place at a step between activation of these receptors and the actin polymerization machinery, because the receptors remain uniformly distributed across the cell surface during chemotaxis (*3, 4*). To explore the mechanism of asymmetry, we used a fluorescent probe of the spatial distribution of an intermediate intracellular signal. We find that this mechanism depends on activities of one or more Rho guanosine triphosphatases (GTPases) and probably also requires activation of phosphatidylinositol 3-kinase (PI3K).

Chemotaxis of a soil amoeba, *Dictyostelium discoideum*, is accompanied by asymmetric recruitment to the cell surface of two GFP-tagged signal transduction proteins, the cytosolic regulator of adenylyl cyclase (CRAC) (*5*) and the pleckstrin homology (PH) domain of the AKT protein kinase (PHAKT) (*6*). In this slime mold, asymmetry of the internal chemotactic signal does not require polymerization of actin (*5*). Although the $\beta\gamma$ subunit of a guanine nucleotide binding protein (G protein) (G$\beta\gamma$) is required for chemotaxis of *Dictyostelium* and for recruiting both probes of receptor activity to cell membranes, it is not clear whether G$\beta\gamma$ serves as an asymmetrically distributed binding site for either probe (*5, 6*).

Here, we stably expressed PHAKT-GFP in an immortalized mammalian cell line, HL-60, which can be induced to differentiate into neutrophil-like cells (*7, 8*). PHAKT-GFP, localized mostly in the cytoplasm of unstimulated differentiated HL-60 cells (Fig. 1A, I), translocated to the plasma membrane when the cells were exposed to a uniform concentration (100 nM) of either of two neutrophil chemoattractants, *N*-formyl-Met-Leu-Phe (*f*MLP) (Fig. 1A, I′) and C5a (see below; Fig. 4B, VII). This translocation, seen in virtually every cell [96%, Web figure 4D (*9*)], was rapid and transient, reaching a peak after ∼30 s and decreasing over the ensuing 2 min [supplemental figures and videos show the time course of PHAKT-GFP translocation (*9*)].

In a gradient of *f*MLP, supplied by a nearby micropipette (*10*), PHAKT-GFP was recruited exclusively to the parts of a cell's surface that received the strongest stimulation (Fig. 1A, II′ and III′). Indeed, translocation of PHAKT-GFP tightly accompanied actin polymerization and formation of a pseudopod at the leading edge (*11*) [for videos of this figure, see (*9*)]. Enrichment of PHAKT-GFP fluorescence at the leading edge contrasted with the uniform distribution of a plasma membrane marker, a GFP-tagged chemoattractant receptor for C5a (C5aR-GFP) (*4*) expressed in HL-60 cells (Fig. 1A, IV) and the exclusively cytosolic signal seen in HL-60 cells expressing GFP alone (Fig. 1A, V) (*11*). The internal gradient of PHAKT-GFP distribution is steeper than that of the extracellular stimulus that elicited it (Fig. 1B). From experiments with a fluorescent dye, sulforhodamine (*12*), we estimate that Femtotips micropipettes generate gradients that are reproducibly linear and rather shallow (∼15% decrease in maximum dye concentration per 10 μm) (Fig. 1B, I). We estimate that the gradient of internal cellular signal was at least six times steeper than that of the chemoattractant itself (Fig. 1B, I and II). The asymmetry of the distribution of PHAKT-GFP probably reflects a parallel asymmetry of signals responsible for restricting actin polymerization to the cells' leading edge.

Neutrophils also polarize their morphology, albeit in random directions, when exposed to a uniformly increased concentration of chemoattractant (*1, 2, 4*). Such a uniform increase in *f*MLP concentration similarly induced asymmetric recruitment of PHAKT-GFP to the pseudopod (morphologic leading edge) in about 50% of polarizing cells (*13*). Recruitment of PHAKT-GFP correlated with the direction of membrane protrusion and the underlying actin polymerization, as revealed by the ruffled leading edge [Fig. 2, A through D; for a video of this figure, see (*9*)]. These observations show the intrinsic capacity of neutrophils to create asymmetric internal signals, not only in shallow chemoattractant gradients, but even in the presence of a uniform concentration of chemoattractant.

The close temporal and spatial association of actin-containing ruffles and pseudopods with PHAKT-GFP fluorescence raised the possibility that actin polymerization is necessary for translocation of PHAKT-GFP to the plasma membrane of HL-60 cells. In these mammalian cells—as in *Dictyostelium* (*5*)—this was not the case, however. Exposure of HL-60 cells to latrunculin-B (*14*), a toxin that sequesters monomeric actin, caused depolymerization of the dynamic actin cytoskeleton, producing a rounded morphology within 3 to 5 min (Fig. 3A). These cells still recruited PHAKT-GFP asymmetrically to the face closest to a pipet containing *f*MLP (Fig. 3B). Thus, the signaling machinery of neutrophils, like that of *Dictyostelium* (*5*), can amplify the external signaling gradient independently of actin polymerization.

Because small GTPases of the Rho family mediate certain neutrophil responses to *f*MLP (*15, 16*) and play important roles in relaying signals to the actin cytoskeleton (*17*), we investigated whether Rho GTPases are required for recruitment of PHAKT-GFP to the neutrophil plasma membrane. A toxin from *Clostridium difficile* inactivates all three Rho GTPases—Rac, Cdc42, and Rho—by glucosylating a conserved amino acid in the effector domain (*18*). This toxin (*14*) induced a round morphology in HL-60 cells (Fig. 4A, IV and VII) and markedly inhibited actin polymerization in response to *f*MLP (*19*). The toxin also blocked *f*MLP- and C5a-in-

---

[1] Department of Cellular and Molecular Pharmacology and [2] Department of Biochemistry and Biophysics, University of California San Francisco, San Francisco, CA 94143, USA. [3] Endocrinology and Reproduction Research Branch, National Institutes of Child Health and Human Development, National Institutes of Health, Bethesda, MD 20892–4510, USA.

*These authors contributed equally to this work.

†To whom correspondence should be addressed. E-mail: bourne@cmp.ucsf.edu

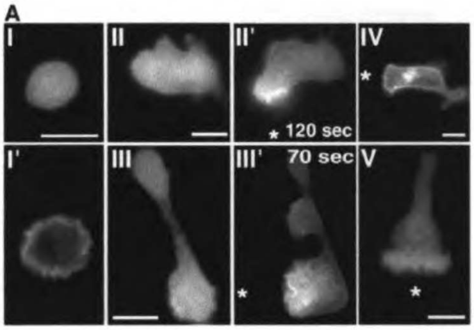

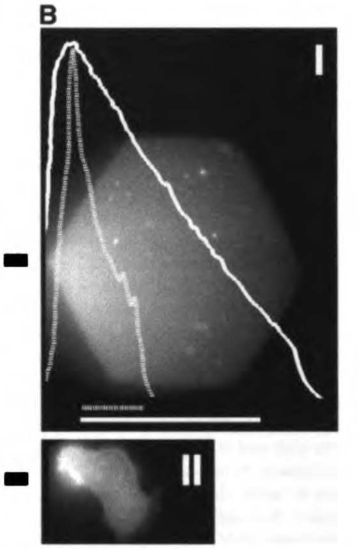

Fig. 1. Translocation of PHAKT-GFP to the plasma membrane of neutrophil-differentiated HL-60 cells. (**A**) PHAKT-GFP–expressing cells (I through III), C5aR-GFP–expressing cells (IV), and GFP-expressing cells (V) were differentiated to neutrophil-like cells (*7*) and plated on glass cover slips as described (*4*). Cells were stimulated either with a uniform increase in *f*MLP concentration, from 0 (I) to 100 nM (I': 60 s post-stimulation) or with a point source of *f*MLP (1 μM) delivered by a Femtotip micropipette (*10*) (II', III', IV, and V), whose position is indicated by an asterisk. Panels II and III correspond, respectively, to cells shown in panels II' and III', but before stimulation with the micropipette. Images were recorded in the fluorescein isothiocyanate (FITC) channel every 5 s as described (*4*). Each result was reproduced in at least 10 experiments (*11*). Bars, 10 μm. Videos of a time course and asymmetric translocation of PHAKT-GFP are available at (*9*). (**B**) Extracellular gradient generated with the micropipette (I), relative to the intracellular gradient of PHAKT-GFP recruitment (II). For the experiment in (I), a Femtotips micropipette filled with sulforhodamine, a fluorescent dye, was lowered onto a cover slip overlaid with the buffer used for cell stimulation (*4, 12*); the image was taken in the rhodamine channel (*4*) 2 min after repositioning the micropipette in a field lacking dye fluorescence. The micropipette tip was located just outside the illumination field, at the left of the hexagon. The solid white line in (I) indicates the intensity of dye fluorescence (*y*-axis) along the *x*-axis at the level of the black horizontal bar shown to the left of the figure; this curve presumably reflects the shape of a gradient of chemoattractant of similar molecular size, such as *f*MLP. The *x*-axis indicates distance across the microscopic field (solid white scale bar, 50 μm). Fluorescence intensities at the ends of this solid scale bar in (I) were 1900 and 300 (arbitrary units, after subtracting a background value of 400, obtained outside the hexagon). The dashed white curve in (I) indicates the intensity of PHAKT-GFP fluorescence measured across a diameter of the neutrophil shown in (II), depicted at the same scale as in (I). This cell was exposed to *f*MLP supplied by a micropipette; the diameter across which PHAKT-GFP fluorescence was measured is positioned at the level of the black horizontal bar in (II). The 15-μm dashed white line in (I) represents the intensity of PHAKT-GFP recruitment across this diameter; fluorescence intensities at the two ends of this line were 900 versus 200 (arbitrary units, after subtracting a background of 100 units measured outside the cell boundary). Maximum fluorescence intensity for rhodamine decreases to half its value over a distance of 30 μm, while maximum fluorescence intensity for PHAKT-GFP decreases to half its value over 5 μm.

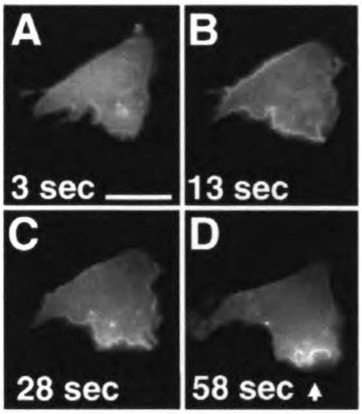

Fig. 2. (**A** through **D**) Asymmetric translocation of PHAKT-GFP at the plasma membrane of neutrophil-differentiated HL-60 cells during polarization in response to a uniform increase in chemoattractant concentration. Differentiated cells (*7*) were plated on glass cover slips as described (*4*). Cells were stimulated with 100 nM *f*MLP at time 0 and images were then recorded as described in the legend of Fig. 1. The arrow in (D) points to the advancing leading edge of the cell. Uniform stimulation was assessed in 13 different sessions, recording the behavior of 68 cells (*13*). Bar, 10 μm. A video of this experiment is available at (*9*).

duced translocation of PHAKT-GFP and membrane ruffling in most cells (Fig. 4A, V and VIII, respectively). A few cells [~9 to 20%, Web figure 4D (*9*)] showed detectable (but limited) translocation of PHAKT-GFP. In contrast, in the absence of toxin treatment a uniform concentration of *f*MLP or C5a induced robust PHAKT-GFP translocation and ruffling in virtually every cell [Fig. 1A, I'; Fig. 4B, IV and VII; Web figure 4D (*9*)]. Cells treated with *C. difficile* toxin were not simply unable to respond to extracellular stimuli: subsequent exposure of toxin-treated, *f*MLP- and C5a-resistant cells to insulin induced translocation of PHAKT-GFP [Fig. 4A, VI and IX, respectively; Web figure 4D (*9*)], although the ruffling response to insulin was inhibited (Fig. 4A) (*20*). At lower toxin concentrations (3.8 to 50 μg/ml), inhibition of the membrane ruffling response to *f*MLP varied widely from cell to cell; under these conditions, *f*MLP induced PHAKT-GFP translocation preferentially in those cells that showed the ruffling response, suggesting that PHAKT-GFP translocation tightly accompanies activation of Rho GTPases. In none of the conditions we tested (varying toxin concentrations and incubation times) did the toxin affect insulin-induced PHAKT-GFP translocation (*19*). Pertussis toxin (*14*) (PTX) blocked both PHAKT-GFP translocation and morphologic responses to *f*MLP, indicating that these events were mediated by G_i, a pertussis toxin–sensitive G protein [Fig. 4A, II; Web figure 4D (*9*)]. Conversely, PTX did not prevent responses to insulin [Fig. 4A, III; Web figure 4D (*9*)].

The PH domain of AKT binds with high affinity to 3'-phosphorylated lipid products of PI3K (*21*), a well-documented mediator of many actions of insulin (*22, 23*). At 100 μM, a specific PI3K inhibitor, LY 294002 (*14*) prevented insulin-induced recruitment of PHAKT-GFP to the plasma membrane (Fig. 4B, III) but did not efficiently block translocation triggered by *f*MLP or C5a [Web figures 4C and 4D (*9*)]. At a higher concentration of LY 294002 (300 μM), translocation induced by either *f*MLP or C5a was almost totally abolished in most cells [Fig. 4B, VI and IX, respectively; Web figure 4D (*9*)]. Point mutations in the PH domain of AKT (K20A and R25C), previously shown to impair translocation of PHAKT in response to PI3K activation (*24*) also blocked or severely impaired PHAKT-GFP translocation in HL-60 cells stimulated with *f*MLP (*19*). The corresponding residues in a PHAKT analog, PHBTK, interact with the 5-phosphate and 3-phosphate of inositol $(1,3,4,5)P_4$ (*25*). Thus, the activity of at least one Rho GTPase and lipid products of PI3K seem to be required for the translocation

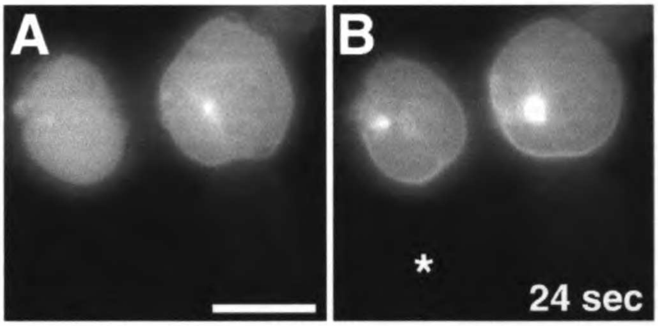

Fig. 3. Asymmetric translocation of PHAKT-GFP in latrunculin-B–treated neutrophil-differentiated HL-60 cells. Differentiated cells (*7*) were plated on glass cover slips as described (*4*). Cells were then pretreated with 20 μg/ml latrunculin-B for 10 min (**A**) (*14*) and then stimulated, in the continued presence of the toxin, with a point source of *f*MLP (10 μM) delivered from a micropipette (*10*) [(**B**), asterisk]. Images were recorded as described in the legend of Fig. 1. Cells showed asymmetric recruitment biased by the micropipette's position in five of nine stimulation sessions performed under these conditions. Bar, 10 μm.

of PHAKT-GFP in neutrophil-differentiated HL-60 cells.

Chemoattractant receptors can activate at least both class 1A and class 1B PI3K's in neutrophils, whereas the insulin receptor only activates class 1A PI3K (*23, 26, 27*). This could explain differing sensitivities of these receptor-induced responses to the PI3K inhibitor. Recent studies in transgenic knockout mice found that chemoattractant-induced formation of 3′-phosphorylated lipids, activation of AKT, and chemotaxis of neutrophils depend entirely on $p110\gamma$, the only known PI3K of class 1B (*28*). Similarly, $p110\gamma$ may be necessary for PHAKT recruitment to the plasma membrane; if so, our experiments with the PI3K inhibitor suggest that chemoattractant-induced translocation of PHAKT only requires activity of a small fraction of the HL-60 cell's complement of $p110\gamma$. PI3K's of class 1A are activated mainly through the recruitment of their regulatory subunit, p85, to the plasma membrane (*23*), whereas $p110\gamma$ is activated directly by $\beta\gamma$ subunits liberated from activated heterotrimeric G proteins (*23, 26*). Thus, it is possible that PHAKT-GFP translocation at the leading edge of motile neutrophils reflect spatially restricted activation of heterotrimeric G proteins. Our results with the toxin suggest, however, that amplification of the PHAKT recruitment requires an intermediate pathway dependent on activity of one or more Rho GTPases.

Our results do not identify the specific Rho GTPase(s) responsible for *f*MLP-induced recruitment of PHAKT-GFP to membranes of HL-60 cells. Although it is likely that recruitment requires more than one Rho GTPase, we speculate that Cdc42 plays a special role in determining the asymmetry of the *f*MLP response. Mutant forms of this GTPase or its exchange factor cause yeast (*29*), macrophages (*30*), and T lymphocytes (*31*) to lose their normal ability to polarize selectively toward an extracellular stimulus; such cells orient in random directions instead, like ships with broken compasses. We imagine that Cdc42 constitutes a key element of the neutrophil "compass," which directs asymmetric translocation of PHAKT-GFP (Figs. 1 through 3) and asymmetric polymerization of actin (*1, 2*) at the cell's leading edge in a gradient of chemoattractant.

References and Notes

1. S. H. Zigmond, *J. Cell Biol.* **75**, 606 (1977); P. N. Devreotes and S. H. Zigmond, *Annu. Rev. Cell. Biol.* **4**, 649 (1988); L. Cassimeris and S. H. Zigmond, *Semin. Cell. Biol.* **1**, 125 (1990); M. J. Caterina and P. N.

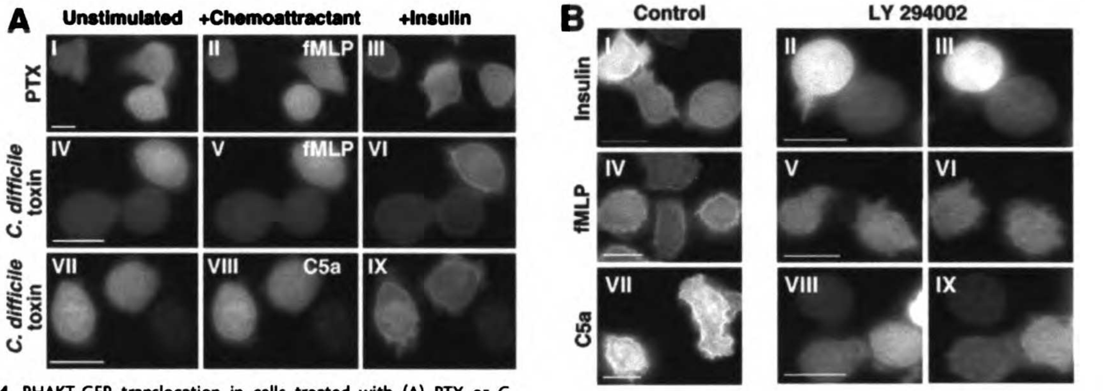

Fig. 4. PHAKT-GFP translocation in cells treated with (A) PTX or *C. difficile* toxin-B and (B) a PI3K inhibitor, LY 294002 (*14*). (**A**) Neutrophil-differentiated cells (*7*), plated on glass cover slips (*4*), were stimulated sequentially with *f*MLP and insulin (panels II and III and panels V and VI, respectively) or C5a and insulin (panels VIII and IX, respectively). *f*MLP or C5a was added first, removed 2 min later, and replaced with insulin, then cells were stimulated for a further 3 min. Panel I through III: treatment with PTX (1 μg/ml). Panels IV through IX: treatment with *C. difficile* toxin-B (90 μg/ml). Panels I, IV, and VII: cells before stimulation with agonists (zero time). Images were recorded as described in the legend of Fig. 1. Stimulation times with the indicated agonists were as follows: II: 65 s; III: 115 s; V: 67 s; VI: 178 s; VIII: 39 s; IX: 161 s. Bars, 10 μm. (**B**) Effect of LY 294002 on chemoattractant- and insulin-induced plasma membrane translocation of PHAKT-GFP in neutrophil-differentiated HL-60 cells. Panels I, IV, and VII: untreated cells stimulated with insulin, *f*MLP, and C5a, respectively. Panels II, V, and VIII: unstimulated cells treated with LY 294002 (100 μM in panel II; 300 μM in panels V and VIII). Panels III, VI, and IX show responses of the same cells to insulin, *f*MLP, or C5a, respectively, in the presence of LY 294002 (100 μM in panel III; 300 μM in panels VI and IX). Images were recorded as described in the legend of Fig. 1. Stimulation times with agonists were as follows: I: 183 s; IV: 46 s; VII: 39 s; III: 199 s; VI: 61 s; IX: 41 s. For each treatment, the result shown is representative of at least eight different stimulation sessions performed on at least two different batches of neutrophil-differentiated HL-60 cells. Bars, 10 μm. Two additional panels of this figure (9) show the effect of 100 μM LY 294002 on chemoattractant-induced plasma membrane translocation of PHAKT-GFP (Web figure 4C) and a histogram (Web figure 4D) of percent cells responding to all three agonists tested in the presence of *C. difficile* toxin or LY 294002 at 100 or 300 μM.

Devreotes, *FASEB J.* **5**, 3078 (1991); G. P. Downey, *Curr. Opin. Immunol.* **6**, 113 (1994).
2. O. D. Weiner *et al.*, *Nature Cell Biol.* **1**, 75 (1999).
3. Z. Xiao *et al.*, *J. Cell Biol.* **139**, 365 (1997).
4. G. Servant, O. D. Weiner, E. R. Neptune, J. W. Sedat, H. R. Bourne, *Mol. Biol. Cell* **10**, 1163 (1999).
5. C. A. Parent *et al.*, *Cell* **95**, 81 (1998); C. A. Parent and P. N. Devreotes, *Science* **284**, 765 (1999).
6. R. Meili *et al.*, *EMBO J.* **18**, 2092 (1999).
7. Culture and differentiation of HL-60 cells with 1.3% dimethyl sulfoxide (DMSO) were performed as described (*4*).
8. The fusions of the PH domains of the protein kinase B (PKB/AKT) kinase and the C5aR with GFP are already described [P. Varnai and T. Balla, *J. Cell Biol.* **143**, 501 (1998)] (*4*). HL-60 cells were transfected by electroporation. Stable cell lines were generated with 1 mg/ml active G-418. Further details of these methods are available at (9).
9. Supplemental material is available at www.sciencemag.org/feature/data/1044239.shl.
10. Microscopic analysis of HL-60 cells was performed at room temperature as already described (*4*). For point-source stimulation, custom-made micropipets with an opening of 0.5 ± 0.2 μm (Eppendorf Femtotips; Fisher Scientific, Pittsburgh, PA) were used. Chemoattractant was back loaded, and air bubbles were pushed out with a microinjection device. The micropipette was placed at the desired coordinates, and a chemotactic gradient was generated with passive diffusion from the tip.
11. Seventeen different sessions of point-source stimulation were performed with PHAKT-GFP expressing HL-60 cells. In these experiments, 15 of 23 cells migrating toward the micropipette showed translocation at the leading edge. Failure to detect recruitment in a minority of the polarizing cells probably indicates a threshold phenomenon. That is, the stimulation received by individual cells exposed to the pipette is weaker than that received by cells in a uniform concentration (100 nM) of *f*MLP, which causes recruitment in 96% of cells [Web figure 4D (9)]. Eleven different sessions of point-source stimulation were performed with GFP-expressing HL-60 cells. In these experiments, as expected, we could not detect any increase of the fluorescent signal at the leading edge of 30 cells migrating toward the micropipette. The C5a receptor-GFP chimera (C5aR-GFP) was shown previously to behave as a spatially unbiased probe of plasma membrane concentration when expressed in a neutrophil-like cell line, PLB-985 (4). Similarly, we detected no apparent increase of C5aR-GFP fluorescence at the leading edge of HL-60 cells.
12. To determine the apparent shape of the chemotactic gradient generated by the Femtotips, we used a fluorescent dye of molecular weight similar to *f*MLP (MW: 437.6): sulforhodamine 101 (MW: 606.7; Molecular Probes, Eugene, OR). Two different Femtotips were tested and similar gradients were observed. IVE software [H. Chen, D. D. Hughes, T. A. Chan, J. W. Sedat, D. A. Agard, *J. Struct. Biol.* **116**, 56 (1996)] was used to calculate fluorescence intensity along the lines indicated for the fluorescent ligand and PHAKT-GFP recruitment (Fig. 1B).
13. Virtually all differentiated HL-60 cells showed recruitment of PHAKT-GFP to the plasma membrane [96%; Web figure 4D (9)] when exposed to a uniform increase in *f*MLP concentration (from 0 to 100 nM *f*MLP), but only ~50% of the cells polarized morphologically within the first 4 min of stimulation. Of the cells that did polarize, ~50% (that is, ~25% of the entire population) showed periods of asymmetric recruitment of PHAKT-GFP to ruffles at the cell's protruding edge.
14. Treatment of HL-60 cells with toxins and inhibitor were as follows: latrunculin-B (Calbiochem, La Jolla, CA) was added on plated cells at a final concentration of 20 μg/ml, and cells were incubated for 5 to 10 min at room temperature. PTX (List Biological Laboratories, Campbell, CA), which acts by inhibiting signal transduction by G_i proteins, was added directly to the cell culture medium a final concentration of 1 μg/ml, and cells were incubated at 37°C for a period of 16 to 22 hours. For LY 294002 (Calbiochem, La Jolla, CA) treatment, a stock solution (100×) was prepared in 100% DMSO just before use. Cells plated on glass cover slips as described (*4*), were incubated for 20 min at room temperature with a freshly diluted solution (100 to 300 μM) of LY 294002 in modified Hank's balanced salt solution (*4*). *Clostridium difficile* toxin-B (TechLab, Blacksburg, VA), was added directly to the cell culture medium at a final concentration of 90 μg/mL. Cells were incubated at 37°C with the toxin for not less than 2 hours and not more than 4 hours, a period in which the best inhibition of *f*MLP-induced ruffling and actin polymerization responses was observed without excessive loss of cell viability. Further experimental details for treatments with LY 294002 and *C. difficile* toxin are available at (9).
15. A. Abo *et al.*, *Nature* **353**, 668 (1991); U. G. Knaus *et al.*, *Science* **254**, 1512 (1991); D. Cox *et al.*, *J. Exp. Med.* **186**, 1487 (1997); G. M. Bokoch, *Blood* **86**, 1649 (1995).
16. Chemotaxis, F-actin generation, and superoxide production induced by chemoattractants are markedly impaired in neutrophils lacking one GTPase, Rac2 [A. W. Roberts *et al.*, *Immunity* **10**, 183 (1999)].
17. A. Hall, *Annu. Rev. Cell. Biol.* **10**, 31 (1994); S. H. Zigmond *et al.*, *J. Cell Biol.* **138**, 363 (1997); S. H. Zigmond *et al.*, *J. Cell Biol.* **142**, 1001 (1998); L. Ma *et al.*, *J. Cell Biol.* **140**, 1125 (1998); L. Ma, R. Rohatgi, M. W. Kirschner, *Proc. Natl. Acad. Sci. U.S.A.* **95**, 15362 (1998); A. Hall, *Science* **279**, 509 (1998); D. J. Mackay and A. Hall, *J. Biol. Chem.* **273**, 20685 (1998); E. Bi and S. H. Zigmond, *Curr. Biol.* **9**, R160 (1999).
18. P. Sehr *et al.*, *Biochemistry* **37**, 5296 (1998); I. Just *et al.*, *Nature* **375**, 500 (1995).
19. G. Servant *et al.*, unpublished data.
20. Preliminary experiments show that PHAKT-GFP–expressing HL-60 cells also migrated toward a micropipette delivering a point source of insulin. However, under these conditions we have not been able to detect translocation of PHAKT-GFP to the plasma membrane.
21. S. R. James *et al.*, *Biochem. J.* **315**, 709 (1996); D. Stokoe *et al.*, *Science* **277**, 567 (1997); T. F. Franke *et al.*, *Science* **275**, 665 (1997); M. Frech *et al.*, *J. Biol. Chem.* **272**, 8474 (1997); A. Klippel *et al.*, *Mol. Cell. Biol.* **17**, 338 (1997); P. J. Coffer, J. Jin, J. R. Woodgett, *Biochem. J.* **335**, 1 (1998); S. J. Isakoff *et al.*, *EMBO J.* **17**, 5374 (1998); J. M. Kavran *et al.*, *J. Biol. Chem.* **273**, 30497 (1998); S. J. Watton and J. Downward, *Curr. Biol.* **9**, 433 (1999).
22. N. B. Ruderman *et al.*, *Proc. Natl. Acad. Sci. U.S.A.* **87**, 1411 (1990).
23. M. P. Wymann and L. Pirola, *Biochim. Biophys. Acta* **1436**, 127 (1998).
24. S. J. Isakoff *et al.*, *EMBO J.* **17**, 5374 (1998).
25. E. Baraldi *et al.*, *Structure* **7**, 449 (1999).
26. L. R. Stephens *et al.*, *Cell* **89**, 105 (1997).
27. A. Ptasznik *et al.*, *J. Biol. Chem.* **271**, 25204 (1996).
28. T. Sasaki *et al.*, *Science* **287**, 1040 (2000); Z. Li *et al.*, *Science* **287**, 1046 (2000); E. Hirsch *et al.*, *Science* **287**, 1049 (2000).
29. Yeast cells expressing an exchange factor for Cdc42 that is unable to bind to the G-protein βγ subunit are unable to orient toward a pheromone gradient [A. Nern and R. A. Arkowitz, *Nature* **391**, 195 (1998)].
30. Bac1.2F5 macrophages microinjected with a dominant-negative Cdc42 mutant are able to migrate but do not polarize in the direction of the chemotactic gradient [W. E. Allen *et al.*, *J. Cell. Biol.* **141**, 1147 (1998)].
31. Expression of either dominant-positive or dominant-negative Cdc42 mutants render cells of a T cell hybridoma, 2B4, unable to polarize their actin cytoskeleton toward the antigen-presenting cell [L. Stowers, D. Yelon, L. J. Berg, J. Chant, *Proc. Natl. Acad. Sci. U.S.A.* **92**, 5027 (1995)].
32. We thank C. Bargmann, D. Stokoe, and A. Weiss for critical reading of the manuscript and M. Rosa for support. Supported in part by NIH grants GM-27800 and CA-54427 (H.R.B.), and GM-25101 (J.W.S.). G.S. is a medical Research Council of Canada Postdoctoral Fellow, and O.D.W. is a Howard Hughes Medical Institute Predoctoral Fellow.

4 August 1999; accepted 20 December 1999

Function of PI3Kγ in Thymocyte Development, T Cell Activation, and Neutrophil Migration

**Takehiko Sasaki,[1,2] Junko Irie-Sasaki,[1,2] Russell G. Jones,[2]
Antonio J. Oliveira-dos-Santos,[1] William L. Stanford,[3]
Brad Bolon,[4] Andrew Wakeham,[1] Annick Itie,[1] Dennis Bouchard,[1]
Ivona Kozieradzki,[1] Nicholas Joza,[1] Tak W. Mak,[1,2]
Pamela S. Ohashi,[2] Akira Suzuki,[1,2] Josef M. Penninger[1,2]***

Phosphoinositide 3-kinases (PI3Ks) regulate fundamental cellular responses such as proliferation, apoptosis, cell motility, and adhesion. Viable gene-targeted mice lacking the p110 catalytic subunit of PI3Kγ were generated. We show that PI3Kγ controls thymocyte survival and activation of mature T cells but has no role in the development or function of B cells. PI3Kγ-deficient neutrophils exhibited severe defects in migration and respiratory burst in response to heterotrimeric GTP-binding protein (G protein)–coupled receptor (GPCR) agonists and chemotactic agents. PI3Kγ links GPCR stimulation to the formation of phosphatidylinositol 3,4,5-triphosphate and the activation of protein kinase B, ribosomal protein S6 kinase, and extracellular signal-regulated kinases 1 and 2. Thus, PI3Kγ regulates thymocyte development, T cell activation, neutrophil migration, and the oxidative burst.

PI3Ks constitute a family of evolutionarily conserved lipid kinases that regulate a vast array of fundamental cellular responses, including proliferation, transformation, protection from apoptosis, superoxide production, cell migration, and adhesion (*1*). These responses result from the activation of membrane-trafficking proteins and enzymes such as the phosphoinositide-dependent kinases (PDKs), protein kinase B (PKB), and S6

CHAPTER SIX

Pathogenic E. coli as a System for Dissecting Signaling to the Cytoskeleton—the Role of the Wiskott-Aldrich Syndrome Protein

Reprinted by permission from *Nature Cell Biology* Vol. 1 No. 6 pp389-391.

Copyright 1999 Macmillan Magazines Limited.

Enteropathogenic *E. coli* acts through WASP and Arp2/3 complex to form actin pedestals

Daniel Kalman*‡†, Orion D. Weiner‡¶, Danika L. Goosney#, John W. Sedat¶, B. Brett Finlay#, Arie Abo and J. Michael Bishop***

**Department of Microbiology and Immunology, G.W. Hooper Foundation Laboratories, University of California at San Francisco, San Francisco, California 94143, USA*
¶Department of Biochemistry, University of California at San Francisco, San Francisco, California 94143, USA
#Biotechnology Laboratory, and the Department of Microbiology and Immunology, University of British Columbia, Vancouver, BC V6T 1Z3 Canada
***Onyx Pharmaceuticals, Richmond, California 94806, USA*
†e-mail: kalman@cgl.ucsf.edu
‡These authors contributed equally to this work

Extracellular stimuli can induce localized actin rearrangements at the site of stimulation. To understand how this occurs, we have been studying enteropathogenic *Escherichia coli* (EPEC), a bacterial pathogen that induces formation of an actin-rich membrane pseudopod or pedestal beneath itself upon adherence to host intestinal epithelia[1]. Infection ultimately results in diarrhoea, which can cause death, especially among infants in developing countries[1]. Here we show that pedestal formation depends on localized recruitment and activation of two host-cell factors involved in actin polymerization: the heptameric Arp2/3 complex (Arp2/3c), which nucleates polymerization[2], and members of the Wiskott–Aldrich syndrome (WAS) family of proteins (WASP and N-WASP)[1], which bind to and activate Arp2/3c (ref. 2). Arp2/3c recruitment depends on WASP, and WASP recruitment depends on its GTPase-binding domain (GBD), suggesting involvement proximally of a Rho family GTPase. This is, to our knowledge, the first demonstration of cellular mediators of EPEC pedestal formation and of localized recruitment of WASP and Arp2/3c as part of a signalling cascade initiated at the cell surface.

Exposure of HeLa cells to wild-type EPEC resulted in the formation of an actin-rich pedestal underneath the bacterium (see Supplementary Information). To determine whether endogenous WAS family proteins localized to the pedestals, HeLa cells were exposed to EPEC and then stained with a polyclonal antiserum that recognized WASP and N-WASP. At low magnification, pedestals are seen as punctate actin staining (Fig. 1c), directly apposed to the bacterium (Fig. 1a). The endogenous WASP-like protein (Fig. 1b) was enriched in the pedestal relative to the cell body.

We next asked whether exogenous WAS family proteins affected pedestal formation or localized to pedestals. Flag-tagged wild-type WASP (WASP-WT) was expressed in HeLa cells, and the cells were exposed to EPEC. The EPEC are shown in Fig. 1e and the WASP-WT, detected by staining with the Flag antibody, in Fig. 1f. WASP-WT had no effect on pedestal formation, as measured by actin staining (Fig. 1g). Like the endogenous WAS-like protein, WASP-WT concentrated in pedestals (Fig. 1e–h, arrowheads). Haemagglutinin (HA)-tagged N-WASP behaved identically to WASP-WT (data not shown). Localization of transfected WASP-WT to pedestals was specific: green fluorescent protein (GFP) fluorescence was not enriched in pedestals relative to the cell body (data not shown).

We determined whether WASP was required for pedestal formation by expressing various domains of WASP or N-WASP. Deletion of the WASP carboxy terminus (ΔC) results in pronounced defects in the capacity of the protein to polymerize actin[1]. Expression of WASP-ΔC blocked pedestal formation in a dominant-negative fashion (Fig. 1i–l). Pedestals, as measured by actin staining (Fig. 1k), were not evident beneath attached bacteria (Fig. 1i arrowheads) in cells expressing WASP-ΔC (Fig. 1j). Blockade occurred even in cells where the construct was expressed at low levels (Fig. 2a cell on right). In such cells WASP-ΔC protein (green, Fig. 2a) localized directly adjacent to the bacteria (blue, Fig. 2a), but no pedestals (red) were evident (compare the cell on the right with the non-expressing cell on the left in Fig. 2a). The C terminus by itself neither localized nor blocked pedestal formation (data not shown).

The WASP C terminus contains a WH2 domain, a cofilin domain and an acidic (A) domain (see Supplementary Information). N-WASP alleles with mutations in the cofilin domain can act in a dominant-negative fashion[3]. However, we could detect no effect of N-WASP-Δcofilin on pedestal formation or localization, even when the protein was expressed at high levels. In contrast, WASP protein lacking the WH2 domain continued to localize beneath the bacteria but blocked pedestal formation only when expressed at high levels (data not shown). The WASP WH2 domain expressed independently neither blocked nor localized. N-WASP-ΔA and N-WASP-ΔA/Δcofilin both blocked when expressed at low levels and were indistinguishable from WASP-ΔC (Fig. 2f–h).

The observation that N-WASP-ΔA blocked pedestal formation led us to consider whether Arp2/3c, which binds to the acidic domain of WASP[2], localizes to pedestals. Subunits p21 (Fig. 2c–e) and p40 (data not shown) of the endogenous Arp2/3c, as well as transfected Arp3-GFP (data not shown), were recruited to the pedestals. As noted above, WASP-ΔC and N-WASP-ΔA blocked pedestal formation but continued to localize beneath EPEC (Fig. 2a for WASP-ΔC; Fig. 2g (arrowheads) for N-WASP-ΔA). WASP-ΔC or N-WASP-ΔA also prevented localization of p41 (Fig. 2f–i, arrowheads), and of p40 and GFP-Arp3 (data not shown), beneath EPEC. We conclude that recruitment of Arp2/3c depends on the WASP acidic domain and that both a WASP-like protein and Arp2/3c are required for pedestal formation. Our *in vivo* results complement *in vitro* studies which show that the C terminus of WASP associates with and potentiates the nucleating activity of Arp2/3c (ref. 2). Whereas the acidic domain directly binds the Arp2/3c subunit p21, both the acidic and WH2 domains are required for activation.

To determine which domains of WASP were required for localization in the pedestal, we expressed WASP proteins containing deletions that disrupt domains outside the C terminus. Deletion of the GBD prevented WASP from localizing specifically in the pedestals (Fig. 1m–p). Quantitation of fluorescence intensity in the pedestal and cell body showed that although WASP-ΔGBD was present in the pedestals, it was not enriched relative to the cell body. The effect was specific: WASP proteins with deletions in the amino terminus encompassing the pleckstrin-homology (PH) and WASP-homology 1 (WH1) domains, or in the polyproline (PP) or N-WASP-Δcofilin domains all localized in a manner comparable to WASP-WT. Thus, the GBD is necessary for recruitment of WASP to pedestals.

When expressed alone at low levels, the WASP GBD domain localized to the pedestals (Fig. 1q–t). When expressed at high levels, WASP GBD blocked pedestal formation but continued to localize beneath the bacterium (data not shown). We surmise that when

© 1999 Macmillan Magazines Ltd

highly expressed, the GBD can competitively inhibit binding of an endogenous WASP-like protein, but that this domain alone is not as effective a competitor as WASP-ΔC, possibly because of the effects of additional domains in WASP. The effect of expressing this domain alone was specific. Expression of PH/WH1 domain or PP domain was without effect on pedestal formation and neither protein localized. Moreover, a GBD from the kinase PAK3, which shares 70% amino-acid homology with the WASP GBD, neither blocked pedestal formation nor localized to pedestals. Thus WASP GBD was necessary and sufficient for localization to pedestals. However, we cannot rule out the possibility that additional domains contribute to localization.

We next determined whether WASP activity was dependent on localization of WASP to pedestals. To do this we assessed whether the dominant-negative effects of the WASP-ΔC required an intact GBD. Expression of mutant WASP with deletions of both the C terminus and the GBD (ΔC/ΔGBD) neither blocked pedestal formation nor localized beneath the bacterium (Fig. 2b). Thus the GBD is required for dominant-negative effects, and localization of WASP through the GBD is required to recruit Arp2/3c and for pedestal formation.

The requirement for WASP GBD suggested that, in pedestal formation, a GTPase both recruits and activates WASP. The Cdc42 GTPase interacts with the WASP GBD[5], but pedestal formation is insensitive to the effects of *Clostridium dificile* toxin B (ToxB)[6], which inactivates Rho family members, including Cdc42. We provide evidence elsewhere that a novel Cdc42 homologue, called Chp[7], is ToxB-insensitive and may mediate EPEC signalling to WASP (D.K. *et al.*, unpublished observations).

Recent evidence has also implicated Arp2/3c, WASP and Rho family GTPases in spatial control of actin polymerization. First, Arp2/3c redistributes to the up-gradient surface of the plasma membrane in neutrophils responding to chemoattractant[8]. Second, artificial targeting of WASP or Cdc42 to a localized site on the plasma membrane is sufficient to generate actin-rich filopodia-like structures at that site[9]. Accordingly, our data suggest that EPEC triggers localized recruitment and activation of WASP and Arp2/3c *in vivo*, leading to localized actin rearrangements.

In summary, we present a model for EPEC pedestal formation (see Supplementary Information). EPEC adheres to the outside of the host cell and inserts the virulence factor Tir into the host plasma membrane using a type III secretion system[1]. Tir then binds the EPEC surface protein intimin, and directly or indirectly recruits

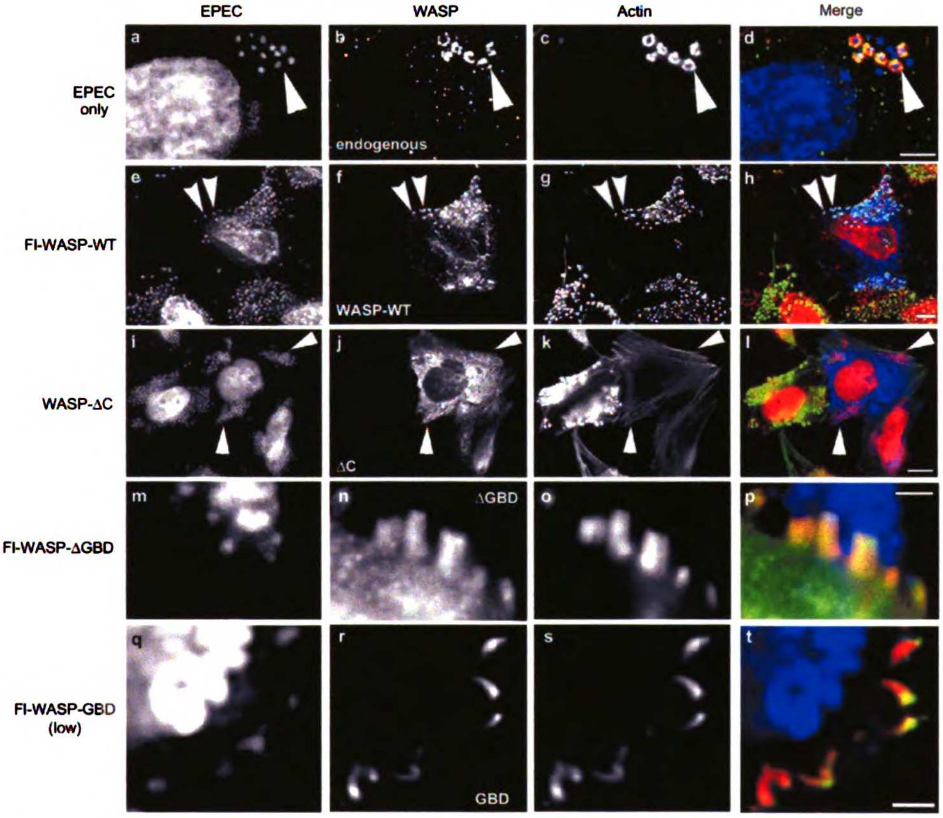

Figure 1 WASP is recruited through its GTPase-binding domain (GBD) to EPEC pedestals. **a–d**, Images of HeLa cells exposed to EPEC. Cells were stained with DAPI, to identify EPEC (**a**), anti-WASP polyclonal Ab (**b**) or rhodamine–phalloidin, to visualize actin (**c**). Arrowheads denote endogenous WASP-like protein localized in pedestals. In the merged images **d**, **p** and **t**, EPEC are pseudocoloured blue, WASP green, and actin red. In **h** and **l**, EPEC are pseudocoloured red, WASP blue, and actin green. **e–h**, Images of cells expressing Flag (Fl)-WASP-WT and exposed to EPEC. In this panel and in **i–t**, cells were stained with DAPI (**e**, **i**, **m**, **q**), anti-Flag mAb (**f**, **j**, **n**, **r**), and rhodamine–phalloidin (**g**, **k**, **o**, **s**). Arrowheads denote Fl-WASP-WT protein localized in pedestals. **i–l**, Images of cells expressing high levels of WASP-ΔC. Note that EPEC on expressing cells have no actin pedestals associated with them (arrowheads). **m–p**, Images of cell expressing Fl-WASP-ΔGBD. Note that WASP-ΔGBD was in pedestals but was not enriched relative to the cytoplasm. **q–t**, Images of cell expressing low levels of Fl-WASP-GBD. Note that the GBD protein localizes to pedestals. Scale bar represents 4 μm in **d**, 5 μm in **h**, 10 μm in **l**, and 2 μm in **p**, **t**.

© 1999 Macmillan Magazines Ltd

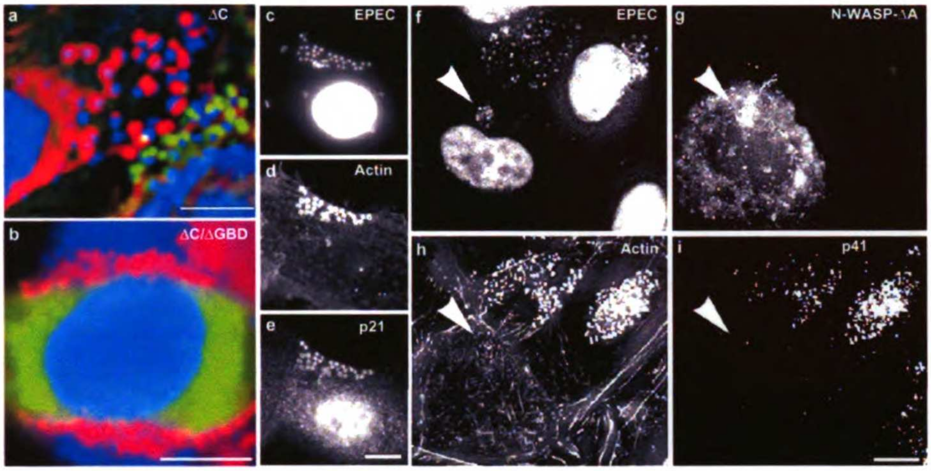

Figure 2 Pedestal formation and localization of Arp2/3c to pedestals require the WASP acidic domain. **a**, Image of HeLa cell expressing low levels of WASP-ΔC and exposed to EPEC. Cells were stained with DAPI, anti-Flag, and rhodamine–phalloidin. In this merged image and in **b**, EPEC are pseudocoloured blue, actin red and WASP green. The cell on the right expresses low levels of WASP-ΔC protein which localizes next to the bacteria (blue) and blocks pedestal formation. The cell on the left did not express the protein and develops pedestals (red). **b**, Image of cell expressing Fl-WASP-ΔC/ΔGBD and exposed to EPEC. Cells were stained and the image pseudocoloured as in **a**. In the absence of C and GBD, pedestals formed and the protein was not localized exclusively within them. Thus, the GBD is required for WASP-ΔC to act as a dominant negative. Unmerged images are provided in Supplementary Information. **c**–**e**, Images of HeLa cell stained for Arp2/3c subunit p21 and exposed to EPEC. The cell was stained with DAPI (**c**), anti-actin mAb and Cy-5-conjugated secondary antibody (**d**), and anti-p21 antiserum and FITC secondary antibody (**e**). Note the recruitment of p21 to pedestals. **f**–**i**, Images of cell expressing N-WASP-ΔA and exposed to EPEC. The cell was stained with DAPI (**f**), anti-HA mAb and FITC secondary antibody, to recognize the N-WASP-ΔA (**g**), rhodamine–phalloidin (**h**), and anti-p41 antibody and Cy-5 secondary antibody (**i**). Note that p41 fails to accumulate beneath EPEC in the cell expressing N-WASP-ΔA, and that the cell fails to make pedestals. Arrowheads denote the lack of p41 accumulation in the cell expressing N-WASP-ΔA. All scale bars represent 10 μm.

and activates a host-cell GTPase of the Chp subfamily. The Chp-like GTPase recruits WASP by binding the GBD, thereby exposing the WH2 and acidic domains in the WASP C terminus. The WASP C terminus in turn recruits and activates Arp2/3c, thereby stimulating actin nucleation and polymerization. Actin polymerization drives membrane protrusion and pedestal formation.

According to this model, WASP-ΔC or N-WASP-ΔA act in a dominant-negative fashion because they compete efficiently with an endogenous WASP-like protein for recruitment, but neither mutant activates Arp2/3c. Notably, the C terminus of WASP blocks activation of Arp2/3c in other systems[10] but does not block EPEC pedestal formation when expressed at similar levels to WASP-ΔC. We suggest that this difference in potency results because WASP-ΔC competes for a limited number of EPEC-generated recruitment sites, whereas the C terminus must titrate the relatively abundant Arp2/3c. Indeed, this capacity makes WASP-ΔC a generally useful probe of WASP function.

In conclusion, WASP and Arp2/3c are the first identified and among the most distal mediators of a signalling cascade initiated at the cell surface by EPEC and culminating in actin polymerization and pedestal formation. An eventual understanding of how EPEC interfaces with the mammalian cellular signalling machinery will provide insight into the molecules that link physiological receptors at the cell surface with reorganization of the actin cytoskeleton. ☐

Methods

HeLa cells were grown on glass coverslips in Dulbecco's Modified Eagles medium (DMEM) supplemented with 10% fetal calf serum and incubated for 6–8 h at 37 °C with WT EPEC at a multiplicity of infection of 10. For some experiments cells were transfected with plasmid vectors using calcium phosphate precipitation or Fugene-6 (Boehringer) 3 days before infection. Constructs are described in Supplementary Information. Cells were processed for immunocytochemistry as described previously[6]. EPEC was recognized by staining with 4′6-diamidino-2-phenylindole (DAPI; 1 μg ml^{-1}; Sigma). Before staining, some polyclonal rabbit antisera were incubated for 20 min with EPEC previously fixed in formaldehyde, and then centrifuged. This procedure removed serum contaminants that nonspecifically bound EPEC. The primary antibodies and concentrations used in this study were as follows: 9E10 monoclonal antibody (mAb) (ascites, 1:200 dilution), anti-Flag mAb (0.1μg ml^{-1}, Sigma), anti-WASP polyclonal antibody (affinity purified, 1:200 dilution), and anti-HA mAb (3F10; 0.1μg ml^{-1}, Boehringer; 1:500 dilution). Secondary antibodies were obtained from Jackson Immunochemicals. Images were acquired with a scientific-grade cooled charge-coupled device on a multi-wavelength wide-field three-dimensional microscopy system[8]. Samples were imaged in successive 0.25-μm focal planes, and out-of-focus light was removed with a constrained iterative deconvolution algorithm[8].

RECEIVED 28 APRIL 1999; REVISED 19 JULY 1999; ACCEPTED 20 AUGUST 1999;
PUBLISHED 16 SEPTEMBER 1999.

1. Goosney, D. L., de Grado, M. & Finlay, B. *Trends Cell Biol.* **9**, 1–4 (1999).
2. Machesky, L. M. & Insall, R. H. *J. Cell Biol.* **146**, 267–292 (1999).
3. Abo, A. *Cell Mol. Life Sci.* **54**, 1145–1153 (1998).
4. Symons, M. *et al. Cell* **84**, 723–734 (1996).
5. Miki, H., Sasaki, T., Takai, Y. & Takenawa, T. *Nature* **391**, 93–96 (1998).
6. Ben-Ami, G. *et al. Infect. Immun.* **66**, 1755–1758 (1998).
7. Aronheim, A. *et al. Curr. Biol.* **8**, 1125–1128 (1998).
8. Weiner, O. D. *et al. Nature Cell Biol.* **1**, 75–81 (1999).
9. Castellano, F. *et al. Curr. Biol.* **9**, 351–360 (1999).
10. Machesky, L. & Insall, R.H. *Curr. Biol.* **8**, 1347–1356 (1998).

ACKNOWLEDGEMENTS
The authors thank A. Mallavarapu and J. Taunton for helpful discussions, S. Keshavarzi for assistance, M. Welch for Arp2/3c antibodies, H.Miki for N-WASP cDNA, and H. Bourne, A. Johnson and J. Engel for commenting on the manuscript. The work was supported by the H.H.M.I. (O.D.W and B.B.F.), the N.S.E.R.C., Canada (D.L.G), and grants from the M.R.C., Canada (B.B.F), from the N.I.H. (J.W.S. and A.A.), and from the N.C.I. (J.M.B.).

Correspondence and requests for materials should be addressed to D.K.

Supplementary information is available on *Nature Cell Biology*'s World-Wide Web site (http://cellbio.nature.com) or as paper copy from the London editorial office of *Nature Cell Biology*.

© 1999 Macmillan Magazines Ltd

CHAPTER SEVEN

Summary

Summary

In conclusion, our primary findings with regards to chemotaxis were that

1. Chemoattractant receptors are uniformly distributed during chemotaxis.
2. Actin polymerization and a nucleator of actin polymerization are strongly asymmetric during chemotaxis.
3. PI(3,4,5)P3 levels are strongly asymmetric during chemotaxis, this asymmetry exceeds that of the external chemoattractant, and Rho GTPases are required for PI(3,4,5)P3 production.

We interpret this data to indicate that gradient amplification (conversion of a small external gradient into a large internal gradient of response) occurs at or upstream of PI(3,4,5)P3. In combination with ongoing experiments (unpublished) that suggest that PI(3,4,5)P3 induces its own production in a positive feedback loop that requires the Rho GTPases, this data suggests the following working model.

Stimulation of uniformly distributed chemoattractant receptors relays a slightly asymmetric (or in the case of uniform stimulation, uniform) pattern of G-protein signaling in the cell interior. This initiates PI(3,4,5)P3 production through the action of the G-protein regulated PI3kinase isoform PI3K-gamma. Small fluctuations in the levels of PI(3,4,5)P3 are amplified through a short-range positive feedback loop involving the Rho GTPases and a longer range (unknown) negative regulator of signaling. This produces a polarized distribution of PI(3,4,5)P3 that can then be used as a through localized activation of Cdc42/Rac and other molecules involved in actin polymerization and leading edge protrusion. Because several other chemotactic cells are known to

exhibit PI(3,4,5)P3 gradients aligned with the external gradient, it will be interesting to determine which of these cells use PI(3,4,5)P3 as a leading edge marker for polarity established through other means versus directly using emergent properties of PI(3,4,5)P3 metabolism to establish appropriate polarity.

Several important future directions include:

1. What are the negative regulators of signaling that restrict PI(3,4,5)P3 and other activities to the leading edge of cells? In general, the study of negative regulators (RGS proteins, lipid phosphatases, etc) has lagged behind that of positive regulators of activity, largely because our currently limited ability to deliver a fixed amount of activity to cells in a relevant way to study its down-regulation.
2. How do we identify new components of the polarity system for chemotaxis? The traditional genetic tools for axon guidance, *Dictyostelium* chemotaxis, etc have been valuable for identifying chemoattractant ligands, receptors, and G-proteins involved in signal relay, but they have yielded surprisingly few insights into the central polarity processing machinery of cells, presumably because these proteins may be required for cell viability. Conditional genetic screens (or chemical genetic ones) and biochemical approaches may be necessary to isolate these new components.
3. Are our GFP-PH-based lipid probes pure readouts of phospholipid distribution, or do they represent a more complex integration of lipid and protein distribution? Manipulations that abolish phospholipid binding also abolish recruitment to the plasma membrane for a variety of PH-based probes, suggesting that this lipid binding is necessary for recruitment. However, lipids are unlikely to be the only factors involved. The observation that PH domains with similar lipid specificities exhibit

different behaviors is some cause for concern-- PHAKT-GFP is recruited well in response to neutrophil stimulation but PH-BTK, which is also a PI(3,4,5P3 binder, fails to recruit to the plasma membrane following stimulation. Some PI(4,5)P2 binding PH domains are strongly recruited to the plasma membrane, others to the Golgi. These should raise important flags, both for the simplistic view that a PH domain = a particular lipid distribution and also that lipid distribution necessarily represents the whole story for spatial regulation of effectors for polarity.

4. How do we design appropriate activity readouts for proteins whose localization doesn't tell the whole story? GFP-tagging proteins and following their distribution has been valuable for analysis of many proteins, but there are a number of interesting proteins that change activation state (GTP-loading, phosphorylation, etc) during chemotaxis but do not alter their distribution. FRET-type analysis, recently developed for small and heterotrimeric G-proteins will be tremendously valuable tools. However, even more sensitive techniques (effectors with carefully engineered chromophores or labeling that only fluoresce upon binding their upstream activator) will probably be necessary for some of the more tightly regulated signal transduction proteins.

The recent tremendous progress in our ability to temporally and spatially study and manipulate activities in cells should greatly accelerate our understanding of the fascinating ability of cells to orient and migrate during chemotaxis. There are, no doubt, many surprises to come.

2723R

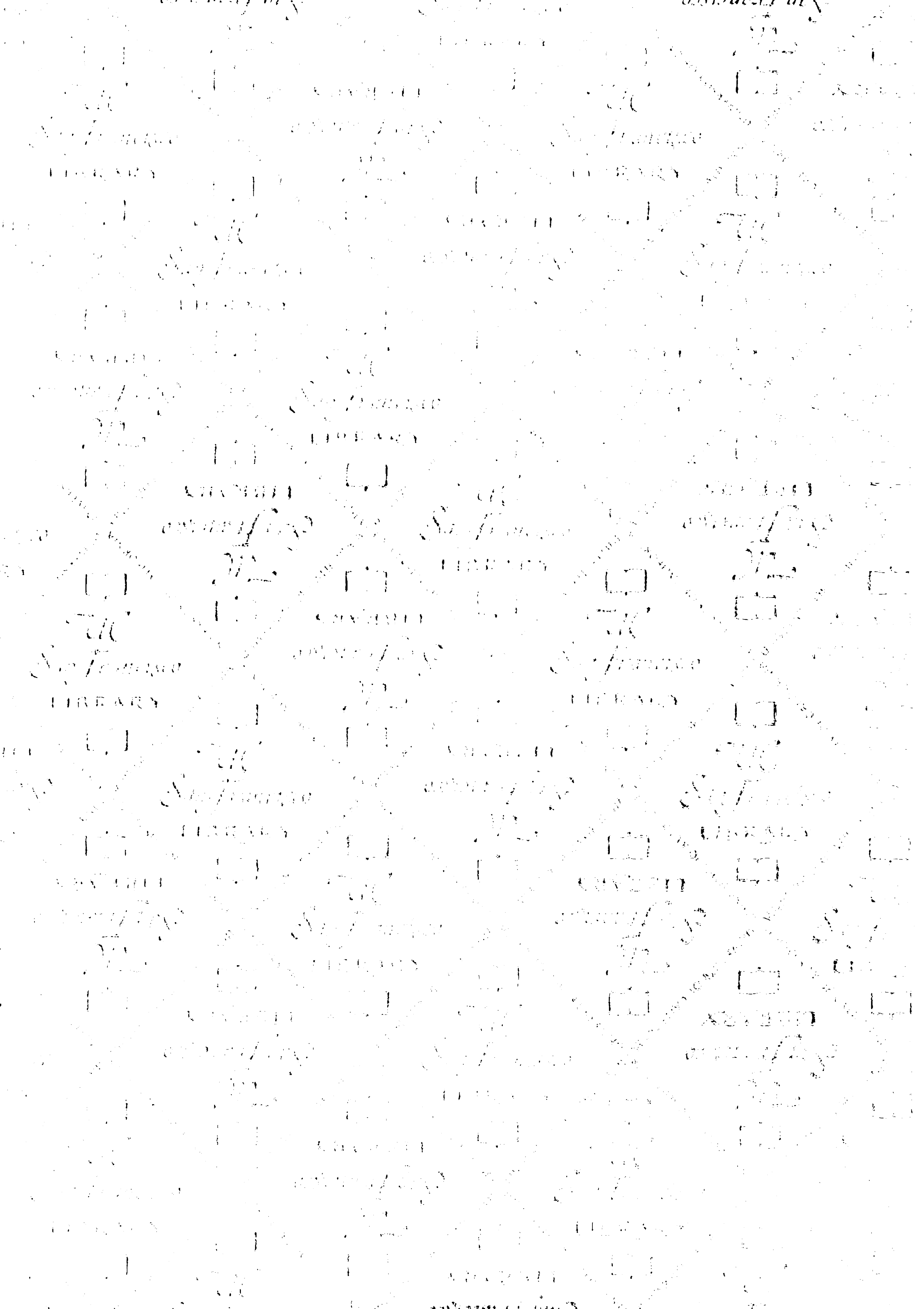

For reference

Not to be taken from the room.

7065769

3 1378 00706 5769